



UIT

THE ARCTIC
UNIVERSITY
OF NORWAY

Faculty of Science & Technology. Department of Geology.

Onshore-offshore correlation in the Andfjorden area and the structural controls on the opening and evolution of the Mesozoic sedimentary basins on Andøya and Andfjorden, northern Norway.

Tore Forthun

Master thesis in Geology, GEO-3900 May 2014



Forord

Der var studietiden over, gitt. Bare et par tastetrykk til så er masteren levert. 1, 2, 3 så er det over, så er jeg voksen. Ikke noe oppstyr, bare helt enkelt – totalt forskjellig fra konfirmasjonen som markerte overgangen fra ungdom til ansvarlig voksen. Følelsen er likevel at det er disse siste tastetrykkene som markerer den *egentlige* overgangen, at det er *nå* jeg blir voksen på ordentlig, at det er dette som burde markeres. Men så tenker jeg meg om; på alle de dumme tingene jeg har gjort siden konfirmasjonen og hvor lite jeg egentlig har forandret meg. Ja, jeg har flyttet ut og er mer selvstendig, men interessene og mange av vennene er de samme. Jeg spiller fotball, går på ski og gleder meg vilt til å kjøpe en Playstation 4, så hvor voksen har jeg egentlig blitt og hvor voksen kan noen få tastetrykk virkelig gjøre meg? Jeg skal jo bare bruke dagene mine på en litt annen, litt *fastere*, måte – ikke bli en helt annen person! Nei, forandringer skjer nok stort sett gradvis og ikke plutselig. De gjøres nok større enn de egentlig er, alt for at vi skal ha en grunn til å feire; vi velger bare noen passende tidspunkt hvor andre kan skåle for oss og si *Det er svært til brand du er blitt!*. Jeg ser derfor lyst på tiden fremover, og tror at den består av noe nytt og mye gammelt.

Kanskje er ikke dette helt sant. Kanskje er tankene mine tomme som Tolstojs, *som en båt med årer og tilbehør, men uten rorskar*, for å sitere Hamsun. Av større betydning er de nå uansett ikke – noe måtte jeg jo fylle forordet med, selv om noen enkle takker og hilsener hadde vært det greieste. Og til de som på dette tidspunktet måtte føle seg snytt – slapp av, de kommer, og det kommer mange av dem.

Først til veilederen min prof. Steffen Bergh. Tusen takk for uvurderlig hjelp i felt, diskusjoner og tips og råde underveis i skriveprosessen. Takk også for at jeg fikk bruke bildene du tok i felt. Jeg hadde ikke kommet langt uten deg. Takk til biveileder Tormod Henningsen ved Statoils kontor i Harstad, som har vært helt utrolig. Under mine opphold på Statoil har du virkelig stått på for meg. Takk for hjelp med seismisk tolkning og ikke minst for at du dro alene til Gapøya etter at været var for dårlig da vi skulle dra sammen. Felldataene herfra fikk dessverre ikke plass i oppgaven, men dette viser hvilken innsats du la ned for å hjelpe meg. En spesiell takk må rettes til feltassistentene mine Anders og Kristian. Dere gjorde feltarbeidet til mer enn stein. Takk også til deres foreldre/steforeldre som tok utrolig godt i mot meg, og gave meg både mat, sengeplass og – ikke minst – godt selskap. Takk til Peter Midbøe og Marco Brønner for diskusjoner og at jeg fikk være med på seismikkinnsamling på Andøya. Alle dere på brakka må selvfølgelig også takkes, spesielt Trude og kakene hennes og de på kontoret, Ingunn, Ingrid og Leif. Leif, det er synd Liverpool ikke vant Premier League mens vi satt ved siden av hverandre, men vi har alltid neste år. Takk også til Daniel for hjelp med tynnslipene mine.

Mor, far, bror Bjørn og resten av familien må så klart nevnes, særlig mor som tok på seg bryet med å lese korrektur. Dere betyr utrolig mye for meg.

Til slutt vil jeg takke min kjære Cathrine. Det er utrolig godt å komme hjem til deg. Du er et lys om jeg er sliten eller har hatt en dårlig dag – en vidunderlig, liten babs!

GIS, GIS, GIS,

Tore Forthun, 14. mai 2014

Abstract

Onshore-offshore correlation of brittle faults has been undertaken in the Andfjorden area defining the boundary between the passive Lofoten-Vesterålen margin and the transform SW Barents Sea margin. This study has focused its efforts on onshore mapping of faults and fractures, the mapping of offshore faults and associated basin-ridge systems from seismic interpretation and the link between fault complexes onshore and offshore by integrating bathymetry data, DEM and magnetic anomaly data. This study demonstrates that both the onshore and offshore part of the Andfjorden area are characterized by NNE-SSW to NE-SW and E-W to ENE-WSW striking faults/fractures, creating a rhombic regional fault/fracture pattern. Kinematic indicators such as fibrous slickensides and geometric relationships (e.g. rotation of older fractures into younger), indicate dominantly normal-slip with components of dextral/sinistral strike-slip movements on all fracture sets. Pre-existing fabrics in the Precambrian basement rocks such as gneiss foliation and lithological boundaries appear, at least locally, to have influenced brittle faulting. Based on the onshore-offshore structural analysis, this study also investigates the structural development of the Mesozoic Andfjorden basin. The following evolutionary model is suggested: (i) Initial basin formation and normal displacement along NNE-SSW and possibly also E-W striking fractures in the Mid Jurassic, resulting in the deposition of a Mid Jurassic rock sequence of uniform thickness that covered a large area. (ii) Rift maxima in the Late Jurassic to Early Cretaceous resulted in the development of the synthetic Senja and Andøya faults as major half-graben basin-boundary faults linked by a c. 30 km wide transfer zone. Propagation of these faults towards each other, or the development of a new fault (the Outer Andfjorden fault) breached the transfer zone, and separated the Andfjorden basin from the Harstad Basin. The separation leads to substantially more subsidence and, consequently, a shift of the depocenter toward the Harstad Basin relative to the Andfjorden basin. (iii) Early Cretaceous footwall uplift along the Andøya fault resulted in an asymmetric exhumation of the Andøya horst, and possibly also the antithetic NNE-SSW striking faults separating the Andfjorden basin from the Mesozoic rocks on Andøya. (iv) Cenozoic uplift related to e.g., ridge-push, a critical taper, post-glacial rebounds, created the Late Cenozoic to recent topography. NW-SE striking fractures observed to cross-cut all other fracture sets are tentatively correlated to these late stage events.

Contents

1	Introduction.....	1
1.1	Background and frame for the project.....	1
1.2	Aim and goals	3
1.3	Regional geology	6
1.3.1	Introduction: Bedrock geology of the study area.....	6
1.3.2	Precambrian basement rocks of Andøya	9
1.3.3	Precambrian basement rocks of the West Troms Basement Complex on Skrolsvik and Bjarkøya.....	10
1.3.4	Mesozoic rocks on Andøya.....	11
1.3.5	Post-Caledonian brittle faults: Rifting, extension and passive margin evolution	14
1.4	Methods	20
1.4.1	Fieldwork	20
1.4.2	Digital Elevation Models (DEM) – topography and bathymetry data	21
1.4.3	Seismic data.....	22
1.4.4	Magnetic anomaly data.....	23
1.5	Definitions	24
2	Description of onshore brittle faults and fractures.....	27
2.1	Introduction.....	27
2.2	DEM images.....	27
2.3	Andøya.....	30
2.3.1	Ramså	30
2.3.2	Skarstein	35
2.3.3	Fiskenes	41
2.3.4	Skarsteinsdalen quarry	44
2.4	Bjarkøya.....	47
2.4.1	Sundsvoll quarry.....	47
2.4.2	Sundsvoll shoreline.....	54
2.4.3	Gammelhamn quarry	57
2.5	Skrolsvik, Senja	60
2.5.1	Field relations and host rock characteristics.....	60
2.5.2	Skrolsvik quarry	61
2.5.3	Senjehesten peninsula.....	66
3	Description of offshore brittle structures.....	71

3.1	Bathymetry data.....	71
3.1.1	General seafloor morphology.....	71
3.1.2	Lineations - Regional trends.....	72
3.2	Magnetic anomaly data.....	72
3.2.1	General description.....	72
3.2.2	Lineaments.....	73
3.2.3	Relation to lithology.....	74
3.2.4	Relation to faults.....	75
3.3	Seismic data.....	76
3.3.1	Introduction.....	76
3.3.2	Database.....	76
3.3.3	Seismic stratigraphy and key horizons.....	76
3.3.4	Seismic interpretation.....	78
3.3.5	Summary and preliminary interpretations.....	85
4	Discussion.....	89
4.1	Discussion of onshore structures relative to the Andfjorden basin.....	89
4.2	Discussion of seismic data and interpretation.....	91
4.3	Onshore-offshore fault correlation using bathymetry and magnetic anomaly data.....	93
4.4	Timing constraints on the fault-fracture sets related to the Andfjorden basin.....	95
4.5	Structural evolution of the Andøya/Andfjorden sedimentary basin.....	100
5	Conclusions.....	105
6	References.....	107

1 Introduction

1.1 Background and frame for the project

This master thesis is part of an ongoing research collaboration with the University of Tromsø (UiT) and Statoil, focusing on land-shelf tectonics in Lofoten and Vesterålen and northwards to the Barents Sea region (Figs. 1, 2 & 8). While previous work in this project has focused on Lofoten and Vesterålen and the Precambrian basement islands Senja, Kvaløya and Vanna, the present work concentrates on Andøya and Andfjorden (Figs. 2 & 3), thus filling an important gap between these areas.

In view of the similarity in crustal thickness (20-27 km), the onshore and offshore areas have experienced roughly similar amounts of post-Caledonian crustal extension and the structural evolution is comparable (Løseth & Tveten, 1996). The focus for this thesis is to map contact relationships to onshore Mesozoic rocks on Andøya (Dalland, 1974, 1975, 1979; Sturt et al., 1979; Dalland, 1981) and analyze relations to the boundary faults to the Andfjorden basin. Special emphasis will be given analyzes of brittle faults and fracture systems close to the Mesozoic rocks on Andøya, in Andfjorden and the nearby islands of Bjarkøya and Senja (Fig. 2) by means of seismic data (Statoil), potential field data (NGU) and digital elevation models (DEM) of topography and bathymetry data in addition to own field observations on land.

Paleozoic and Mesozoic faults and rift-related basin structures on the shelf outside Lofoten and Vesterålen is reflected in the structuring of the shallow shelf and land areas around Vestfjorden-Andøya and northwards (Figs. 1, 2 & 8). There are for example clear indications on fault controlled lineaments (narrow fjords, cliffs, asymmetric morphology, rotated fault blocks, etc.) corresponding with regional normal faults delimiting Mesozoic rocks on the shelf (Hansen et al., 2012). Seafloor data from the shallow shelf show similar structures in the bedrock, allowing direct correlation of faults from land to deeper basins. New data from land and Vesterålen fjords (e.g. Sortlandsundet), show that rotated and partly eroded Paleozoic (?) and Mesozoic (?) fault blocks with associated sedimentary successions may have covered large parts of the coastal areas (Davidsen et al., 2001; Hendriks et al., 2010; Osmundsen et al., 2010; Fig. 2 this study). Such structures and paleo-relief may have been preserved on land as a result of fast Cenozoic uplift, coastal erosion and a land-shelf drainage and sedimentation that followed established directions since the Cretaceous.

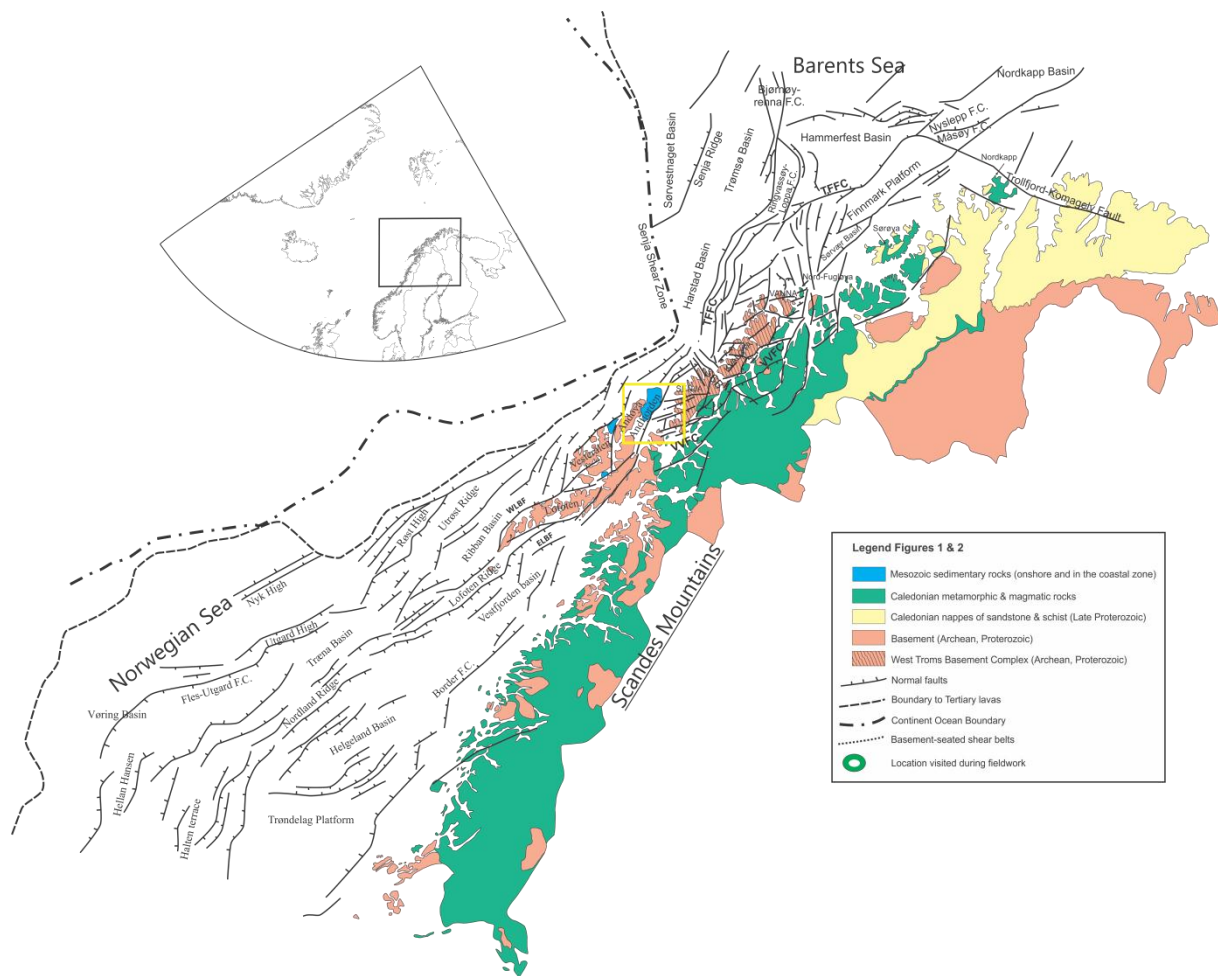


Figure 1 Structural elements from the Mid-Norwegian to the SW Barents Sea Margin and the main lithological units of the Mid-North Norway. From Indrevær et al. (2014).

Table 1 Abbreviations used in this thesis

AF = Andøya fault	SF = Senja fault
AB = Andfjorden basin	SFZ = Stonglandseidet Fault Zone
EAF = East Andøya Fault Zone	SiFZ = Sifjorden fault zone
ELBF = East Lofoten Border Fault	SsF = Sortlandsundet fault
GF = Gullfjorden Fault	TFFC = Troms-Finnmark Fault Complex
HB = Harstad Basin	VVFC = Vestfjorden-Vanna Fault Complex
OAF = Outer Andfjorden fault	WLBF = West Lofoten Border Fault

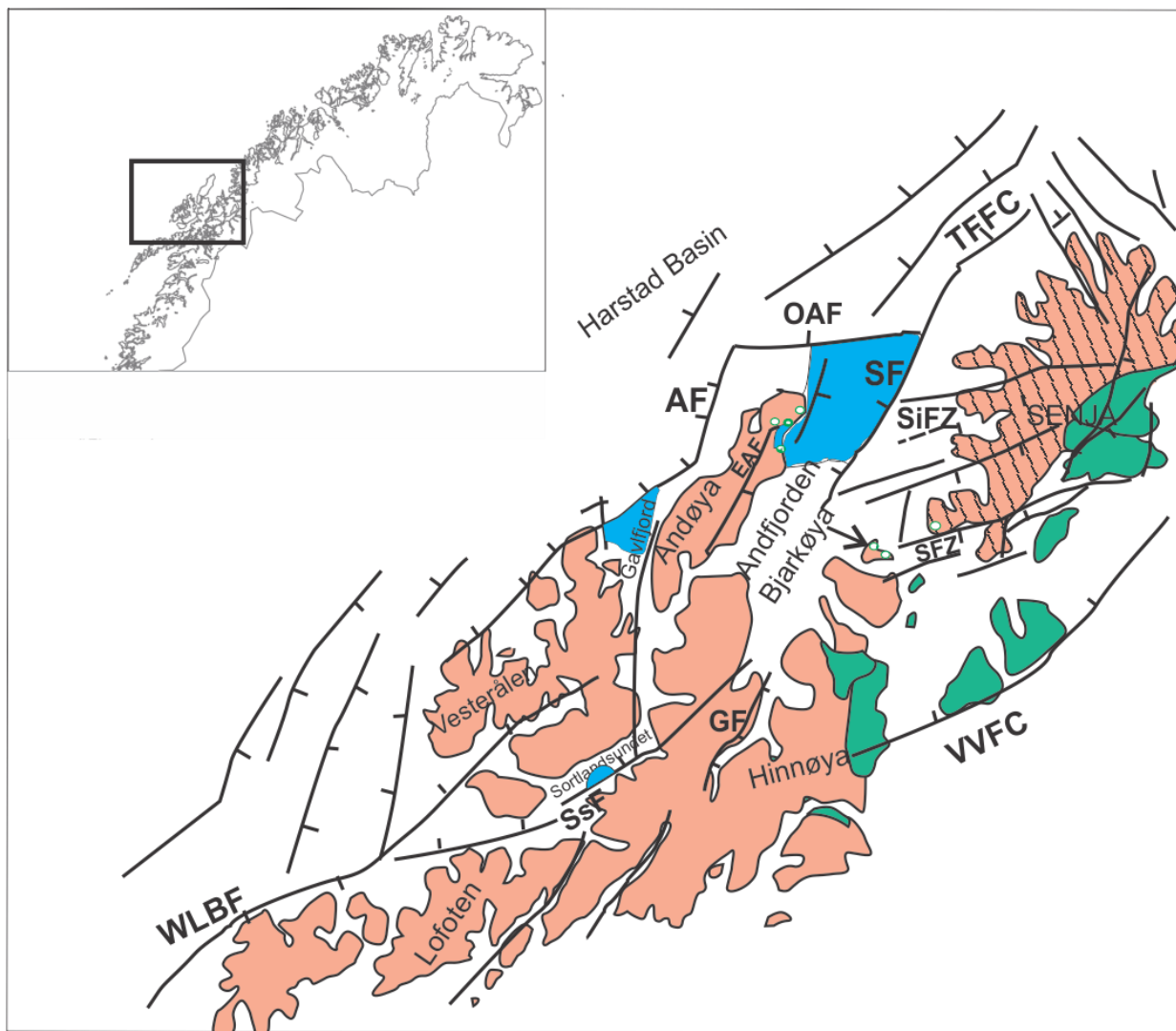


Figure 2 Simplified geological and structural map of the study area showing Precambrian basement rocks, Caledonian nappes and Mesozoic sedimentary rocks. Modified after Indrevær et al. (2014). Abbreviations are given in Table 1. Legend in Figure 1.

1.2 Aim and goals

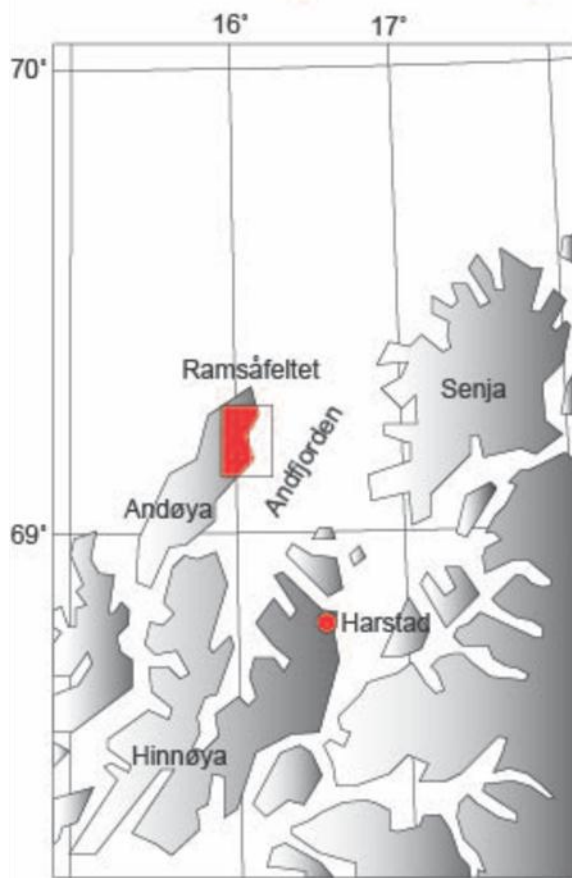
The specific tasks for this thesis are defined as follows:

- 1) Map and analyze brittle faults and fractures in the Precambrian bedrock in selected localities around Andfjorden, including Andøya, Bjarkøya and western Senja, using DEM data of bathymetry and topography and structural fieldwork. Special attention will be given to studies of faults near Ramså and Skarstein, delimiting the Mesozoic basin on Andøya (Figs. 3, 4 & 5), to illuminate fault orientations, kinematics and implications for basin formation.
- 2) Regional studies of bathymetry data from Andfjorden (MAREANO) with emphasis on separating Paleozoic and Mesozoic faults from glacial/morphological elements and

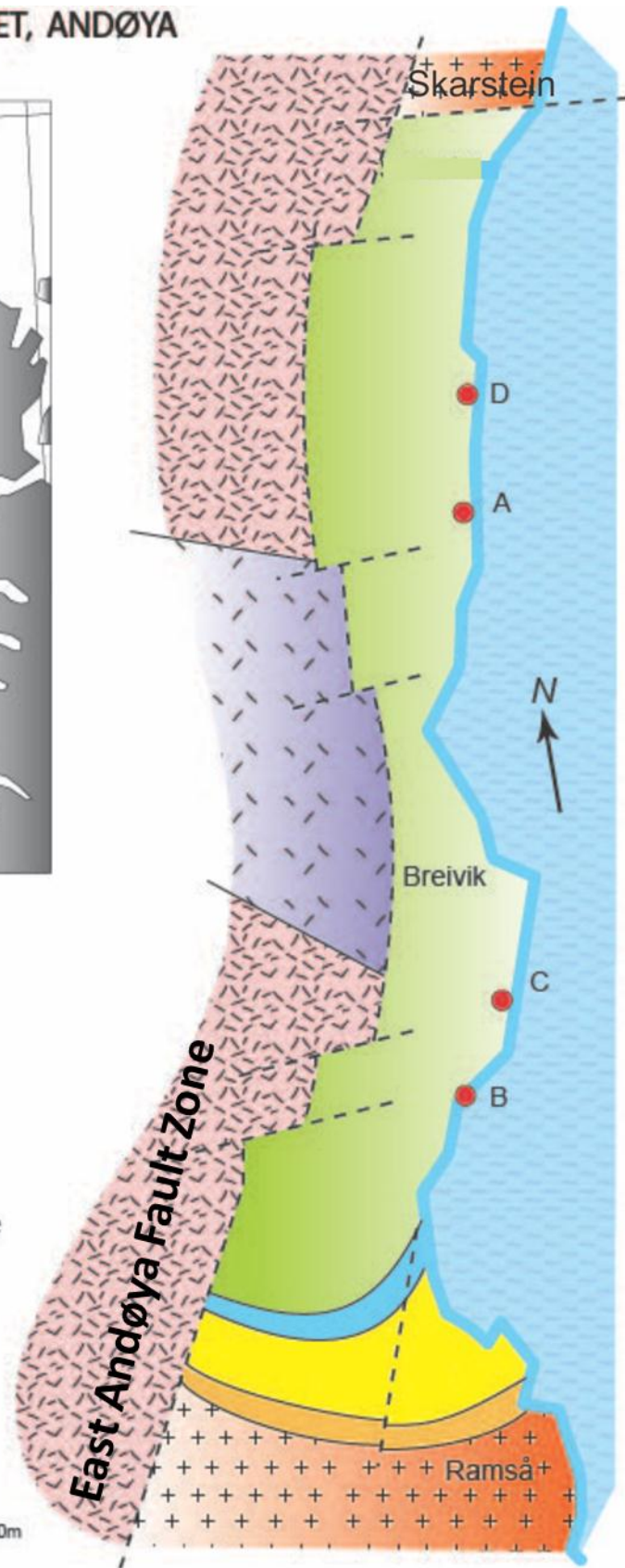
discuss fault formation and compare with directions for tectonically generated landscapes and similar faults/structures on land.

- 3) Regional studies of magnetic anomaly data to identify tectonic lineaments and possibly structural boundaries within the study area (both onshore and offshore). Findings may be used to support or negate interpretations from other data sets e.g., DEM, bathymetry and seismic data.
- 4) Seismic interpretation of selected 2D seismic lines from Andfjorden and the shallow shelf further out. The purpose is to interpret faults that can be linked to basin-ridge systems and to unravel their geometry and evolution in space and time. In doing so, one can achieve a better understanding of the architecture and structure of the Andfjorden basin and its relation to the Harstad Basin further out on the shelf.
- 5) Use the different datasets to correlate onshore and offshore basins, brittle faults and fractures and discuss this in relation to known tectonic events that affected the Nordland, Troms and SW Barents Sea margins, in order to present a model for the evolution of the Andøya and Andfjorden sedimentary basins.

GEOLOGICAL MAP, RAMSÅFELTET, ANDØYA



- Skarstein Formation
- Nybrua Formation
- Dragneset Formation
- Ramså Formation
- Gabbro and gabbro-norite
- ++ Andøy Granite
- / / / / Archean gneiss
- Fault
- Rock Boundary
- Borehole



Modified from Dalland, 1980

Figure 3 Geological map of the sedimentary basin between Ramså and Skarstein, Andøya. The basin is bounded in the east by one or several NNE-SSW striking faults, and laps on to basement in the south. Modified from Midbøe (2007).

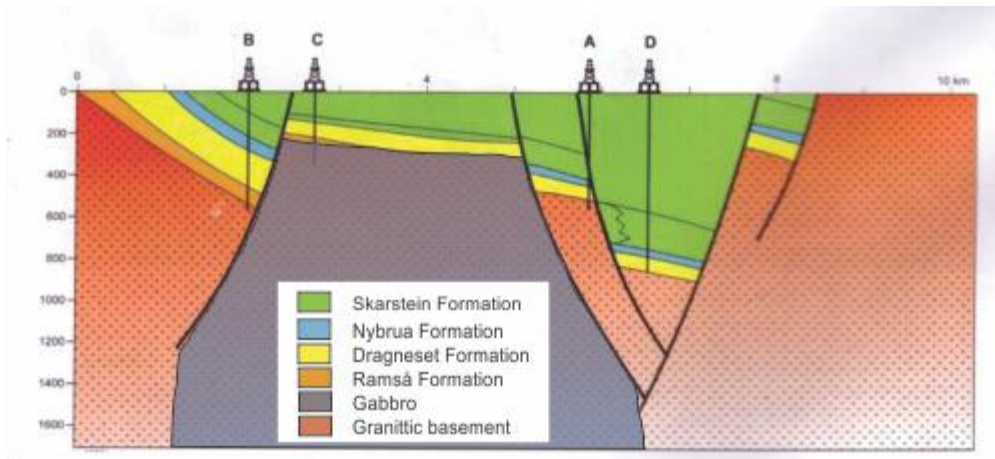


Figure 4 S-N striking cross-section of the sedimentary basin on Andøya. The basin consists of a graben and a half-graben separated by a horst. Modified from Rasmussen (1985).

1.3 Regional geology

1.3.1 Introduction: Bedrock geology of the study area

The regional geology of Lofoten, Vesterålen and Senja is dominated by Precambrian basement provinces in addition to offshore shelf areas with Paleozoic through Cenozoic strata and local Mesozoic rocks exposed on Andøya, Vesterålen (Henningesen & Tveten, 1998; Zwaan & Grogan, 1998).

The Precambrian rocks of Lofoten and Vesterålen (Figs. 1 & 2) consists of a magmatic province of Proterozoic anorthosites, mangerites, charnockites and granitic rocks (1870-1790 Ma) intruded in Archean/Proterozoic high grade ortho- and paragneisses assumed to be part of the Fennoscandian Shield (Griffin et al., 1974; Corfu, 2004). The rocks in Lofoten are massive with weakly developed foliation, while the rocks in Vesterålen show more variation and are dominated by various Archean and Paleoproterozoic ortho- and paragneisses.

Andøya (Fig. 2) consists of (i) Archean migmatitic gneisses intruded by (ii) Proterozoic plutonic (granite) rocks belonging to the Lofoten eruptives and (iii) an overlying (?) series of meta-supracrustal rocks (Skogvoll Group) of likely Proterozoic age (Henningesen & Tveten, 1998). These Precambrian units are all located in the north of the island and border to the Jurassic-Cretaceous Ramså basin (Dalland, 1974, 1975, 1979; Sturt et al., 1979; Dalland, 1981). On Senja, further north east (Fig. 6), Precambrian rocks belonging to the West Troms Basement Complex (Bergh et al., 2010) are well exposed. The rocks are generally well foliated and define a linear pattern of NW-SE striking units containing Neoproterozoic gneisses, Paleoproterozoic meta-supracrustal belts, granitoid plutonic rocks and numerous ductile shear zones.

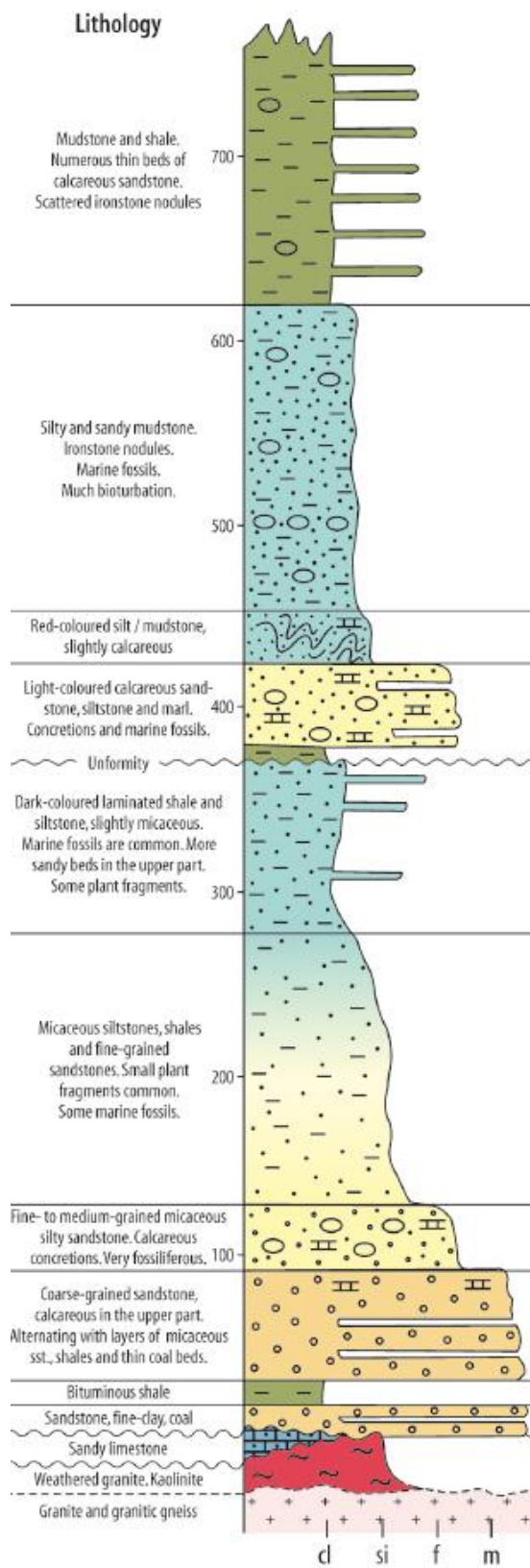


Figure 5 The sedimentary succession on Andøya. The succession consists of two Mesozoic fining-upwards sequences overlying a sandy limestone of unknown age and weathered basement grading into unweathered basement. From Bøe et al. (2010).

Mesozoic rocks of Middle Jurassic – Early Cretaceous age are exposed in a small area onshore between Ramså and Skarstein (Figs. 2, 3, 4 & 5) on Andøya, and consist of the Holen (disputable) and Ramså formations deposited directly on weathered basement, followed by the Dragnes, Nybrua and Skarstein formations with a total thickness of over 700 meters (Sturt et al., 1979; Dalland, 1981). Sandstones, calcareous schists, bituminous shales, micaceous fine-grained sandstones with numerous marine fossils (bivalves and belemnites are most common, but vertebrate remains have also been found) and frequent coal layers characterize the series (Dalland, 1974; 1975; Fig. 5 this work).

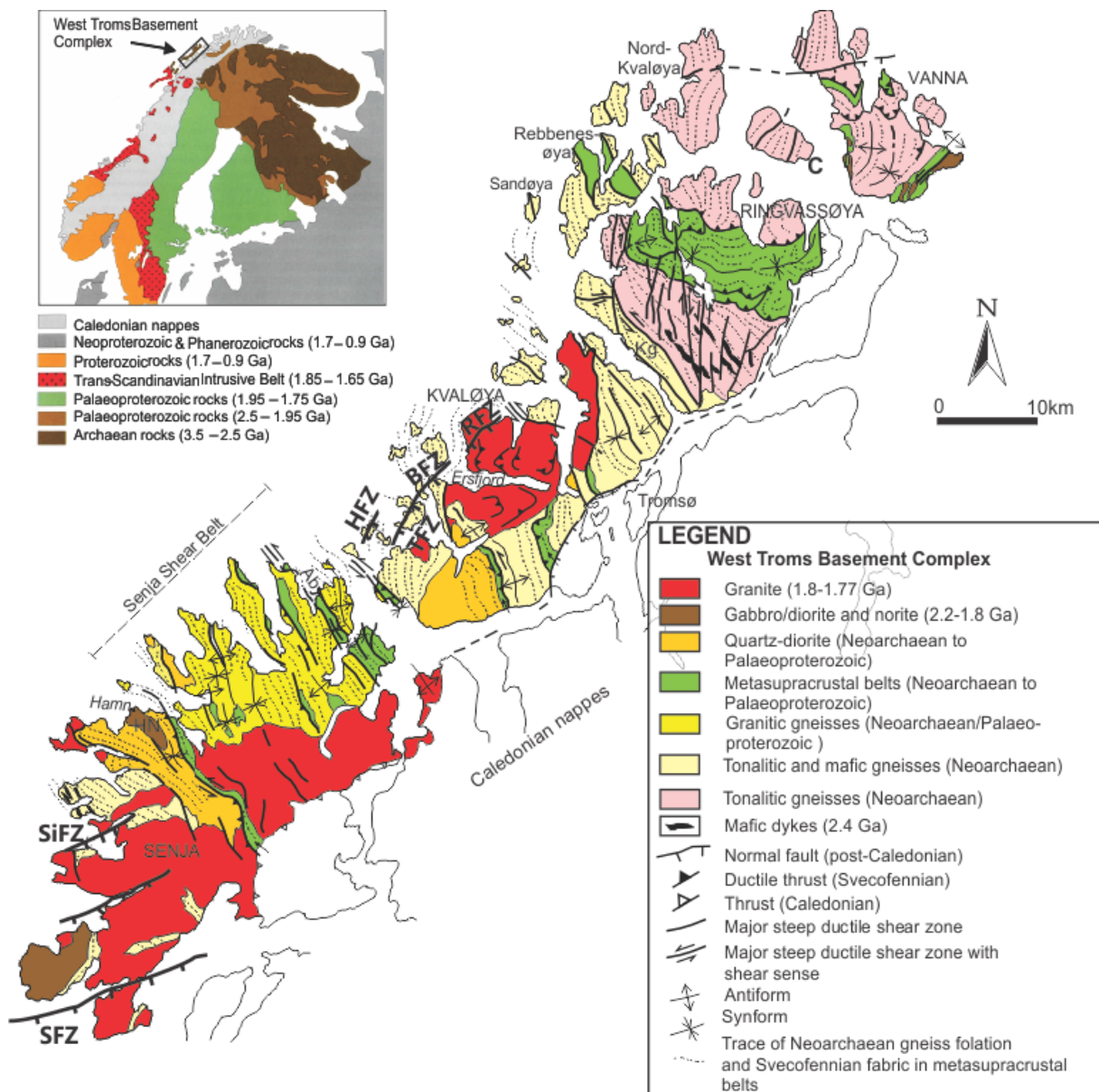


Figure 6 Regional geologic-tectonic map of the West Troms Basement Complex showing Precambrian fabrics and post-Caledonian brittle fault zones. Modified after Bergh et al. (2010) with new faults from Koehl (2013).

1.3.2 Precambrian basement rocks of Andøya

The Precambrian rocks on Andøya are divided into three groups: Neoproterozoic migmatitic gneiss, Paleoproterozoic igneous rocks (1.8-1.6 Ga) belonging to the Lofoten-Vesterålen Complex and igneous rocks of Archean to Paleoproterozoic age with the overlying meta-supracrustal rocks of the Skogsvoll Group (Henningsen & Tveten, 1998).

The Neoproterozoic gneisses are light gray and of various tonalite, trondhjemite and granitoid (TTG-gneiss) compositions, and metamorphosed in amphibolitic facies. They can be traced over to Hinnøya, where the metamorphic grades are up to granulite facies (Henningsen & Tveten, 1998). The age of the TTG-gneisses has not been determined on Andøya, but Zwaan and Grogan (1998) state that samples from Hinnøya have been dated to 2.8 Ga and that this likely represents the age of metamorphism rather than the age of formation. Although the host rock may have been both supracrustal rocks or intrusive, it seems most likely, based on the texture, that the gneisses were metamorphosed from a protolith of granodioritic to dioritic composition at mid-crustal levels (Henningsen & Tveten, 1998).

Coarse grained mangerite, gabbro and gabbronorite have intruded the Neoproterozoic gneiss in a similar manner to what Griffin et al. (1974) and Corfu (2004) observed in Lofoten and Vesterålen. Although the mangerite has not been found in direct association with the gabbro or gabbronorite, leaving their relationship somewhat unclear, Henningsen and Tveten (1998) decided to include these rocks in what they named the Lofoten-Vesterålen Complex. The rocks appear to be little deformed, implying also that they were not disturbed by the later Caledonian orogeny.

Red granites are exposed in numerous isolated locations and may thus consist of several granitic intrusions of different age, but these are together to the Andøy granite for simplifications (Henningsen & Tveten, 1998). The granite has not been dated, but isotopic investigations of a meta-basalt in the overlying Skogsvollgroup indicate a Paleoproterozoic minimum age and a possible relationship to the Lofoten-Vesterålen Complex.

The Skogsvoll Group is found in the flat central part of the island (Henningsen & Tveten, 1998). The lower part of the group (Vet Formation) overlies a thin zone of weathered granite, and consists of quartzite and quartzite conglomerate underlying marble, mica schist, while the upper part (Arnip Formation) consists of a smaller layers of mica schists, metabasalts (amphibolites) and marbles (Henningsen & Tveten, 1998). The rapid lithological changes in the upper part of the formation indicate deposition in a shallow marine area with volcanic activity (Henningsen & Tveten, 1998). It was long assumed that the Skogsvoll Group was of early Caledonian age, but unpublished radiometric dating of the amphibolite, although not very accurate, yields a minimum age of 1.8-1.6 Ga (Henningsen & Tveten, 1998).

1.3.3 Precambrian basement rocks of the West Troms Basement Complex on Skrolsvik and Bjarkøya

The rocks on Skrolsvik, and Senja in general, belong to the West Troms Basement Complex (Fig. 6). The West Troms Basement Complex is a major basement province situated west of the Caledonian thrust nappes, and composed of TTG gneisses, igneous-intrusive and meta-supracrustal rocks (Bergh et al., 2010). These rocks were split into four major rock types: Neoproterozoic gneisses (2.89-2.56 Ga), Neoproterozoic to Paleoproterozoic supracrustal rocks (2.40-1.97 Ga), early Paleoproterozoic mafic dykes (2.67-2.22 Ga), and Paleoproterozoic granitic and mafic plutonic intrusions (1.80-1.75 Ga) (Bergh et al., 2010).

While TTG gneisses with mafic intercalations are dominant in the northeastern part, the southwestern part (Senja) is made up of more granitic rocks, forming a compositional boundary that corresponds largely with the NW-SE striking Senja Shear Belt (Zwaan, 1995). The gneisses have a dominant foliation varying in trend between N-S and NW-SE, and a steep dip to the NE. Migmatite zones are common and seem to be associated with foliation parallel shear belts like the Senja Shear Belt (Bergh et al., 2010). The metamorphic grade of most rocks is commonly amphibolite facies, with local retrogression to greenschist facies along major ductile shear zones.

Metasupracrustal rocks are concentrated in belts between the gneiss regions (Astridal-, Svanfjellet- and the Torsnes belts), and commonly consist of meta-conglomerates, metapsammites, meta-schists, meta-volcanites and a number of distinct banded iron formations and massive sulphide ore bodies (Sandstad & Nilsson, 1998) with a steep SW and NE dipping mylonitic foliation (Bergh et al., 2010).

Huge igneous plutonic rocks intruded the West Troms Basement Complex in the Paleoproterozoic. Gabbro and quartz diorite commonly occur together, and are often associated with swarms of diabase dykes in the TTG gneisses. Similar mafic dyke swarms in Ringvassøya have been dated at 2.4 Ga (Kullerud et al., 2006). In southern part of Senja, near Skrolsvik (Figs. 2 & 9), a major quartz diorite pluton was dated to 1926 ± 3 Ma while associated granitic and gabbroic rocks were dated to 1.8 Ga (Zwaan & Grogan, 1998). Zwaan and Grogan (1998) also describe smaller, but similar intrusive rocks within the meta-supracrustal belts, but these were strongly deformed (lense-shaped) and even mylonitized during the Svecofennian orogeny (1.8-1.75 Ga). The Tranøybotten and Kaperdals granites (1768 ± 49 Ma and 1822 ± 5 Ma; Zwaan and Grogan (1998) intruded the basement rocks on Senja and are very similar to the large Ersfjord granite pluton on Kvaløya (1792 ± 5 Ma; Corfu et al. (2003), a coarse-grained igneous body that shows steep, sheared and mylonitized contacts with the surrounding gneisses. The granites are all accompanied by felsic pegmatite dykes of seemingly the same composition, likely representing the final stage of this intrusion event.

Bjarkøya (Figs. 2 & 9) is located in the southeastern part of Andfjorden, about ten kilometers outside Skrolsvik and is composed of rocks thought to belong to the West Troms Basement Complex, with a granite pluton in the south accompanied by a gabbro and a granitoid in the north.

The West Troms Basement Complex extends from Bjarkøya in the south to Vanna in the north, and the relationship to the Precambrian basement rocks on Andøya is thus uncertain. NGU has constructed a magnetic map over the area illustrating a clear relationship between magnetic anomalies of the Skogvoll Group on Andøya and anomalies on the eastern side of Andfjorden (Fig. 44). However, more work focusing on the Precambrian of Andøya is needed before a reliable correlation of basement rocks can be made across Andfjorden.

1.3.4 Mesozoic rocks on Andøya

The Mesozoic succession on Andøya (Figs. 3, 4 & 5) is thought to be a relic portion of the Mid-Norwegian continental rift margin succession, which was deposited in the Paleozoic, Mesozoic and Cenozoic time periods (Brekke, 2000; Vajda & Wigforss-Lange, 2009). The sedimentary strata on Andøya was first detected by T. Dahl in 1867 (Ørvig, 1960) and is still the only known succession of Mesozoic sedimentary rocks onshore mainland Norway (Bøe et al., 2010). The presence of numerous coal layers led explorers to drill for coal in the last part of the 19th century and hydrocarbons in the 1970s (Bøe et al., 2010). Mesozoic rocks also occur in very near-shore positions in Andfjorden, Sortlandsundet between Langøya and Hinnøya and in Gavlfjorden between Andøya and Langøya (Davidsen et al., 2001; Fig. 2 this study) and in similar half-graben systems in fjords further south (Bøe et al., 2010). These rocks are interpreted to represent the remains of a much more extensive Jurassic-Cretaceous sedimentary succession that covered large parts of coastal Norway (Sturt et al., 1979; Bøe et al., 2010) prior to the Late Cenozoic to Quaternary uplift and erosion (Bøe et al., 2010).

The stratigraphy of the Mesozoic rocks in northeastern Andøya is shown in Figure 5. From the granitic basement there is a gradual transition into a thick interval of weathered granite/granitic gneiss overlain by an enigmatic sandy limestone (the Holen Formation) (Dalland, 1974, 1975, 1979, 1981). The Holen Formation consists of an up to 6 meters thick sandy limestone that has not been observed in outcrops, but is known from boreholes I, II and V (cf. Dalland, 1974; Dalland, 1981). Its age depends on the heavily disputed age of the deep weathering. K/Ar-dating of the weathering profile indicate that weathering occurred in the Paleozoic (Sturt et al., 1979), but it has also been correlated to Jurassic weathering profiles offshore (Smelror et al., 2001). The Holen Formation may thus represent either the

lowermost unit of the Mesozoic succession (Dalland 1974, Smelror et al. 2001) or the last remnants of a previously very thick Paleozoic sedimentary cover that was uplifted and eroded in the Triassic (Sturt et al., 1979; Dalland, 1981; Manum et al., 1991). It has also been suggested to belong to the basement rocks (Voct, 1905).

The total thickness of the *confirmed* Mesozoic succession is more than 500 meters, consisting of two major fining-upwards sequences: (i) A lower unit of Middle Jurassic (Bajocian/Bathonian-Ryazanian) non-marine sedimentary rocks that gradually grade into marine deposits, which again are truncated by an unconformity or a hiatus, and (ii) a lower Cretaceous fining upwards sequence grading from shallow to deep marine facies upwards in the stratigraphy (Dalland, 1974, 1975, 1979, 1981).

The lowermost Middle Jurassic Ramså Formation is about 100 meters thick and made up by the Hestberget Member (Figs. 13 & 14), consisting of braided river sands with interlayers of kaolin-rich shales representing outwash from the kaolin-rich weathered basement, the Kullgrøfta Member (Fig. 14) with lagoonal bituminous shales and the fluvial to beach and shallow-marine sandstones of the Bonteigen Member (Dalland, 1974, 1975, 1979, 1981). The overlying Dragneset Formation is up to 290 meters thick and divided into three members, grading from calcareous sandstone (Breisanden Member) in the lower part to siltstone and shale in the upper part (Taumhølet and Ratjønn members) (Dalland, 1974, 1975, 1979, 1981). The formation contains abundant marine fossils, including remains of Ichthyosaurs, bivalves, ammonites and belemnites (Ørving, 1960; Dalland, 1975). The youngest sedimentary rocks of the Dragneset Formation is of Upper Volgian or possibly Berriasian age, while the oldest in the overlying Nybrua Formation is dated to the Valanginian (Dalland, 1975), indicating an erosional or non-depositional hiatus of 20-30 Ma. The Nybrua Formation is a little less than 80 meters and forms a regionally extensive unit of shallow-marine marl and sandstone in the lower Cretaceous (Leira and Skjærmyrbekken members). Overlying this unit are intermediate- to deep marine mudstones of the at least 200 meters thick Skarstein Formation (Nordelva and Hellneset members), deposited from the Hauterivian to the Aptian (Dalland, 1974).

On a larger scale, the basin sequence is bounded by NNE-SSW striking faults that probably follow lines of weakness from e.g. older brittle faults of Late Paleozoic to Mesozoic age (Dalland, 1975). On the landward side, this basin succession is believed to be separated from the crystalline basement by the East Andøya Fault Zone (Løseth & Tveten, 1996; Henningsen & Tveten, 1998; Figs. 2 & 3 this work) but maps from new gravity data do not confirm the presence of such a fault, and rather indicate an onlap sequence on basement rocks to the west and south, along with further inland reaching sedimentary rocks (Brønner et al., 2008).

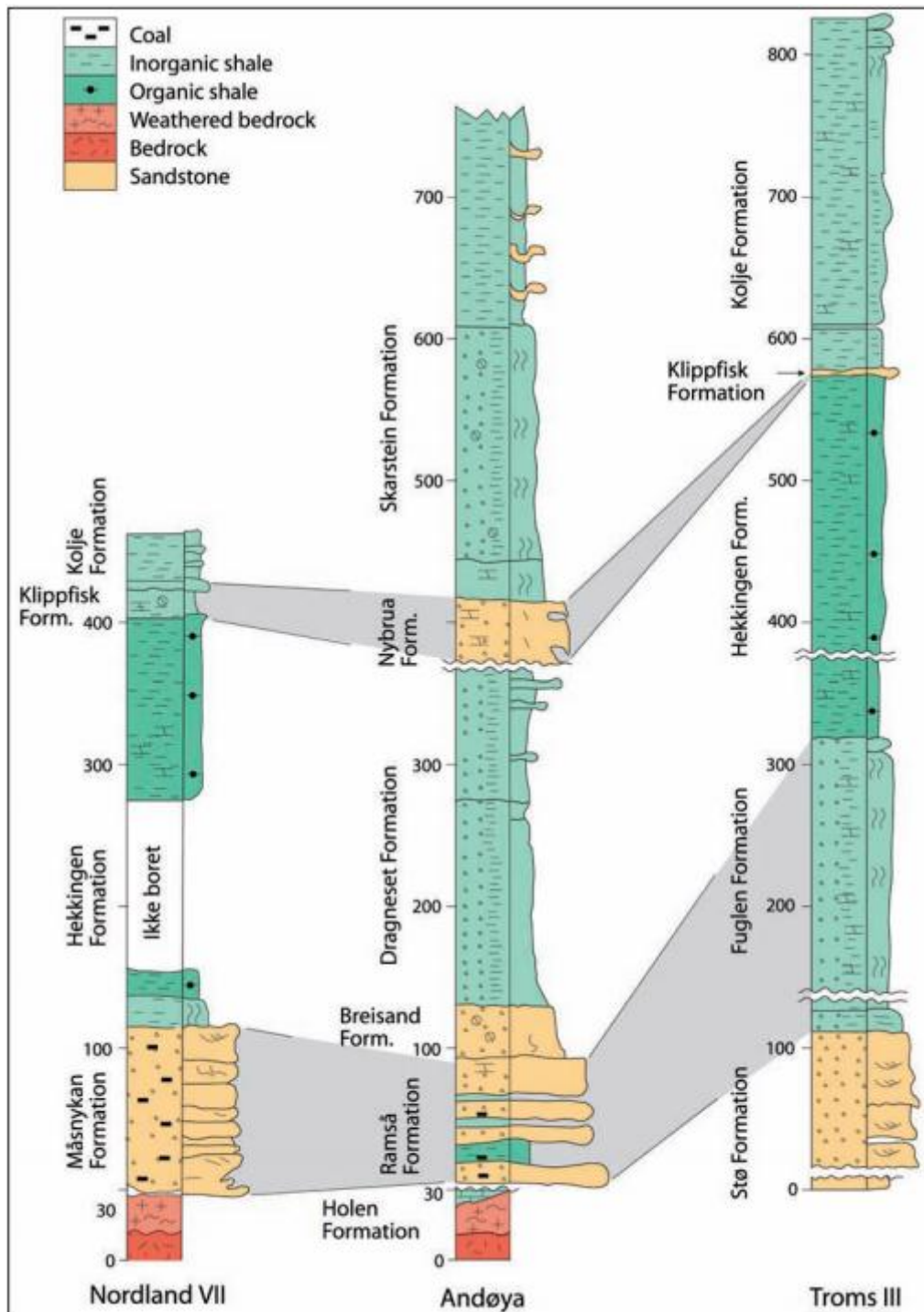


Figure 7 Lithostratigraphic and sequence stratigraphic correlation of cored successions in Nordland VII, Andøya and Troms III. Form Bøe et al. (2010), modified from Smelror et al. (2001).

A N-S trending well-correlation profile shows the internal structuring of the basin as it is interpreted by Rasmussen (1985) (Fig. 4). The sedimentary rocks are likely located in a half-graben to the south and another graben to the north, separated by a gabbroic basement horst (Figs. 3 & 4). The architecture and filling pattern is largely controlled by several normal faults dipping to the south and north (Dalland, 1981). While the contact between sedimentary

strata and crystalline basement rocks appears to be faulted in the north (Skarstein), possible onlap is indicated in the south (Ramså) (Fig. 4).

Little information has been published from the offshore Andfjorden basin (Fig. 2), but it is believed to be a downfaulted graben representing the continuation of the basin onshore and likely reflects the same tectonic and depositional events (Dalland 1981). It is bounded by the NNE-SSW striking Senja fault in the east (Zwaan & Grogan, 1998; Tsikalas et al., 2001; Hansen et al., 2012; Fig. 2 this study) and is believed to continue into the deep Harstad Basin to the north (Dalland, 1981; Henningsen & Tveten, 1998; Zwaan & Grogan, 1998). This is also supported by lithostratigraphic correlations between Nordland VII, Andøya and Troms III (Smelror et al., 2001; Bøe et al., 2010; Fig. 7 this study). There has not been published data of the kinematic history of the Andøya and Andfjorden basins, but is it likely that the kinematics reflect those depicted from nearby areas and the shelf as a whole (chapter 1.3.5). It is one of the aims of this study to develop a more detailed tectonic model, based on fieldwork, seismic data, DEM data and magnetic anomaly data, that explains the geometry and kinematics of faults bounding the Andfjorden basin offshore and onshore, as well as fault timing and spatial relationships to basin formation in the Andfjorden area (see chapter 4.5).

1.3.5 Post-Caledonian brittle faults: Rifting, extension and passive margin evolution

The more than 300 million years long post-Caledonian extensional history of the North Norwegian passive continental margin resulted in the deposition of large piles of sedimentary strata in fault-bounded basins, and the formation of numerous brittle faults and fractures (cf. Ziegler, 1989; Gabrielsen et al., 1990; Blystad et al., 1995; Larssen et al., 2002; Hansen et al., 2012) until the rifting culminated in the Early Cenozoic (Eocene) with break-up and ocean floor volcanism (cf. Doré et al., 1999; Faleide et al., 2008).

1.3.5.1 Basin-ridge architecture

Figures 1., 2. and 8. show the main structural elements (basins and ridges) of the Mid to North Norwegian offshore continental margin. From Lofoten to western Troms and Finnmark, the shelf is characterized by a series of NNE-SSW and NE-SW trending, partly curved basement ridges and basins bounded by dominantly extensional faults of variable orientation (cf. Blystad et al., 1995; Løseth & Tveten, 1996; Olesen et al., 1997; Bergh et al., 2007; Hansen et al., 2012). The main basement high is the Utrøst Ridge, which runs parallel to the Lofoten Ridge offshore (Figs. 1 & 2). Major basins include the Røst Basin on the seaward side of the shelf, the Ribban Basin on the central shelf, the Træna Basin to the southwest, the Vestfjorden Basin on the landward side (Mokhtari & Pegrum, 1992; Blystad et al., 1995) and the Harstad Basin north of Andøya (Figs. 1 & 2).

1.3.5.2 Basin-bounding faults and major onshore-offshore fault systems

Major basin-bounding faults adjacent to the Lofoten Ridge include the West Lofoten and East Lofoten Border Faults bounding the Lofoten Ridge (Løseth & Tveten, 1996; Bergh et al., 2007) the eastward dipping Pyramiden Fault that can be traced along strike for more than 80 km west of Langøya (Hansen et al., 2012) the Andøya Fault and the East Andøya Fault Zone, the Senja fault on the eastern edge of Andfjorden (Hansen et al., 2012), that may represent a continuation of the Troms Finnmark Fault Complex running parallel to the coastline of Troms and Finnmark (Indrevær et al., 2014), and bounding the eastern limit of the Harstad Basin (Gabrielsen et al., 1990) and the Vestfjorden-Vanna Fault Complex that runs from Vestfjorden to Vanna. The latter fault complex down drops the Caledonian nappes from the basement islands (Forslund, 1988; Opheim & Andresen, 1989; Olesen et al., 1997) - and largely mimics the zigzag/rhombic geometry of the offshore Troms-Finnmark Fault Complex (Fig. 1). However, while the Troms-Finnmark Fault Complex and most other faults off Lofoten and Vesterålen are characterized by a listric geometry and large-magnitude displacement/extension, a planar geometry is depicted for the Vestfjorden-Vanna Fault Complex (Indrevær et al., 2014).

A number of regional studies on the Lofoten-Troms margin have enabled characterization and linking of offshore basins, basin bounding fault systems and morphotectonic lineaments (Olesen et al., 1997; Tsikalas et al., 2001; Wilson et al., 2006; Bergh et al., 2007; Eig, 2008; Hansen et al., 2009; Osmundsen et al., 2010; Indrevær et al., 2014). Bergh et al. (2007) compiled a map of all the main onshore lineaments, including brittle faults and fractures, in the Lofoten-Vesterålen area (Fig. 8), and the authors proposed the existence of at least three genetically related lineaments striking: (i) NNE-SSW, (ii) ENE-WSW to E-W, and (iii) NW-SE, similar to the conclusions of Gabrielsen and Ramberg (1979) and Gabrielsen et al. (2002). Brittle faults in western Troms have not been studied as detailed as those in Lofoten and Vesterålen, but the same major fault-fracture sets have been observed here as well (Forslund, 1988; Gagama, 2005; Antonsdóttir, 2006; Thorstensen, 2011; Koehl, 2013; Indrevær et al., 2014).

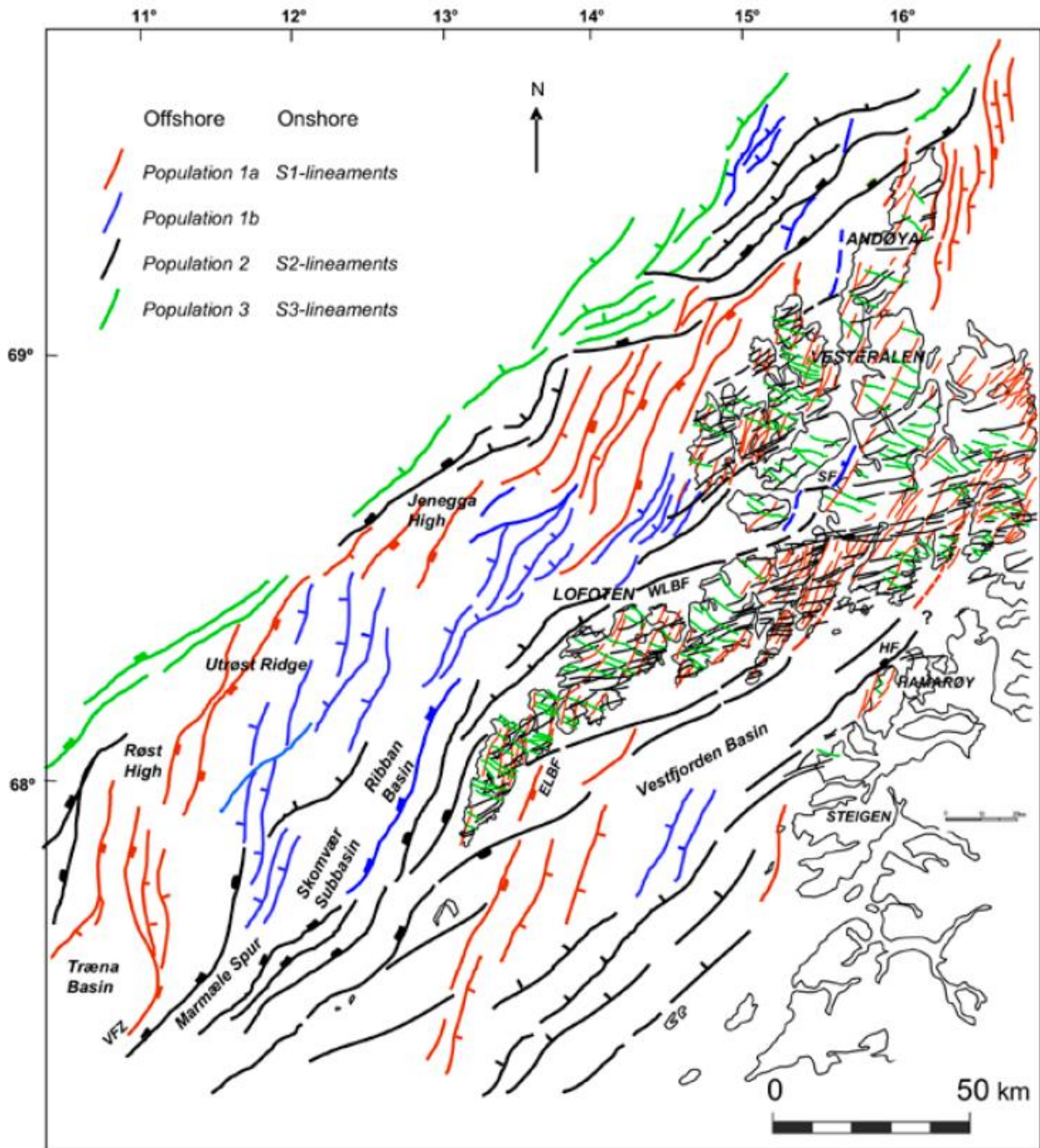


Figure 8 Regional composite map linking offshore and onshore faults-fractures patterns along the Lofoten-Vesterålen margin. From Bergh et al. (2007).

1.3.5.3 Sedimentary deposits

The offshore basins are all bounded by normal faults and filled with predominantly Lower to Upper Cretaceous sedimentary rocks that are locally near 7 km thick (Bergh et al., 2007). Jurassic units have a constant thickness or increase in thickness when approaching the Vesterålen islands. Since no pronounced boundary faults seem to separate the offshore basins from onshore areas this indicates that large parts, if not all, of the now exposed and denudated basement rocks onshore Vesterålen were covered by Middle and Upper Jurassic sedimentary sequences (Hansen et al., 2012). This is supported by the preserved Mesozoic

rift basin on Andøya ((Dalland, 1974, 1975, 1979, 1981) erratic blocks found in coastal areas (Fürsich & Thomsen, 2005), the presence of fault-bounded Mesozoic basins in shallow fjord areas in Vesterålen (Davidsen et al., 2001; Bøe et al., 2010), and inferred Mesozoic faults onshore (Sturt et al., 1979; Dalland, 1981; Bartley, 1982; Løseth & Tveten, 1996; Bergh et al., 2007). The Vesterålen margin thus resembles the western flank of a graben that probably covered the entire islands of Vesterålen (Hansen et al., 2012).

Pre-Cretaceous (possibly Permo-Jurassic) sedimentary strata have also been identified offshore, in the Træna Basin and the Vestfjorden Basin, and they were also inferred to lie beneath the Cretaceous sequence in the Harstad Basin, located at 5 s TWT or more on seismic data (Brekke & Riis, 1987). Paleozoic and Early-Mid Mesozoic sedimentary rocks are also known from the Loppa High and Finnmark Platform (Gabrielsen et al., 1990) as well as the Wandel Sea basin on North East Greenland (cf. Stemmerik et al., 1998), which, according to paleogeographic reconstructions, was located near this study area before the development of the transform Barents Sea margin in the Cenozoic (Mosar et al., 2002).

1.3.5.4 Fault timing

Timing of offshore fault activity can be indirectly dated from sedimentary successions in the basins (cf. Bergh et al., 2007). Mesozoic rifting on the Lofoten-Vesterålen Margin occurred during the Early Triassic, Mid/Late Jurassic (Bajocian to Volgian), Early Cretaceous (Valanginian to Albian) and latest Cretaceous to breakup (Campanian/Maastrichtian to Eocene) (Hansen et al., 2012). The timing of main fault activity in the Harstad Basin is more difficult to infer due to the quality of the seismic data and lack of geological information, but it seems that the main fault activity ceased at the Jurassic/Cretaceous boundary in south and in the Late Cretaceous further north (Brekke & Riis, 1987). The Harstad Basin is bordered to the east by the Troms-Finnmark Fault Complex, which is likely an old (Precambrian?) zone of weakness that has been reactivated several times until the Eocene (Gabrielsen et al., 1990). It has been proposed that extensional faulting (in the basin) started in the Mid Jurassic and continued during a period of major subsidence in the Early Cretaceous and that renewed normal faulting, combined with inversion along some major faults, took place in the Late Cretaceous (Gabrielsen et al., 1990). As there is little published literature from the area, fault activity in the offshore Andfjorden basin remains even more dubious. However, Late Jurassic - Early Cretaceous extension on the shelf has been correlated with contemporaneous faults on Andøya (Tsikalas et al., 2001).

Absolute dating of onshore brittle fault rocks in the area between Lofoten and Western Troms have been undertaken recently (Olesen et al., 1997; Hendriks, 2003; Davids et al., 2010; Hendriks et al., 2010; Stelthenpohl et al., 2011; Davids et al., 2012a; Davids et

al., 2012b; Davids et al., 2013). K-Ar illite ages ((Davids et al., 2010; 2012a; 2012b; 2013), apatite fission-track analysis (AFT; Hendriks (2003); Hendriks et al. (2010)) and $^{40}\text{Ar}/^{39}\text{Ar}$ K-feldspar data (Stelthenpohl et al., 2011) show a contrast in the timing of fault activity and exhumation between the Troms and Vesterålen regions. K-Ar illite data from fault gouges indicate that the onshore brittle faulting may have initiated as early as in the Devonian with faulting along both N-S and NE-SW trending faults on Andøya and farther inland in Central Troms (Davids et al., 2013). Carboniferous rifting events have been demonstrated in the Nordkapp Basin NE of Finnmark, which was simultaneous with the initiation of the offshore Troms-Finnmark Fault Complex that bounded the Hammerfest and Tromsø basins southward (Davids et al., 2013). While faulting continued at least into the Cretaceous and possibly into the Cenozoic (Hendriks, 2003; Hendriks et al., 2010), in the Lofoten-Vesterålen part of the margin, major faulting on the onshore Troms margin appears to have ceased after the Permian faulting event. Most of the post-Permian rifting in northern Norway must therefore have occurred either offshore west of Troms or further southwest onshore and offshore adjacent to the Lofoten-Vesterålen and Andøya basement horst (Davids et al., 2013).

On Andøya, Sturt et al. (1979) reported normal faults parallel to the East Andøya Fault Zone (trending NNE-SSW) in sedimentary rocks of Aptian age near Ramså. K-Ar dating of samples from semi-brittle/mylonitic fault zones in the weathering profile yields Late Cretaceous-Early Cenozoic ages, while Dalland (1981) also inferred movement to have occurred in the Middle Jurassic (Bajocian-Bathonian), Ryazanian and Turonian times. AFT ages from Andøya document the overall exhumation of the island to have occurred between 127 ± 11 Ma to 142 ± 14 Ma (Hendriks, 2003).

1.3.5.5 Basement control

The network of brittle faults that frame the Lofoten-Vesterålen and SW Barents Sea margins may to some extent have been controlled by ductile basement fabrics. Bergh et al. (2007) made a short comment on how steeper brittle faults merged into favorable foliation attitudes at Eggum, and (Hansen et al., 2009) supported the idea that ENE-WSW and NW-SE trending faults developed along inherited fabric from the basement rocks such as foliation, ductile shear zones (e.g. the NW-SE trending Senja Shear Belt), Caledonian thrusts and lithological boundaries. Indrevær et al. (2014) concluded that onshore brittle faults in western Troms formed close to, or along favorably oriented Precambrian and/or Caledonian structures, at least on a local scale, and that, on the larger scale, steep basement-seated Precambrian ductile shear zones, e.g. the NW-SE trending Senja Shear Belt and the Bothnian-Kvænangen Fault Complex, seem to have affected the NE-SW trending brittle fault

complexes by accommodating shifts in polarity and/or the stepping of fault segments along strike.

The Ribban, Træna and Vestfjorden basins have been interpreted to be situated above spoon-shaped depressions in the underlying basement developed during Late-Caledonian extension (Eig, 2008), and that Devonian extensional detachments were uplifted to form metamorphic core complexes on the Mid-Norwegian margin, including Lofoten, in the Permian (Eig, 2008; Stelthenpohl et al., 2011). These exhumed, basement-inherited depressions and highs likely became the template for younger faults and basins that developed along their flanks from the Late Paleozoic to Early Cenozoic (Eig, 2008).

1.3.5.6 Margin evolution

Various onshore-offshore tectonic and evolution models have been proposed to explain the formation of the different fault-fracture populations and their relationship to basins, including progressive successions, step-wise and/or synchronous events, e.g. due to shifts in regional strain fields in Mesozoic-Cenozoic times (Wilson et al., 2006; Bergh et al., 2007; Davids et al., 2010; Eig & Bergh, 2011; Hansen & Bergh, 2012; Hansen et al., 2012). From the indirect timing of sedimentary strata and faulting events in offshore basin, Eig (2008) believed the main fault patterns formed during three discrete tectonic events. The first took place in the Permian-Jurassic and was responsible for the development of the right-stepping *en echelon*, NNE-SSW trending faults due to WNW-ESE orthogonal extension. A shift in the extension direction from WNW-ESE to NNW-SSE was supposed to have occurred in the Mid/Late Jurassic-Early Cretaceous, in order to enable the development of the ENE-WSW striking faults. Hansen and Bergh (2012), however, argued for simultaneous formation of the ENE-WSW and NNE-SSW trending faults. The ENE-WSW striking faults potentially acted as sinistral strike-slip soft- and hard-linked transfer faults to the NNE-SSW striking faults, resulting in the zigzag pattern described by Bergh et al. (2007). The fault-segment linkage also caused the development of major boundary faults, establishing the Lofoten Ridge as a prominent structural element at this time (Hansen et al., 2012). Olesen et al. (1997) proposed the presence of NW-SE striking transfer zones to explain the change of polarity of offshore faults, as for example the Bivrost Lineament south of Lofoten and the Vesterålen transfer zone or the Lenvik transfer zone along Andfjorden in southwestern Troms. They also stated that the offshore continuation of these NW-SE striking lineaments were linked to oceanic transforms such as the Bivrost Fracture Zone for the Bivrost Lineament (Olesen et al., 1997). This hypothesis was later rejected by (Olesen et al., 2007) who attributed these offshore fracture zones to navigation errors. Finally, NW-SE trending transtensional fractures

formed during a third stage in the Late Cretaceous-Paleocene under NW-SE contraction and NE-SW extension, possibly due to ridge-push forces (Eig & Bergh, 2011).

By contrast, (Wilson et al., 2006) proposed a different model, where the margin would be segmented in distinct domains, each domain deforming differently with regard to an extension direction constantly oriented WNW-ESE. Plate reconstructions by Mosar et al. (2002) indicate that the regional extension direction changed from WNW-ESE to NW-SE during the Late Cretaceous, and the latest Cretaceous to Palaeogene oblique-normal to strike-slip fault zones are interpreted to reflect NW-SE directed extension (e.g. Bergh et al., 2007; Hansen et al., 2012).

The timing and nature of the uplift and exhumation of the basement ridges in Lofoten, Vesterålen, Andøya and western Troms is still much debated (cf. Olesen et al., 1997; Mosar et al., 2002; Eig, 2008; Hendriks et al., 2010; Osmundsen et al., 2010; Redfield & Osmundsen, 2013; Indrevær et al., 2014). Various causes of uplift have been proposed, e.g. rapid switches in the regional strain and stress fields (Bergh et al., 2007; Eig et al., 2008) stress perturbations within transfer zones (Eig & Bergh, 2011), passive margin exhumation due to NW-SE directed ridge push forces (cf. Grønlie et al., 1991; Doré et al., 2002; Gabrielsen et al., 2002; Mosar et al., 2002) and asthenospheric diapiric rise due to emplacement of the Iceland Plume and later climate deterioration with increased erosion (e.g. Rohrman & van der Beek, 1996; Nielsen et al., 2002; Pascal & Olesen, 2009). Recent work suggest that the nature of the uplift has been controlled by the hyper-extended character of the Norwegian passive margin (Osmundsen & Redfield, 2011; Redfield & Osmundsen, 2013). The contrast in geometry between the listric Troms-Finnmark Fault Complex and the planar Vestfjorden-Vanna Fault Complex, is believed to have resulted in the formation of a short tapered, hyper-extended margin after final break-up in the Paleocene/Eocene (c. 55 Ma), uplifting and exhuming the West Troms Basement Complex as a short-tapered margin due to unloading and crustal flexure with continued uplift and erosion to the present stage level (Indrevær et al., 2014).

1.4 Methods

1.4.1 Fieldwork

The onshore observations and interpretations made in this work are the result of fieldwork carried out in June, July and August 2013. It led to the identification of the main lithological boundaries and the mapping and description of brittle fractures on the islands of Andøya, Bjarkøya and Senja (Figs. 12, 15, 20, 30 & 41). The lithological units are from Dalland (1981), Henningsen and Tveten (1998) and (Zwaan & Grogan, 1998). The field localities on Andøya were chosen because of their exposures of Mesozoic sedimentary rocks, and were

thus vital to understanding fracture systems related to the formation of the sedimentary basins on land and in Andfjorden. Bjarkøya was chosen because it is situated in the central part of Andfjorden (just south of the boundary between Precambrian basement rocks and Mesozoic sedimentary rocks) (Figs. 2 & 9) and therefore possibly experienced faulting syntectonic to faults in the Andfjorden basin. The island also contains two quarries with excellent kinematic indicators on fault/fracture surfaces (Figs. 28, 34 & 35). Skrolsvik was visited as it lies a few kilometers east of the Senja fault (Figs. 1 & 2) thought to define the eastern limit of the Andfjorden basin. Another interesting factor, is the close vicinity to the major Stonglandseidet fault zone that is believed to continue out into Andfjorden (Zwaan & Grogan, 1998; Figs. 2 & 9 this study).

The resulting maps (Figs. 12, 15, 20, 30 & 41) show the rock type and lithological boundaries, structural orientation data (strike and dip), kinematic data (slickensides, sense of shear, offsets, duplexes, etc.) presented by photographs, sketches and interpreted drawings as well as in the form of stereoplots obtained via the Orient software. The structures were investigated in both traverses and along strike. In addition to the general maps of the localities, specific fault-fracture zones were chosen for more detailed geometric and kinematic analysis at Bjarkøya (chapter 2.4.2), Skrolsvik (chapter 2.5.2) and Senjehesten (chapter 2.5.3). Such fracture analysis can convey information on the tectonic stress field which was active at the time of fracture formation, and thus be used to infer the character of the ancient stress field and its variation through time (e.g. Dunne & Hancock, 1994; Mandl, 2005).

Relative timing for the different fault-fracture patterns has been deduced from the field observations using criteria of crosscutting relations. As the network of brittle faults in Lofoten-Vesterålen and the SW Barents Sea margins may to some extent have been controlled by ductile basement fabrics (e.g. Bergh et al., 2007; Eig et al., 2008; Hansen et al., 2009; Koehl, 2013; Indrevær et al., 2014) orientation measurements of ductile gneiss foliations were recorded at each locality in order to see if the orientation coincides with that of the brittle fractures.

1.4.2 Digital Elevation Models (DEM) – topography and bathymetry data

In recent years, high-resolution topographic and bathymetric data (MAREANO) have become an important tool for lineament analysis fault trace mapping (Bergh et al., 2008; Osmundsen et al., 2010; Roberts et al., 2011; Indrevær et al., 2014).

A clear relationship between the distribution of alpine topography and Late Cretaceous-Cenozoic and recent fault patterns and rejuvenation in Norway has been well documented (Osmundsen et al., 2010). 3D satellite images (DEM) and photo analysis (e.g. Virtual Globe from www.norgei3d.no, www.norgeskart.no) were thus used to locate and map structurally

controlled lineaments, scarps, depressions, uplifts, terraces and lithological boundaries in the landscape on Andøya, Senja and Bjarkøya. To validate these interpretations, some of these localities were later visited for detailed field work (see chapters 2.3, 2.4 & 2.5)

Bathymetry data from the MAREANO project were used to identify and separate brittle structures from glacial lineations in the Andfjord and to study the transition from land to shallow shelf. Bathymetry must be used with caution, and only together with other data such as field observations, magnetic anomaly data and seismic data (see chapters 3.2 & 3.3) to avoid misinterpretations. However, used correctly, bathymetry data is one of the best tools to bridge the gap between geological data collected onshore and seismic data offshore.

1.4.3 Seismic data

The seismic data used in this investigation consists of conventional 2D sections collected by NPD, WesternGeco and Norsk Hydro. The most important seismic sections chosen for this study are LO88R0711, LO88R0713 and LO88R0752 (Fig. 45) collected by Norsk Hydro in Andfjorden in 1988 and reprocessed by StatoilHydro in 2007.

The basic technique of seismic surveying involves mapping geological structure by creating seismic waves with artificial sources and observing the arrival time of the waves reflected from interfaces (seismic reflections) in the rocks, called seismic reflectors (Andreassen, 2009). Four major groups of systematic reflections are distinguished on seismic sections (Veeken, 2007):

- Sedimentary reflections representing bedding planes
- Unconformities or discontinuities in the geological record
- Artefacts; like diffractions, multiples, etc.
- Non-sedimentary reflections; like fault planes, fluid contacts etc.

Seismic exploration is the best tool to render a graphic representation of the geological structure of the Earth's subsurface (Andreassen, 2009). However, although seismic sections can bear striking resemblance to geological cross-sections, limitations in the horizontal and vertical resolution of the data in addition to artefacts of the method (e.g. random noise generated by other boats, waves, fish, shoals, wrecks etc., multiples or velocity distortions), can make it difficult to make a simple and direct link between geology and seismic sections (Badley, 1985). To attain the best result, it is thus very important that all phenomena unrelated to geology are recognized and disregarded in an interpretation.

The offshore Troms 2 and Andfjorden areas are structurally complex areas (cf. Brekke & Riis, 1987; Kløvjan, 1988; Indrevær et al., 2014), and diffractions from faults as well

as velocity anomalies across faults are expected. Due to such velocity anomalies, even perfectly processed time sections are not always ideal for structural interpretations (Badley 1985). Seafloor multiples are also common, occasionally masking primary structures. This is especially problematic in areas of very poor signal-to-noise ratio, e.g. the northern part of seismic section LO88R0713 (Fig. 47). Along with random noise, these distortions give the seismic sections in Andfjorden a generally poor to medium signal-to-noise ratio.

1.4.4 Magnetic anomaly data

Magnetic susceptibility is an important property of the lithosphere that depends on the concentration of *ferro-* and/or *ferrimagnetic* minerals in the bedrock (cf. Reynolds, 1997). In fact, the mixed iron oxides of iron and titanium (Fe and Ti) and one sulphide mineral, pyrrhotite, display significant magnetic properties, and in comparison to magnetite, even the susceptibility of the other Fe-Ti oxides is very small (Reeves, 2005). Consequently, magnetite and pyrrhotite are by far the most important minerals in aeromagnetic mapping.

The comprehensive review by Clark and Emmerson (1991) shows a wide range of magnetic susceptibilities in rocks, but in general it follows that sedimentary rocks often possess little significant susceptibility and that the major proportion of the magnetic signal is generated at crystalline (igneous or metamorphic) basement level (Reynolds, 1997). Faults and fracture zones are commonly displayed as linear negative magnetic anomalies that are caused by hydration and oxidation of magnetite to e.g. hematite (Henkel & Guzman, 1977). For the same reason, areas of deep weathering are also often displayed as negative anomalies in aeromagnetic surveys (Henkel & Guzman, 1977; Reeves, 2005).

In this work, magnetic anomaly data from the Geological Survey of Norway (NGU) have been used to map brittle faults and tectonic lineaments in the onshore and offshore areas surrounding Andøya (Fig. 44). Magnetic anomaly data has been extensively used along the Lofoten-Vesterålen and SW Barents Sea margins, and has proven to be a useful tool in determining basement depth and structure (e.g. Olesen et al., 1997; Gernigon & Brønner, 2012) as well as onshore-offshore fault correlation (e.g. Hansen et al., 2012; Indrevær et al., 2014).

As a concluding remark, it should be noted that magnetic models are non-unique, i.e. many earth models can produce the same magnetic response (cf. Reynolds, 1997; Reeves, 2005). However, by using several independent sources of information, the virtual endless possibilities can be limited to a very small number of geologically reasonable models (Reeves, 2005). In this thesis, magnetic anomaly data are used together with geological maps, seismic data, bathymetric and topographic data, and detailed field work at key localities.

1.5 Definitions

This section provides an introduction to the terminology (presented in alphabetic order) used in the thesis. It is important to avoid ambiguity on some geological terms that have been defined differently by several authors.

Table 2 Definitions of some geological and structural terms used in this work

Term	Description
Accommodation zone	Area of deformation that transfers strain or displacement between two overlapping faults that need not to have been active at the same time (Colletta et al., 1988; Peacock et al., 2000).
Antithetic fault	Minor fault that has a similar orientation but opposite dip to a related major fault; also used to describe two related faults with opposite shear senses (Gibbs, 1984).
Cataclastic rock	Mainly chaotic fault rock that developed with cohesion, which is generated by mainly frictional flow (Braathen et al., 2004).
Conjugate faults	Two intersecting faults that formed under the same stress field. Such faults show opposite sense of shear and make 30° to σ_1 (Fossen, 2010).
Core zone	Area accommodating most of the displacement in a fault zone (Caine et al., 1996).
Damage zone	Area of fracturing around and mechanically related to a fault (McGrath & Davison, 1995).
Detachment	Low-angle or horizontal fault/shear zone separating a hanging wall from a footwall. Detachments are typically reactivated weak layers or structures (Fossen, 2010)
Dextral	Right-lateral, moving right relative to a point of reference (Fossen, 2010).
Extensional duplex	Duplex forming along an extensional fault, where individual riders are separated by extensional faults and bound by a roof fault and a floor fault (Fossen 2010).
Fault breccia	Mainly chaotic, noncohesive fault rock generated by fractional flow (Braathen et al. 2004).
Fault gouge	Fine-grained and clay-rich non-cohesive rock located in the core to faults, formed by crushing and chemical alteration of the rock (Fossen, 2010).

Fault rocks	Commonly formed through strain concentration within a tabular or planar zone that experiences shear stress (Braathen et al., 2004).
Growth fault	A shallow normal fault that has moved during deposition of sediments on the hanging-wall side. The hanging-wall strata thicken toward the fault and may also be more coarse-grained close to the fault. The fault displacement increases downwards as fault dip decreases (Fossen, 2010).
Horse	In extensional duplexes, fault-bounded block located between low-angle normal faults (Root, 1990).
Lineaments	Lineaments are topographic/bathymetric alignments that are visible on remote-sensing images (e.g. air photographs, satellite images, DEM models) or on topographic/bathymetric maps (Goldstein & Marshak, 1988).
Listric fault	Spoon-shaped faults that are downward flattening (Fossen, 2010).
Mylonite	Fault rock with distinct mineral fabric, dominated by plastic flow (Braathen et al., 2004).
Pure shear	Plain strain coaxial deformation where particles move symmetrically around the principal axes of the strain ellipse in the XY-plane (Fossen, 2010).
Relay ramp	Folded area in a relay formed by flexing of layers between fault tips. Usually for sub-horizontal layers that are given a ramp-like geometry in the overlap zone. The folding is due to strain transfer between the two faults (Fossen, 2010).
Riedel shears	Sets of subsidiary slip surfaces arranged en echelon (stepwise), each Riedel or R-shear being oblique to the zone or main slip surface. An antithetic set (R') also occurs, although less commonly than R-shears (Fossen, 2010).
Roll-over	The fold structure defined by the steepening of otherwise horizontal hanging-wall layers toward a normal fault. Normally related to a listric fault (Fossen, 2010).
Sinistral	Left-lateral, moving left relative to a point of reference (Fossen, 2010).
Simple shear	Non-coaxial plane strain deformation where particles move along straight lines (Fossen, 2010).
Slickenside	Polished fault surface that can be used to determine movement direction and shear sense along a fault zone (Passchier & Trouw, 2005).

Strike-slip duplex	Imbricate fault arrays develop along a sub-vertical, mostly strike-slip major fault defining a straight-bend geometry (Woodcock & Fischer, 1986)
Synthetic fault	Minor fault that has a similar orientation and the same displacement sense as a related major fault; also referring to two related faults having the same shear senses (Gibbs, 1984).
Transfer fault	Fault that links, is at a high angle to, and that transfer displacement between two normal faults (Gibbs, 1984). May be either hard-linked (fault surfaces joined) or soft-linked (fault surfaces are isolated, but linked by ductile strain of the rock volume between them) (Trudgill & Cartwright, 1994).
Transfer zone	Area of deformation and bed rotation between two normal faults that overstep in map view and that were active at the same time (Morley, 1995).

2 Description of onshore brittle faults and fractures

2.1 Introduction

The islands of Andøya, Bjarkøya and Senja (Figs. 2 & 9) display brittle fractures with varying attitudes and cross-cutting relationships, and are part of a major N-S to NE-SW striking fracture and topographic lineament pattern distributed throughout Lofoten, Vesterålen and western Troms and Finnmark (see chapter 1.3.5.). This tectonic pattern is well obtained from satellite and DEM images (Fig. 9) and the various lineament trends can be identified and addressed further, as a basis for more detailed investigations. Selected outcrops were chosen for more detailed structural analysis (Figs. 9, 11, 24, 36). In outcrops, the brittle faults and fracture sets were analyzed and when possible, the kinematics and timing relationships sorted out. Although numerous *slickensides* were found on fresh fracture surfaces in quarries on Andøya (chapter 2.3.4), Senja (chapter 2.5.2; Fig. 39) and especially Bjarkøya (chapters 2.4.1 & 2.4.3; Figs 33 & 34) there is a general absence of direct kinematic indicators on faults in shore localities of the study area. As most of the localities are situated close to larger fault zones with significant offset, it is expected that there have been some movement along the fracture surfaces but, given the vicinity to the sea, it is possible that most of the kinematic indicators were later removed by waves.

The purpose of this field work was twofold: *Firstly*, to investigate various aspects of the fracture groups, the geometry and nature of interaction, possible mechanisms of initiation and propagation, and their relationship to the local and regional strain-stress field through time, as well as the sedimentary basins on Andøya and in Andfjorden and regional fault systems like the Troms-Finnmark- and the Vestfjorden-Vanna fault complexes. *Secondly*, to discuss the possible relationships/links and implications of these fractures in terms of (locally) the opening and development of the Andfjorden and Ramså basins and (regionally) to the development of the North Atlantic passive margin.

The description of the brittle structures will be organized systematically, starting with the large scale characteristics obtained from DEM satellite images (Norgei3d) of the locality followed by a description of the brittle fractures and kinematic indicators (if present). A short mention of pre-existing ductile fabrics and their (possible) relation to the brittle structures will then be followed by a summary and a preliminary interpretation of the structures observed at the locality. The interpretations will, along with DEM, seismic and magnetic data, form the basis for kinematic and dynamic analysis in chapter 4.

2.2 DEM images

DEM data and aerial/satellite photos (Norgei3D) were studied prior to the fieldwork in order to identify regional lineament trends and localities with good bedrock exposures that could be

visited during the fieldwork. During this investigation, three major sets of lineaments were identified (Fig. 9). The *first* set is oriented NNE-SSW parallel to fjords and sounds such as Andfjorden, Gofjorden, Gullsfjorden and Risøysundet (Figs. 2 & 9). The lineaments are dominantly straight and show left- or right-stepping and relay geometry where the individual lineaments die out. Curved traces are also common, and NE-SW striking lineaments are observed to rotate clockwise and bend into parallelism with the ca. E-W striking ones. A second form of curvature is observed on the northeastern side of Andøya, where the NNE-SSW striking lineaments appear to bend sharply towards the east. The length of the individual segments is highly variable, from several kilometers to only a few.

The *second* lineament set strikes ENE-WSW, parallel to fjords such as Astafjorden and Solbergfjorden (Figs. 2 & 9). Whereas this set is well developed on Senja and on the islands in Andfjorden, it is much less prominent on Andøya (Fig. 9). Interference between the first two sets of lineaments produce the rhombic pattern known from brittle faults along the whole northern Norwegian continental margin (Gabrielsen et al., 2002; Bergh et al., 2007; Hansen et al., 2012; Indrevær et al., 2014), including the sedimentary basins in Andfjorden, Gavlfjorden and Sortlandsundet (Davidsen et al., 2001; Fürsich & Thomsen, 2005; Fig. 2 this work). The *third*, and least prominent set of lineaments, is NW-SE to WNW-ESE striking. It can be observed on Andøya, as well as Senja and the Andfjorden islands, and generally abut and/or cross-cut the other lineaments (Fig. 9)

Asymmetric landscapes in Lofoten and Vesterålen have been attributed to normal faults (Osmundsen et al., 2010), and a brief investigation of the topography of northern Andøya was performed to see if this too could be tectonically controlled. The landscape on Andøya is very characteristic, and can roughly be divided into three mountainous regions separated by large areas of almost flat terrain covered by peat (Fig. 10 a). Fieldwork was conducted in the north-eastern part of the island. This portion is very flat and covered by peat, except for narrow bedrock exposures along the coastline. The character of the landscape changes dramatically westwards, as the north-western part of the island is defined by a series of cirques. The back walls of these cirques rise nearly vertical to 400 meters plus, giving the northern island a characteristic, asymmetric topography (Fig. 10 b), that potentially can be related to faulting.

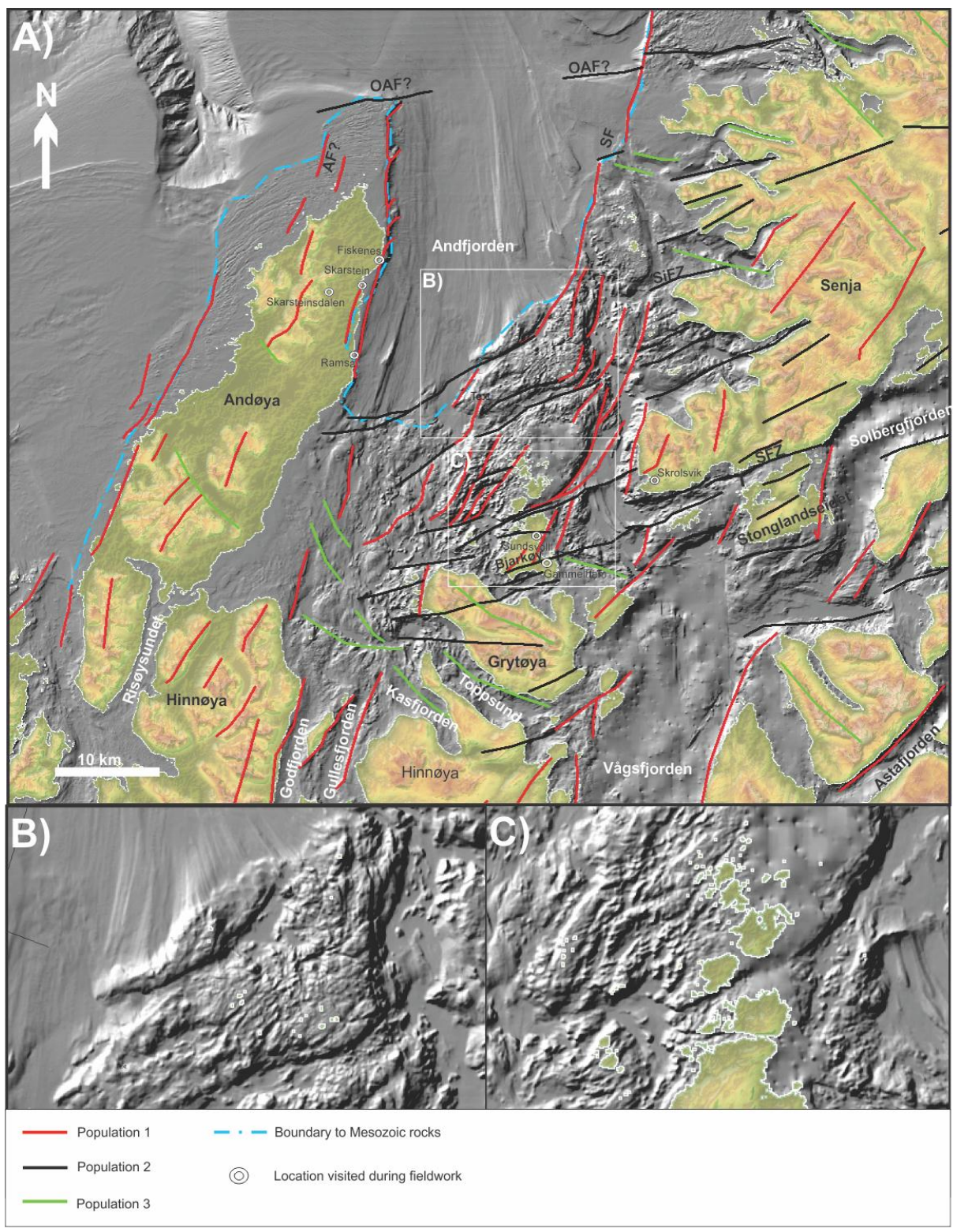


Figure 9 A) Topographic and bathymetric map (DEM data) of the study area. Tectonic lineaments are interpreted onshore and offshore, and can roughly be divided into three groups. B) and C) Detailed images illustrating how NNE-SSW striking lineaments seemingly bend into parallelism with ENE-WSW striking lineaments, creating rhombic to lense-shaped blocks. See Table 1 for abbreviations.

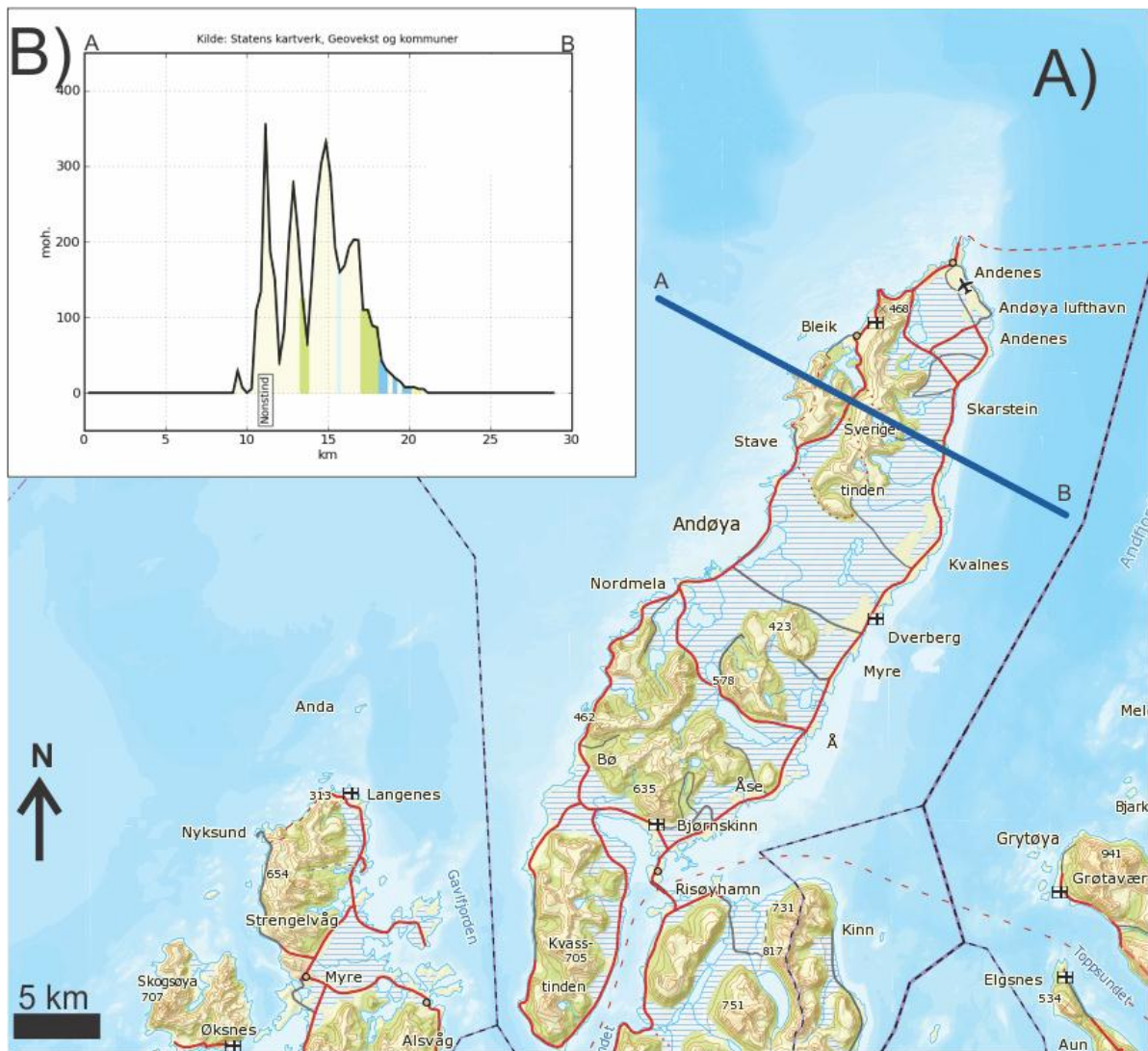


Figure 10 A) Topographic map of Andøya illustrating how the island can be divided into three mountainous regions separated by large, flat-lying areas. B) ENE-WSW oriented cross-section illustrating northern Andøya's asymmetric character towards the southeast. See A) for location.

2.3 Andøya

2.3.1 Ramså

2.3.1.1 Field relations and host rock characteristics

Ramså is located on the north-eastern shore of Andøya (Fig. 11 a). The sedimentary basin between Ramså and Skarstein on Andøya is the only known Mesozoic basin onshore Norway (chapter 1.3.4). Between the exposures and towards the sea, granitic gneisses and amphibolitic gneiss intercalations are the dominant bedrocks of the area. (Fig. 3 & 12). North of the river mouth, the Jurassic Hestberget Formation is exposed as benches of coarse grained sandstone with layers striking NE-SW and dipping gently to the northwest (Fig. 13). In the Ramså River there are several exposures of fractures and/ or faulted sand- and siltstone units with thin interlayers of coal (Fig. 14), belonging to the Hestberget and Kullgrøfta members of the Ramså Formation (Fig. 5).

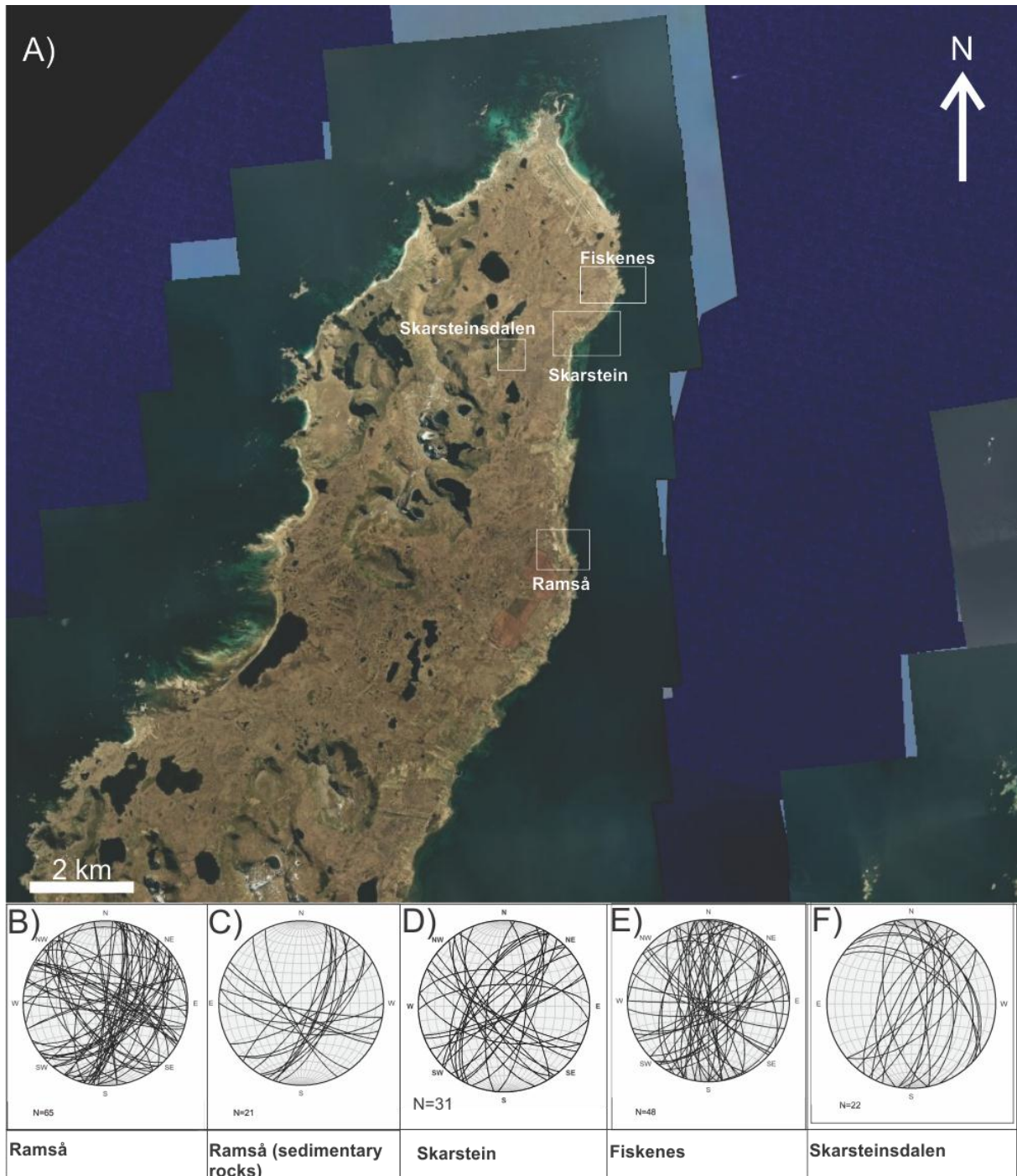


Figure 11 A) Aerial photo of northern Andøya showing areas visited during the fieldwork. B) - F) Lower-hemisphere Schmidt stereonets displaying fracture orientation data from the field localities on Andøya.

The sedimentary rocks are locally well-bedded and the strata on average dip gently to the northwest (Fig. 4, 5 & 13) (Dalland, 1974, 1975, 1979, 1981). The rocks locally contain internal fractures with a dominating NE-SW strike and subvertical dip to the southeast, but minor NW-SE trending, steep fractures are also common (Fig. 12).

The south side of the river mouth is characterized a red granite (the Andøy Granite), rich in kalifeldspar, with a weakly developed foliation (Fig. 12). Mafic intrusions are common,

and the contacts between the two lithologies are parallel with the fracture directions (NNE-SSW to NE-SW).

The contact between the Mesozoic rocks and the basement granite is not exposed, but the sedimentary rocks appear to lap conformably onto the basement gneisses (Fig. 4). Alternatively, the contact may be tectonic.

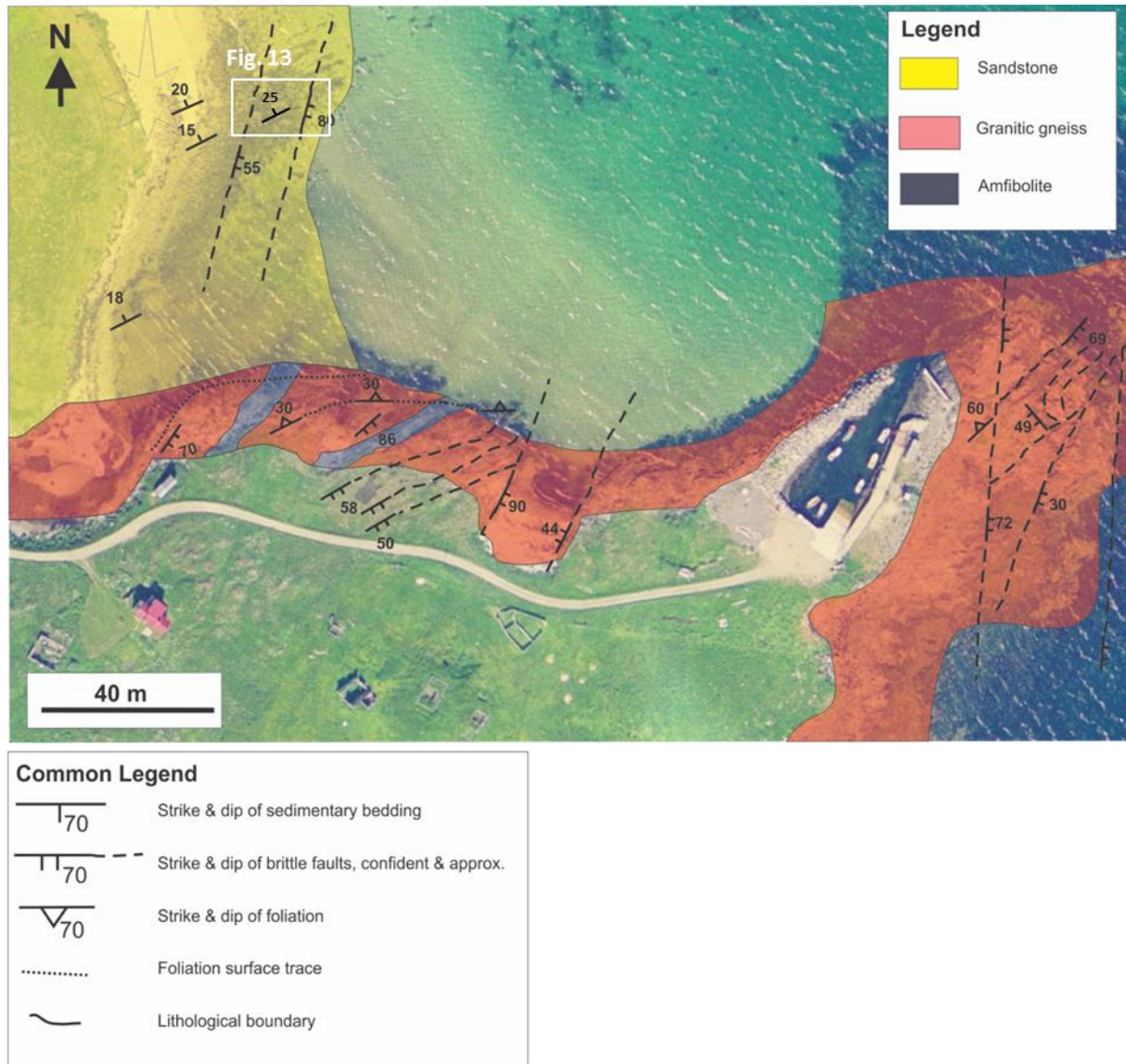


Figure 12 Structural and lithological map of the Ramså area, showing the outcrops of Mesozoic sandstones along with Precambrian gneisses with intercalations with amphibolite.

2.3.1.2 Description of brittle fractures and associated structures in the sedimentary strata and adjacent gneisses at Ramså

The brittle fractures observed in the Mesozoic sedimentary strata and adjacent gneisses at Ramså display variable strike directions, with a preference of NNE-SSW to NE-SW striking surfaces and dips towards the east to southeast (Fig. 12). Steep NW-SE striking fractures are however also present, especially in the granite south of the pier. When comparing stereonet plots of fractures in the sedimentary rocks to the fracture trends in the crystalline

bedrock, it becomes evident that the ratio between the fracture orientations is similar (Figs. 11 b & c). Strictly N-S striking fractures are however not observed in the sedimentary rocks, but they become increasingly abundant in the surrounding basement rocks farther south. NW-SE striking fractures are also significantly more common in the basement rocks, while WNW-ESE striking fractures are better evolved in the sedimentary rocks.



Figure 13 Benches of sandstone (*Hestberget member, Ramså Fm*) outcropping in the intra tidal zone at Ramså.

2.3.1.3 Description of kinematic data

No slickensided fracture surfaces were observed in the sedimentary rocks or the basement rocks located within or in the vicinity of the intra-tidal zone. Slickensides do however occur in the coal layers further up the river, but the layers were too thin for reliable measurements to be made.

2.3.1.4 Pre-existing fabrics along the fault zone

The granitic gneisses and amphibolitic gneiss intercalations have a weakly developed foliation that generally strikes E-W to NE-SW with dips to the north or northwest (Fig. 12). Fractures apparently cut through the foliation, but also run parallel to it south of the pier (Fig. 12).

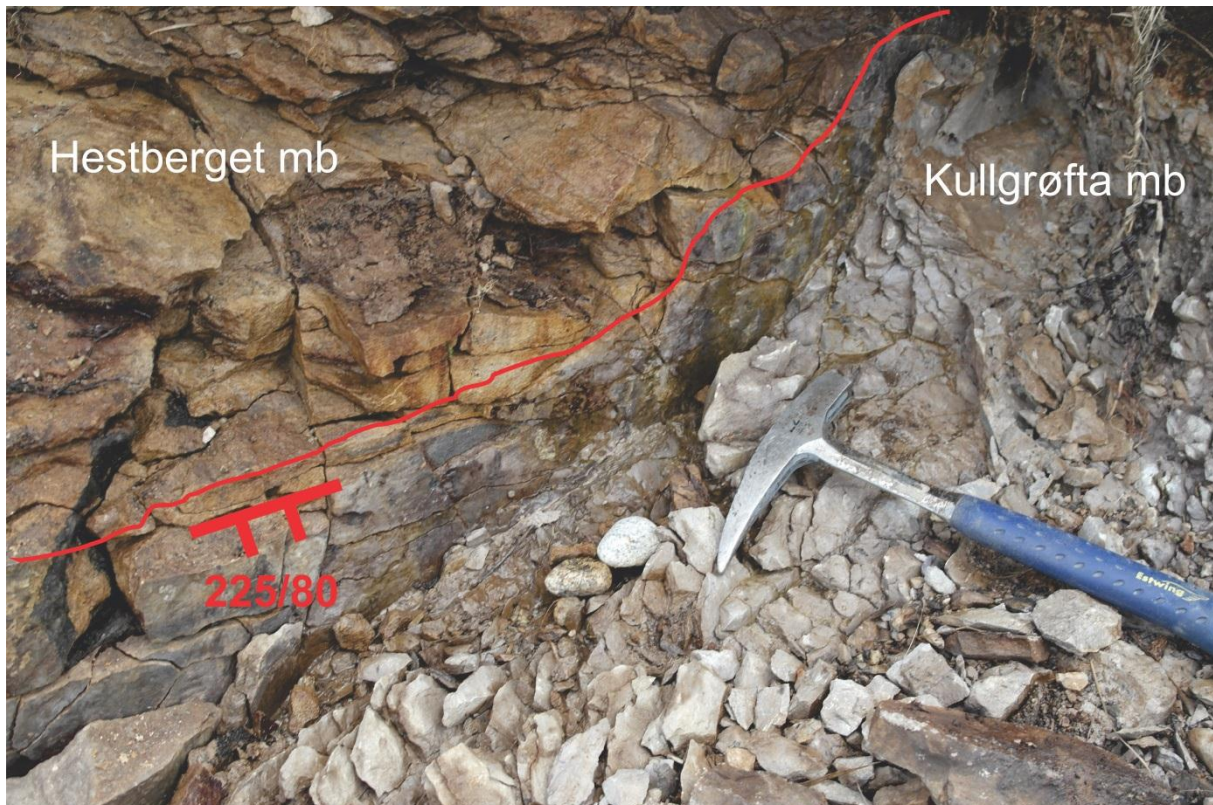


Figure 14 Small NE-SW striking fault (red line) in the Hestberget and Kullgrøfta members of the Ramså Formation upstream the Ramså river.

2.3.1.5 Summary and preliminary interpretations

The lithology at Ramså consists of Precambrian granitic gneisses, amphibolitic gneiss intercalations and Jurassic sand- and siltstones with abundant coal stringers (Figs. 12, 13 & 14). Sedimentary rock exposures are few, and most of the sedimentary strata is covered by vegetation and/or Quaternary sediments (Figs. 11 & 12). Consequently, the contact between gneisses and sedimentary strata is not exposed, making it difficult to determine its nature (tectonic or depositional). If the contact is tectonic, i.e. a large normal fault dipping to the north, a significant increase in fracture intensity would be expected towards the contact, but this is not observed. However, the sedimentary rocks dip gently to the northwest (Figs. 12 & 13), away from the contact, and may rather support an onlap relationship, as is also the most likely interpretation of potential field modelling (Fig. 4).

The ratio of fracture trends in the sedimentary rocks exposed at Ramså largely overlap with fractures in the crystalline basement rocks, displaying in general NE-SE to NNE-SSW and WNW-SSE to NW-SE trends (Figs. 11 b & c). The sedimentary rocks exposed at Ramså are of Bathonian to Kimmeridgian age (166.1 - 157.3 Ma, Mid-Late Jurassic) and although they cannot yield a definite age constraint to fracture formation, they certainly prove that later rift phases known from the continental margin (Late Jurassic/Early Cretaceous or Late Cretaceous/Early Cenozoic) produced NE-SW to NNE-SSW and WNW-ESE striking fractures and faults. This is supported by several studies onshore and offshore along the

margin from Lofoten to Finnmark, e.g. Gabrielsen et al. (1990), Løseth and Tveten (1996), Olesen et al. (1997), Tsikalas et al. (2001), Roberts and Lippard (2005), Bergh et al. (2007); Hansen et al. (2012); Davids et al. (2013); Indrevær et al. (2014), but especially by Sturt et al. (1979) who dated NNE-SSW striking faults in the sedimentary rocks at Ramså to the Aptian (125 - 112 Ma, Early Cretaceous).

Kinematic indicators such as fibers and/or slickensides were likely common on fault surfaces, but these have most likely been removed by erosive processes like wave action.

Locally, the ductile foliation is parallel to brittle fractures (Fig. 12), and may in these circumstances have been favorably oriented for reactivation as brittle fractures. However, on the large scale, pre-existing basement fabrics does not seem to have controlled the location and/or orientation of brittle faults and fractures - and thus the initiation of the sedimentary basin - at Ramså.

2.3.2 Skarstein

2.3.2.1 Field relations and host rock characteristics

The Skarstein village is located just north of the presumed boundary zone for the onshore Mesozoic rocks (Figs. 3, 11 & 15), however, Mesozoic rocks in the area are commonly found as erratic blocks with a large abundance of marine fossils (Fig. 16). The northernmost boundary between the sedimentary rocks and the crystalline basement is characterized by an NE-SW to E-W striking fault dipping moderately to the south (Dalland, 1974; Figs. 3 & 4 this work) (Dalland, 1974, Fig. 3 this work), but the boundary was not observed during the fieldwork.

The shoreline in the Skarstein area runs parallel to the basin bounding N-S to NNE-SSW striking fault in the fjord. The rocks in the Skarstein area are granitic gneisses and amphibolites with steep, NW-SE trending foliation and NE-SW striking brittle fractures. The fractures locally display matrix supported cataclastic fault rocks present in unfoliated red granite (the Andøya Granite) (Figs. 15,17 & 18). The dominating fractures are NNE-SSW to NE-SW, and thus semi-parallel to the major fault in the fjord (Figs. 2, 3 & 15), and are characterized by hematite precipitation (Fig. 19) on the fracture surfaces. The trends of the fractures are overall, oblique or truncating relative to the main gneiss foliation of the area.

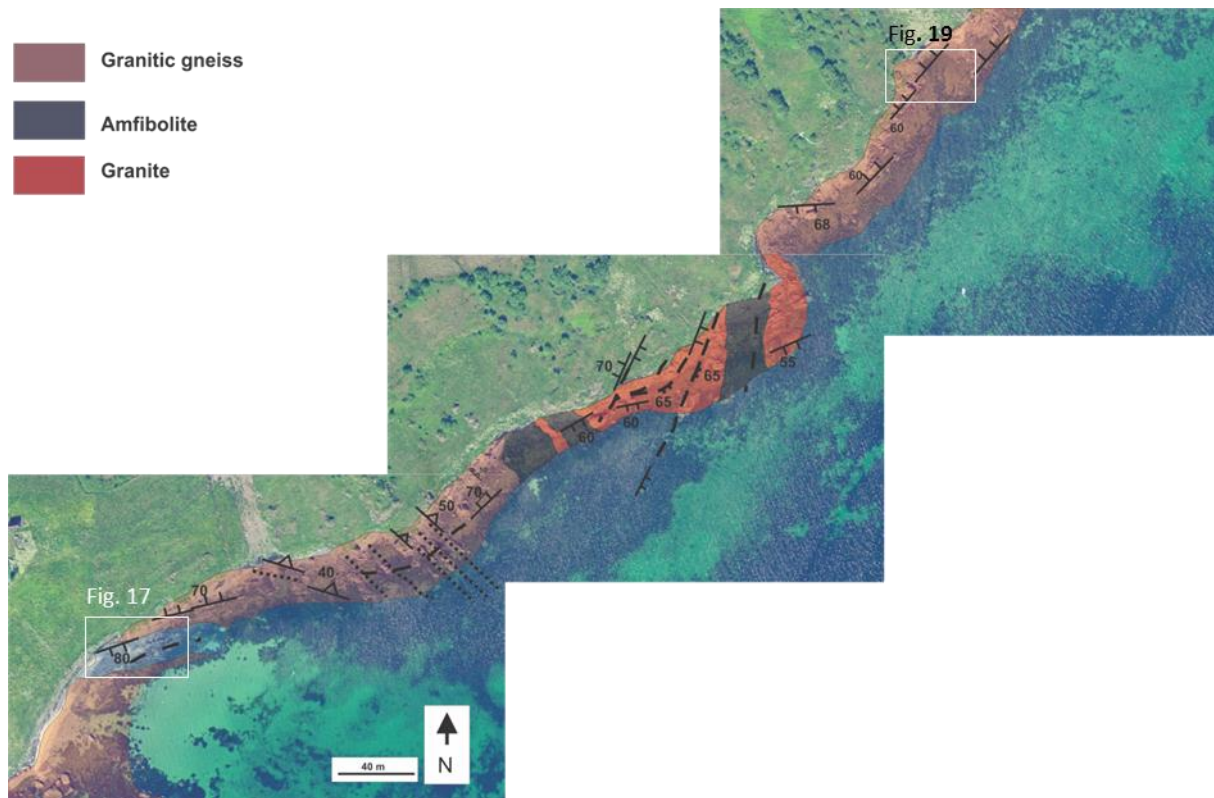


Figure 15 Structural and lithological map of Skarstein. The lithology consists of granitic gneiss and unfoliated granite with intrusions of amphibolite. NE-SW striking cataclasites are the most prominent structural features. For structural legend, see Common legend in Figure 12.

2.3.2.2 Description of brittle fractures in basement rocks

The fractures observed along the shore northwards from Skarstein towards Fiskenes (Fig. 15) display great variations in attitude and dip. In the south, NW-SE striking fractures are the most conspicuous, and they are mostly sub-parallel with the foliation of the basement gneisses (Fig. 15). On a larger scale, however, NNE-SSW to NE-SW striking fractures seem to be the most dominating (Figs. 11 c & 15). The fractures generally seem to be steeply dipping, but fractures trending E-W to WNW-ESE appear to dip more gently, and mainly to the north. Merging and cross-cutting relationships are complex in map-view, and a clockwise rotation of NE-SE striking fractures into NNE-SSE striking fractures are observed, merging into parallelism with the ENE-WSW striking fractures (Fig. 15).

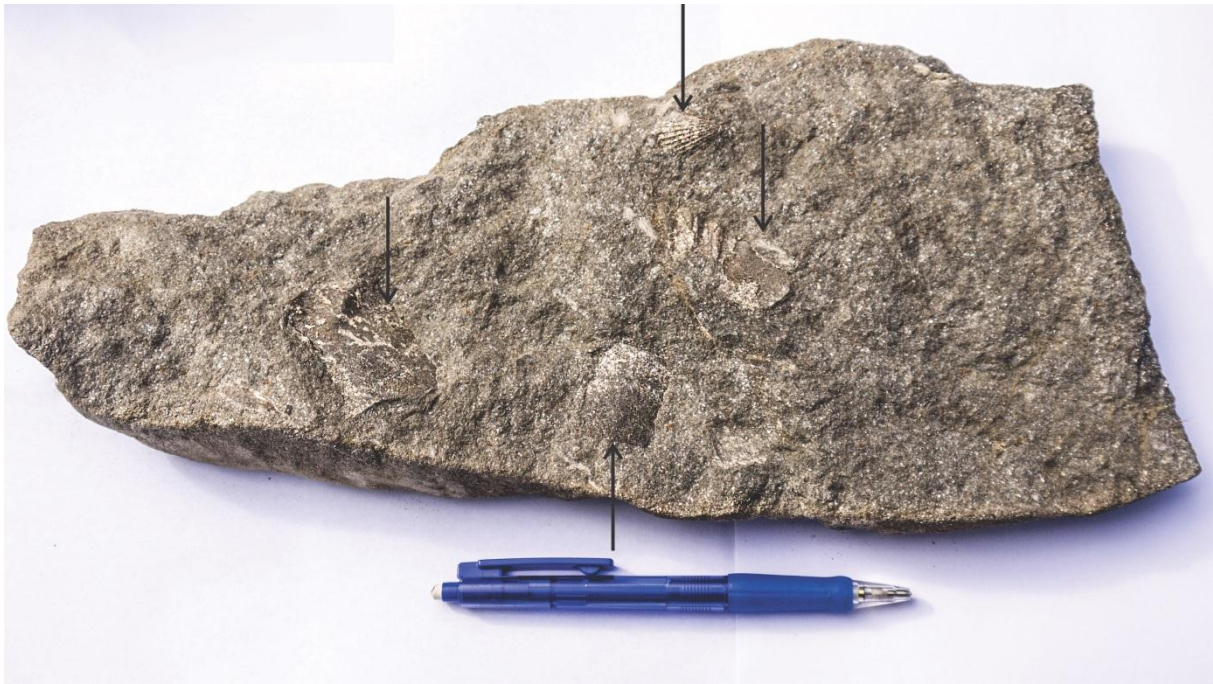


Figure 16 *Erratic block containing several fragments of marine fossils discovered along the Skarstein shoreline.*

2.3.2.3 Description of kinematic data

Due to the absence of slickensided surfaces and offsets, the shear sense of fractures and/or faults at Skarstein remain difficult to assess. Thin-section studies of cataclasites confirm that the rocks are brittle fault rocks, but it was not possible to retrieve kinematic data from these samples (Fig. 18). Hematite was occasionally found on NNE-SSW to NE-SW striking fractures planes, but the surfaces were smooth and possible lineations must have weathered off (Fig. 19). However, the clockwise rotation of NE-SW striking fractures into NNE-SSW striking fractures might serve as evidence for dextral strike-slip movements along the NNE-SSW and/or ENE-WSW striking fractures.

2.3.2.4 Pre-existing fabrics along the fault zone

A steep NW-SE striking foliation is developed in the granitic gneiss and amphibolite lenses, but is not observed in the unfoliated granite. While NNE-SSW to NE-SW and approximately E-W striking brittle fractures, including the cataclastic fault rocks, seem to have developed independent of the gneiss foliation, NW-SE striking fractures appear parallel to this foliation and are locally well-developed (Fig. 15).



Figure 17 NE-SW to ENE-WSW striking steep fractures with cataclastic fault rocks in massive granite, Skarstein, Andøya. For structural legend, see Common legend in Figure 12; location in Figure 15.

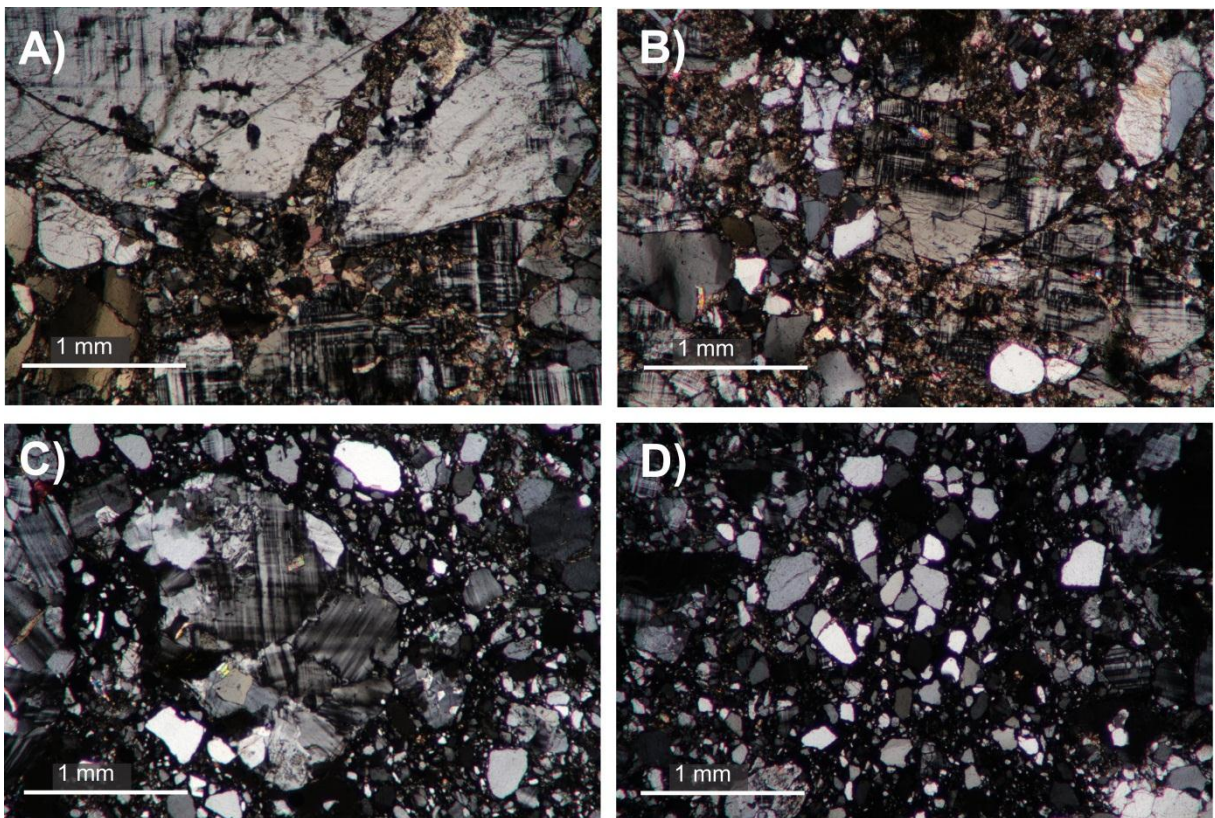


Figure 18 A)-D) Microphotographs of thin sections from the cataclastic fault rocks at Skarstein.

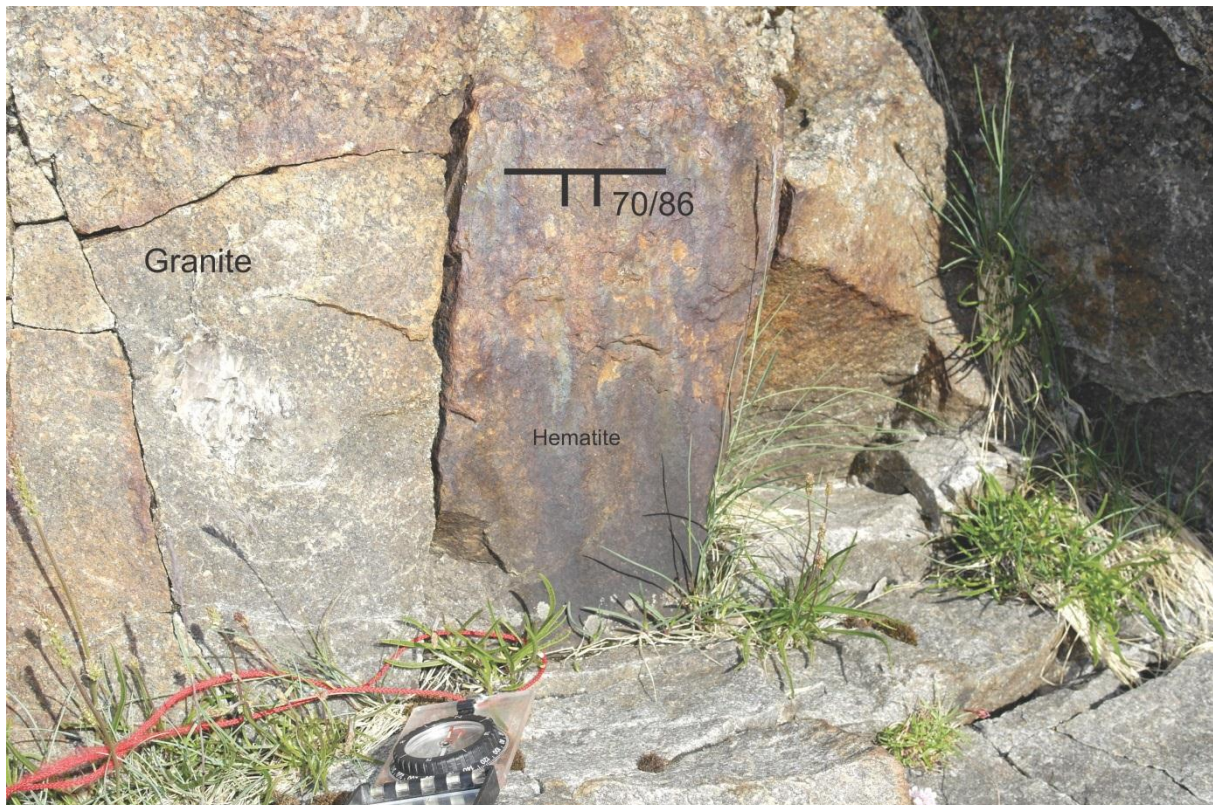


Figure 19 Hematite precipitation on ENE-WSW striking fracture in granite. For structural legend, see Common legend in Figure 12; location in Figure 15.

2.3.2.5 Summary and preliminary interpretations

The bedrock at Skarstein is made up of granitic and amphibolitic gneisses and unfoliated granite (Fig. 15). Occasional erratic blocks of sedimentary rocks from the sedimentary strata further south, inland or offshore are also present. The contact between the crystalline basement rocks and the sedimentary basin is characterized by an NE-SW to E-W striking fault and believed to be located just south of Skarstein (Dalland, 1974; Figs. 3 & 4 this work), but it was not observed during the fieldwork. The presence of NE-SW striking cataclastic fault rocks at Skarstein (Figs. 15, 17 & 18), may however support the interpretation of a tectonic contact.

The area between Skarstein and Fiskenes is characterized by a network of NNE-SSW to NE-SW, E-W and NW-SE striking fractures that are both parallel to and/or oblique to the gneiss foliation of the host rocks (Figs. 3, 11 & 15). Two NE-SW striking fracture zones contain cataclastic fault rocks up to one meter wide indicate the presence of a major (?) brittle fault zone in the area. Cataclastic rocks were not detected further inland or southward towards the contact to the sedimentary outcrops, but rather seemed to continue northeastward into the fjord. As the cataclasites do not occur along with sedimentary rocks, the deformation cannot be directly linked to the Mesozoic basin and/or -rift phases. However, given the close vicinity to the basin in Andfjorden and the abundance of NE-SW striking faults/fractures in this basin (Henningsen & Tveten, 1998; Zwaan & Grogan, 1998) and the

sedimentary rocks at Ramså (Dalland, 1974, 1975, 1979; 1981; Fig. 11 c this work), it is a strong possibility that the cataclasites are part of a major fault merging into the fjord bounding and/or offsetting Mesozoic sedimentary strata. If so, the fault is interpreted as a dip-slip normal/oblique-slip fault, and may thus have developed during Mesozoic rifting, perhaps in relation to the NNE-SSW striking boundary fault present in the eastern part of Andfjorden (Henningesen & Tveten, 1998; Zwaan & Grogan, 1998). Recently, a N-S striking fault in Skarsteinsdalen (Fig. 23) has been dated to the Late Devonian/Early Carboniferous (Davids et al., 2013; see chapters 1.2.5.4 & 2.3.4), and a second alternative is thus that the cataclasites and related fault zones may have formed in this Paleozoic rift phase.

The clockwise rotation and merging into parallelism of NE-SW striking fractures into respectively NNE-SSW and ENE-WSW striking fractures, may indicate that dextral strike-slip movements have occurred on one or both of the latter fracture sets. If the ENE-WSW striking fractures have accommodated dextral strike-slip movements, the NNE-SSW striking fractures would be expected to display the same geometry as the NE-SW striking fractures. This is not observed, suggesting that (a) the NNE-SSW striking fractures are younger than both the NE-SW and ENE-WSW striking fractures; or (b) that the NNE-SSW striking fractures are younger or synchronous with the NE-SW striking fractures, and that the dextral strike-slip motion was restricted to the NNE-SSW striking fractures. In the last scenario, it is possible that the clockwise rotation of the NE-SW striking fractures is the result of local stress perturbations caused by the dextral strike-slip movement along the older/synchronous NNE-SSW striking fractures (Dyer, 1988; Hansen & Bergh, 2012; Koehl, 2013; Fig. 49 this study). Shear is however not needed to create the stress perturbations, and the NNE-SSW and NE-SW striking fractures may thus have developed as synchronous tension joints. If the NE-SW striking fractures are the oldest, the drag effect is a result of dextral strike-slip movement along the younger NNE-SSW striking fractures.

That hematite was only identified on the NNE-SSW to NE-SW fractures, further indicate that these fracture may have developed at a different stage than the ENE-WSW striking fractures.

Also, given their similar orientation, the gneiss foliation appears to have controlled or at least been related to the formation of NW-SE striking fractures at Skarstein. The foliation possibly acted as zones of weakness that were reactivated as brittle fractures during a later extensional phase. The other brittle fracture populations, including the cataclastic fault rocks, are oblique to the gneiss foliation, and no obvious connection to the foliation can be made.

2.3.3 Fiskenes

2.3.3.1 Field relations and host rock characteristics

Fiskenes is a harbor located about a kilometer north of the Mesozoic basin on Andøya (Fig. 11). Overall, the shoreline in the Fiskenes area runs approximately N-S. However, it is highly irregular and characterized by several small NE-SW oriented headlands and bays (Fig. 20). The bedrock of the area consists of unfoliated granite and migmatitic and mylonitic gneisses with dykes of amphibolite, with a sub-vertical E-W to NW-SE striking foliation (Fig. 20) that are fractured by NNE-SSW to NE-SW, E-W and NW-SE foliation parallel fractures (Figs. 11 e & 20).

2.3.3.2 Description of brittle fractures in the basement rocks at Fiskenes

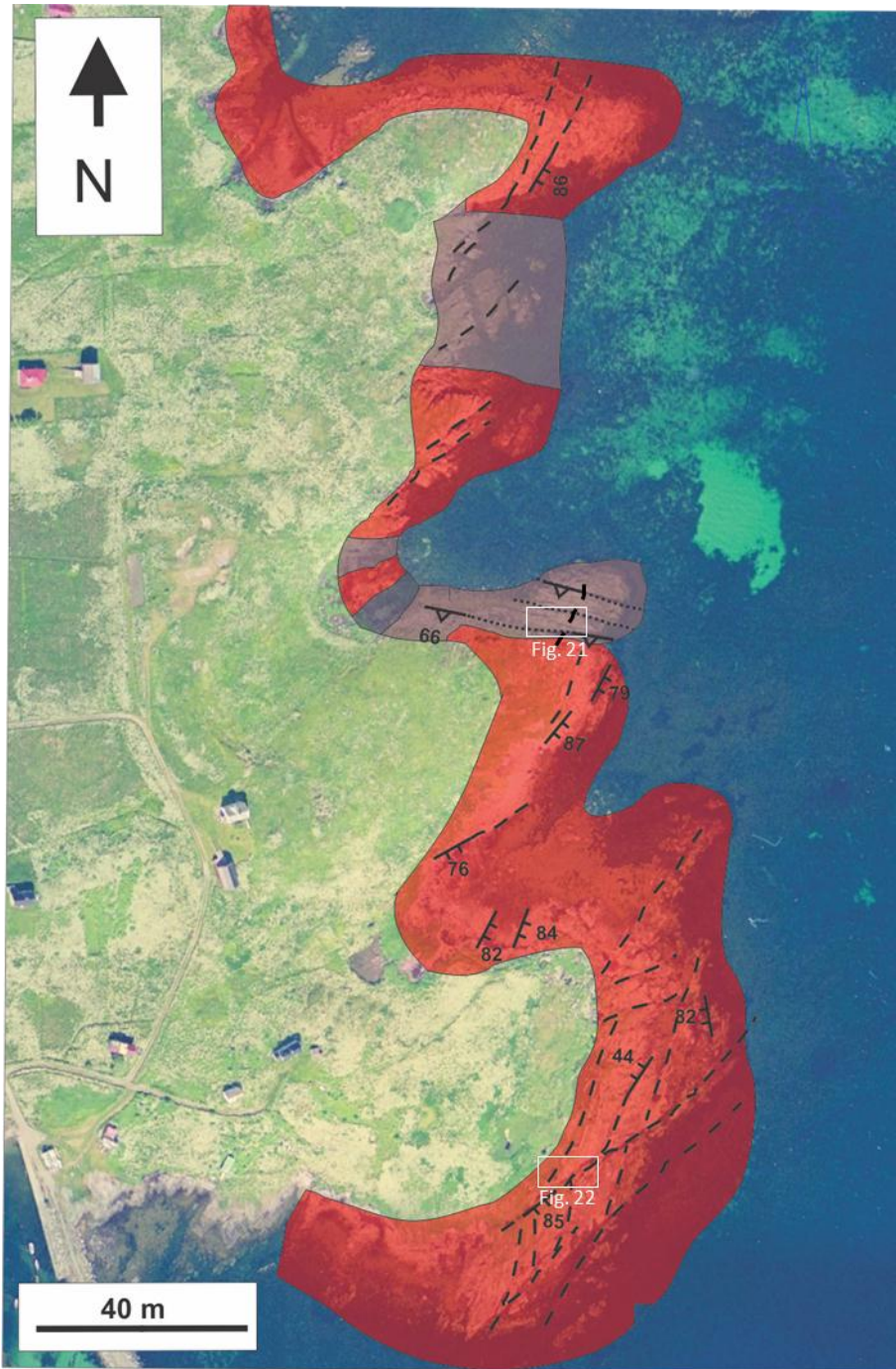
The brittle fractures at Fiskenes are moderately to steeply dipping and generally strike NNE-SSW to NE-SW, although E-W and foliation parallel NW-SE striking fractures also occur (Figs. 11 e, 20 & 21). The map pattern is complex: The NNE-SSW striking fractures have a stepping geometry and cross-cut the foliation parallel fractures, while showing a clockwise rotation towards the NE-SW and the ENE-WSW striking fractures (Figs. 20 & 21).

2.3.3.3 Description of kinematic data

Again, the kinematic indications come from geometric analysis rather than kinematic indicators on the fracture planes: The clockwise rotation of NNE-SSW striking fractures toward the ENE-WSW striking fractures might be a result of dextral strike-slip movements along the NE-SW striking fractures (Fig. 22).

2.3.3.4 Pre-existing fabrics along the fault zone

An older, ductile NW-SE to E-W striking gneiss foliation was observed in the gneisses and amphibolites at Fiskenes (Figs. 20 & 21), and appears to be sub-parallel/parallel to the NW-SE and E-W striking brittle fractures. The change in foliation strike could potentially indicate macroscale folding of the basement rocks, but this was not further investigated.



- Unfoliated granite**
- Amfibolite**
- Granitic gneiss**

Figure 20 Structural and lithological map of Fiskenes, Andøya. Unfoliated, red granite dominate the lithology, but outcrops of granitic gneiss and amphibolite also occur. The gneiss is affected by a WNW-ESE to NW-SE striking ductile foliation, while NNE-SSW to NE-SW striking lineaments affect the whole bedrock complex. For structural legend, see Common legend in Fig. 12.

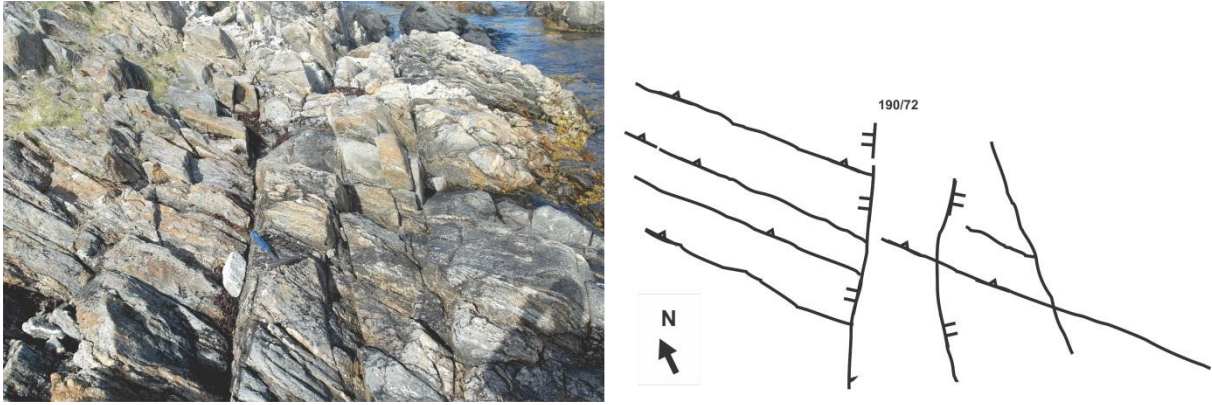


Figure 21 A) NNE-SSW striking fractures cut NW-SE striking foliation parallel fractures at Fiskenes, Andøya. B) Sketch of the picture, better illustrating the relationship between foliation and NNE-SSW striking fractures. For structural legend, see Common legend in Figure 12; location in Figure 20.



Figure 22 Clock-wise bending of NNE-SSW striking fractures (red) against ENE-WSW striking fractures (black) at Fiskenes. For location, see Figure 20.

2.3.3.5 Summary and preliminary interpretations

Fiskenes is located about a kilometer from the northern limit of the Mesozoic basin on Andøya and a couple of hundred meters from the eastern boundary fault of the Andfjorden basin (Henningsen & Tveten, 1998; Zwaan & Grogan, 1998), and is characterized by bedrock made up by migmatitic and mylonitic gneisses with dykes of foliated amphibolite and unfoliated granite. Even though Fiskenes is located farther away from the onshore and offshore sedimentary basins, the fracture pattern is similar to what was observed in closer vicinity to these basins (chapters 2.3.1. and 2.3.2). NNE-SSE to NE-SW striking fractures are most abundant, while E-W and NW-SE striking fractures define the landscape to a lesser

extent. NNE-SSW striking fractures are observed to merge into parallelism with NE-SW striking fractures, rotating in a clockwise manner. This geometry can either be formed if older NNE-SSW striking fractures are dragged toward younger NE-SW striking fractures during dextral shearing and due to material rotation along the NE-SW striking fractures, or if the NNE-SSW striking fractures merge into parallelism with older/synchronous NE-SW striking fractures (Dyer, 1988; Hansen & Bergh, 2012; Koehl, 2013). In the latter scenario, the clockwise curving is due to stress perturbation along potentially sinistral NE-SW striking fractures (Fig. 49). The stress perturbation can also occur without shearing, making it possible that the NNE-SSW and NE-SW striking fractures formed synchronously as tension joints (Dyer, 1988; Mandl, 2005).

The NW-SE and the E-W striking fractures run sub-parallel or parallel to the pre-existing NW-SE to E-W striking foliation (Figs. 20 & 21). It is therefore suggested that this foliation influenced the development of the NW-SE and E-W striking fractures at Fiskenes.

2.3.4 Skarsteinsdalen quarry

2.3.4.1 Large scale field relations and host rock characteristics

A large quarry is located in Skarsteinsdalen approximately two kilometers west of Skarstein (Fig. 11 a). The bedrock of the quarry is unfoliated gabbro/amphibolite and felsic gneisses with a steep NW-SE striking foliation dipping to the SW (Fig. 23). The contact between the two lithologies is defined by a large N-S striking fault zone dipping moderately to the east (Fig. 23). The fault zone is up to eight meters thick and consists of a floor and a roof fault dipping between 30° and 50° to the east, linked by hematite filled, high frequency N-S trending faults/fractures that show anticlockwise sigmoidal bending towards the floor and roof surfaces (Fig. 23). A 5-10 cm thick layer of fault gouge separate strongly fractured gabbro in the footwall from massive migmatitic gneiss in the hanging wall. This fault gouge has recently been used in radiometric dating of the fault zone (Davids et al., 2013), yielding Late Devonian or Early Carboniferous age with no later reactivation. Due to the intense deformation of the rocks, movement in the area is difficult and hazardous, and the analysis of the fault zone thus rely more on geometrical analysis from pictures than data collected in the field.

2.3.4.2 Description of brittle fractures and associated structures in the fault zone

The fault zone is up to ten meters thick and defined by a floor and a roof fault dipping c. 40° to the east, linked to hematite-filled, high frequency N-S trending fractures that show anticlockwise sigmoidal bending towards floor and roof surfaces (Fig. 23). A 5-10 cm thick layer of fault gouge separate strongly fractured gabbro in the footwall from massive migmatitic gneiss in the hanging wall. NW-SE striking fractures appear sub-parallel to the

gneiss foliation in the felsic gneiss, but are also observed in the unfoliated gabbro/amphibolite.

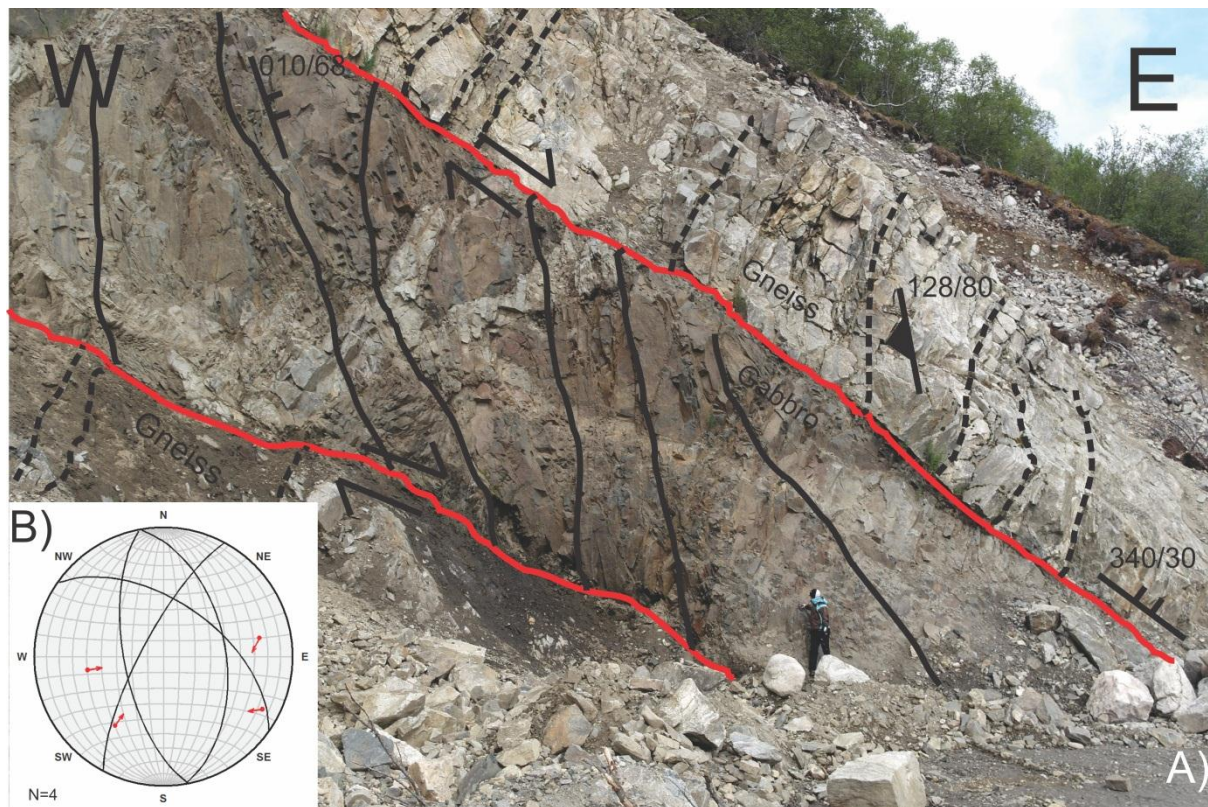


Figure 23 A) Major NNE-SSW striking fault zone cross-cutting gneiss foliation (dotted black lines) in Skarsteinsdalen. Subsidiary faults (solid black lines) merge and show sigmoidal anti-clockwise bending towards floor and roof faults (red lines). B) Stereonet showing the slickenside data recorded from subsidiary faults in Skarsteinsdalen. For structural legend, see Common legend in Figure 12.

2.3.4.3 Description of kinematic data

As no offsets were observed in the fault zone, the kinematic data consists of slickenside striations and geometric fracture analysis (Figs. 23 a, b & 49). Slickenside striations are numerous on minor faults/fractures of various orientations observed in and around the Skarsteinsdalen fault zone. The slickensides recorded define fibrous hematite and illustrate normal dip-slip movements; sometimes also with a sinistral slip component, along NNW-SSE, NW-SE and NE-SW striking faults/fractures (Fig. 23 b). The bending of the subsidiary N-S striking faults towards the roof and floor faults (Fig. 23), may be used to infer the overall slip direction of the fault zone: Either the subsidiary faults are the oldest and were dragged toward younger roof and floor faults during reverse dip-slip movements on the latter faults, or the fractures formed synchronously, with the anticlockwise rotation bending being caused by local stress perturbations likely related to normal dip-slip movements along the roof and floor faults (Figs. 23 & 49).

2.3.4.4 Pre-existing fabrics along the fault zone

A ductile gneiss foliation striking NW-SE (dipping to the east) has been mapped in the gneiss, but is not apparent in the gabbro. The fault zone is located in the lithological boundary between a gabbro/amphibolite and a migmatitic gneiss and cuts through foliation of the gneiss (Fig. 23). The foliation is sub-parallel to the NW-SE striking fractures in the felsic gneisses (Fig. 23).

2.3.4.5 Summary and preliminary interpretations

The host rocks of the Skarsteinsdalen fault zone is unfoliated gabbro/amphibolite and felsic gneiss with a NW-SE striking foliation (Fig. 23). An E-W oriented vertical profile display the up to eight meters thick core zone of the fault zone (Fig. 23). The core zone may represent a brittle duplex made up by fault-bounded blocks (horses), stacked on top of each other and contained by moderately eastward dipping roof and floor faults (Fig. 23).

The anticlockwise bending of the subsidiary faults towards the floor and roof faults may be explained in two ways: (i) either the subsidiary faults formed earlier and were dragged toward the roof and floor faults by reverse dip-slip movements on the latter faults, or (ii) the faults developed synchronously, with the anticlockwise rotation of the subsidiary faults toward the roof and floor faults likely resulting from normal dip-slip movements along the latter faults (Figs. 23 & 49).

Combined with the slickenside data (Fig. 23 b) and the radiometric dating (Davids et al., 2013), the most likely geometrical interpretation seem to be alternative (ii), indicating that the fault zone may have been active as a normal fault during the Devonian collapse of the Caledonides. It is also possible that the fault initially developed as a thrust fault during the Caledonian orogeny, before being reactivated as a normal fault during the following collapse of the orogen. Reactivation of Caledonian thrusts and Paleozoic normal faults are common on the Norwegian passive margin, and although the presence of Mesozoic sedimentary rocks in a fault bounded basin speaks for significant Mesozoic and even Cenozoic movement along faults in this area, the Skarsteinsdalen fault is believed to have been inactive, and the boundary fault is expected to be located closer to the sea. Due to an extensive peat cover, the boundary fault of the basin has yet to be identified, but recent seismic and aeromagnetic surveys performed by NGU and the University of Bergen as part of the RABIS project suggest this might be resolved in the near future.

Given the similar orientation of NW-SE striking foliation in the felsic gneisses and the NW-SE striking brittle fractures, it is possible that the foliation influenced the development of this fracture set. However, the NW-SE striking fractures are also present in the unfoliated gabbro/amphibolite, and evidently also developed without favorably oriented zones of

weaknesses. The N-S roof and floor faults are located in the lithological boundaries between gneiss and gabbro (Fig. 23 a). Thus, it is likely that these boundaries acted as zones of weakness and influenced the development of the roof and floor faults.

2.4 Bjarkøya

2.4.1 Sundsvoll quarry

2.4.1.1 Large scale field relations and host rock characteristics

The quarry at Sundsvoll, Bjarkøya, is the largest quarry visited during the fieldwork. It is located on northern Bjarkøya, just by the Sundsvollsundet, a prominent E-W striking escarpment separating Bjarkøya from Helløya (Figs. 24 & 25). The bedrock in the quarry is made up of Archean, hornblende and amphibole rich gabbro with precipitations of iron oxides and sulfides, and Early Proterozoic granitic pegmatites and spheroidal weathered tonalitic granite with sub-horizontal layers with dark material (Fig. 26 & 27). The contact between the granite and the gabbroid rocks sometimes appear to be faulted, and is distinguished by thin layers of possible fault gouge (Fig. 26). Possible fault gouge also appear as sub-horizontal 15 cm thick dark zones internally in the weathered granite (Fig. 27). Samples were collected with hope for age determination, but at closer examination, the samples looked and felt quite sandy, and although it is possible that they are breccia from the fault zone, they could just as well be dirt-sediment that has fallen into an open crack.

From DEM data, the quarry seems to be located in an area where several fracture orientations are conspicuous (Figs. 9 & 24 a), and measurements done in the field confirms this. Although the topography appears to be controlled by NE-SW to N-S lineations, faults and fractures striking NW-SE and E-W seem to be just as common at outcrop scale. Faults/fractures in the quarry are often characterized by hematite or chlorite precipitations on the fracture surfaces, that commonly also contain slickensides (Fig. 28).

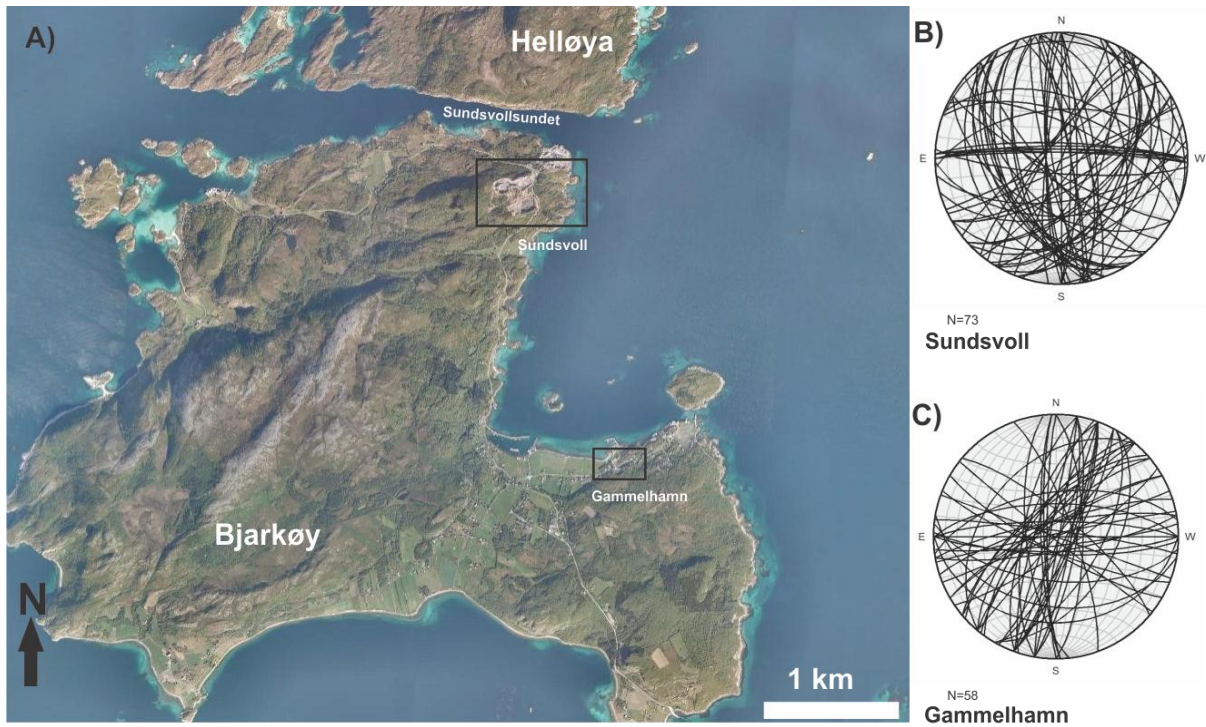


Figure 24 A) Satellite photo of Bjarkøya and southern Helløya, showing large scale lineament patterns and fieldwork locations. B) and C) Lower-hemisphere Schmidt stereonets displaying fracture orientation data from the Sundsvoll Gammelhamn quarries, respectively.

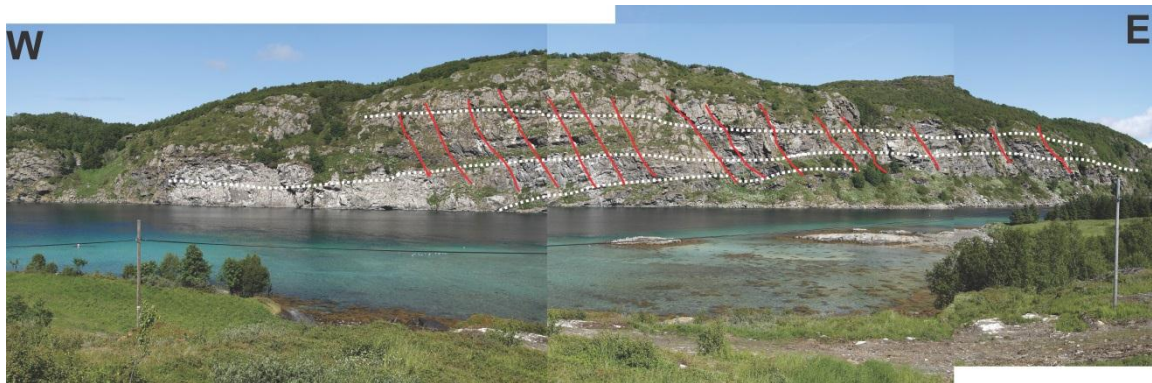


Figure 25 The E-W trending escarpment separating Bjarkøya from Helløya. NNE-SSW striking fractures (red) cut through almost horizontal foliation (white).

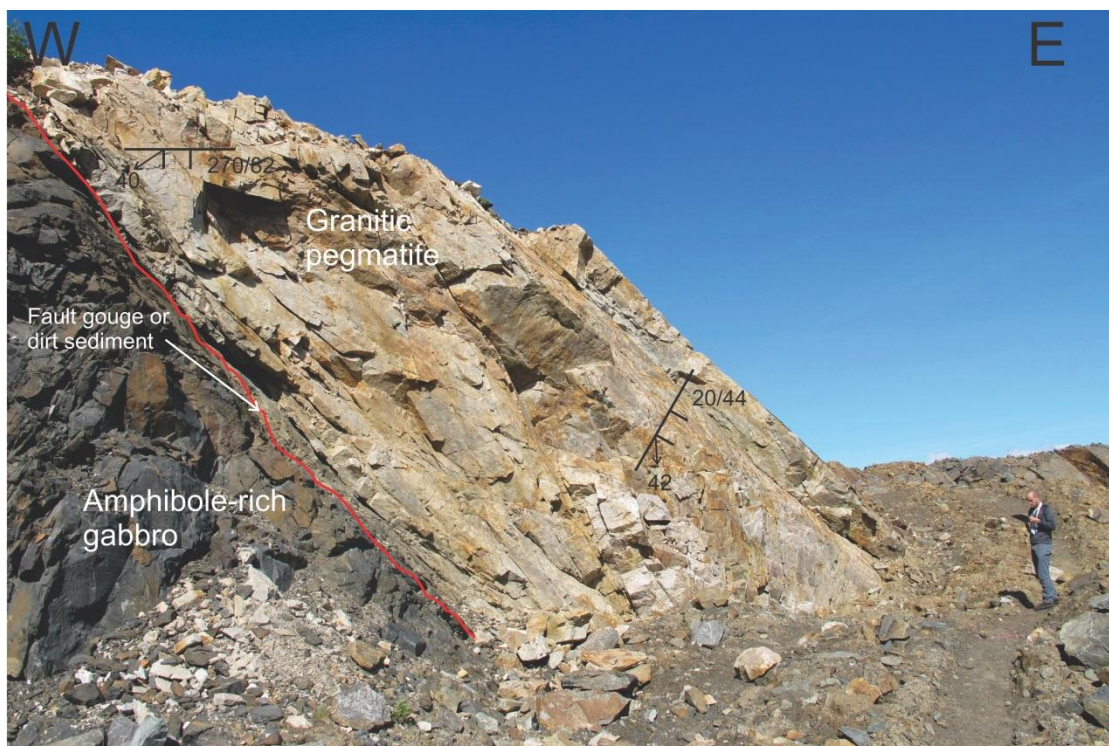


Figure 26 Lithological boundary (red) between the two major lithologies in the Sundsvoll quarry: Gabbro and granitic pegmatites. Contact may be faulted and contain fault gouge or dirt sediment. Slickensides are recorded along both E-W and NNE-SSW striking fractures. For structural legend, see Common legend in Figure 12. Photo: prof. Steffen Bergh.

2.4.1.2 Description of brittle fractures in basement rocks

Numerous brittle fractures occur in the quarry at Sundsvoll, and they have been studied in cross-sections striking in different directions (Figs. 26 & 29). Fractures are common within the separate rock units, but the contact between the different lithologies very often appear to be faulted (Figs. 26 & 29). Faults are sometimes distinguished by thin layers of possible fault gouge (Fig. 26), and possible fault gouge also appear as sub-horizontal c. 15 cm thick dark zones internally in the weathered granite (Fig. 27).

The quarry is large, and fractures/faults striking almost every direction were identified: N-S striking faults/fractures dipping steeply to the east and west, NE-SW striking faults/fractures commonly dipping moderately to the southeast, NW-SE striking faults/fractures dipping moderately to the southwest, and E-W striking faults/fractures with sub-vertical dips to the north and south (Fig. 24 b). Finally, the chlorite and hematite-coated fracture/fault surfaces often display fibrous slickensides that provided substantial information regarding the kinematics of these faults.

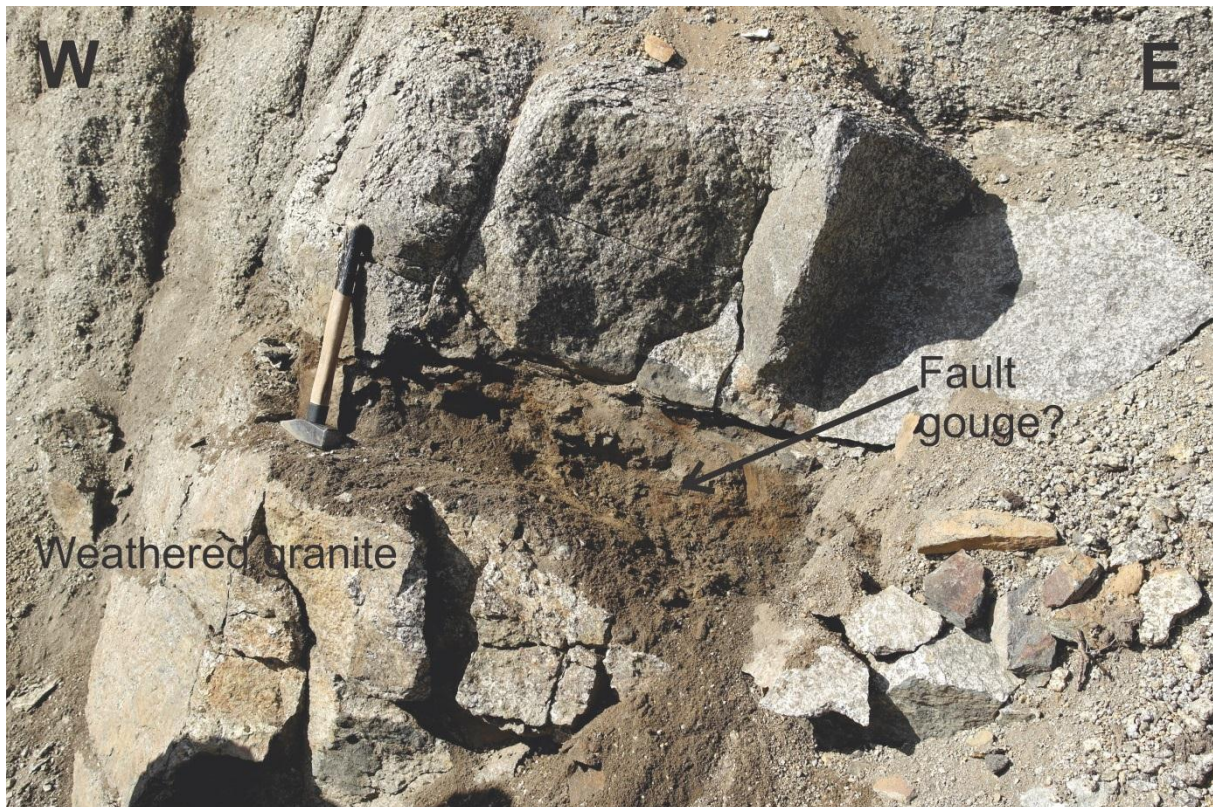


Figure 27 Weathered granite in the Sundsvoll quarry with internal fault zone possibly composed of unconsolidated Fe-enriched fault gouge. Photo: prof. Steffen Bergh.

Slip-linear data, Sundsvoll

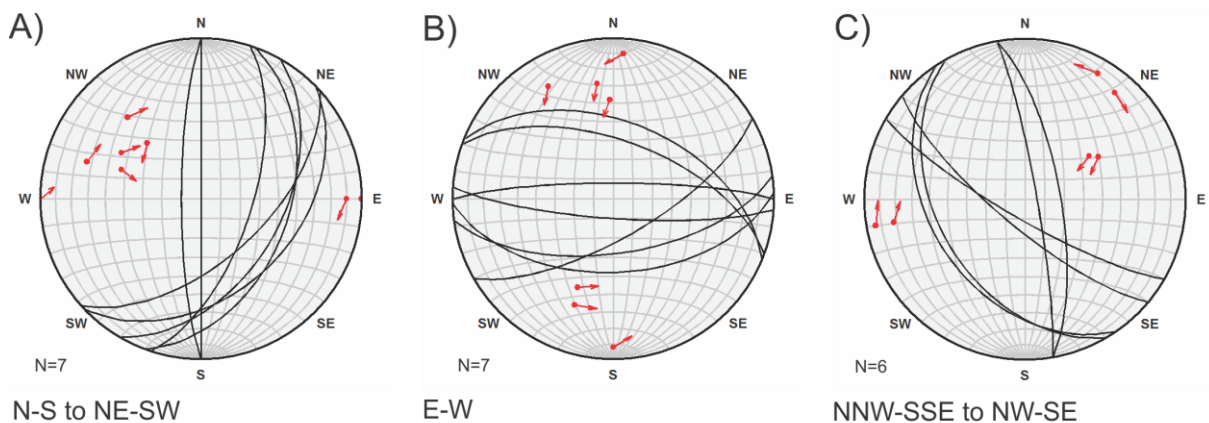


Figure 28 Stereonets displaying the slickenside data recorded in the Sundsvoll quarry. A) N-S to NE-SW striking fractures are dominantly oblique-slip with both dextral and sinistral components. B) E-W striking fractures dipping to the south show dominantly normal dip-slip movements, while north dipping ones are entirely dextral. C) NNW-SSE to NW-SE striking fractures show a great variation of shear sense, from almost pure normal dip-slip to pure dextral/sinistral-slip.

2.4.1.3 Description of kinematic data

Slickensides were observed on fracture sets in all orientations and the data are plotted as slip-linears in stereonets (Fig. 28). The N-S trending fractures dominantly show sinistral oblique-slip, but there is also evidence of pure dip-slip normal motion (down to the east). Slickensides on the E-W trending fractures indicate mostly dextral oblique-slip (Fig 28), but as for the N-S trending fractures, almost pure dip-slip normal movement (down to the south)

is also observed (Fig 28). The NE-SW trending fractures displays a lot of differently plunging slickensides, with movement indicated to be both sinistral and dextral oblique as well as pure dip slip normal (down to the southeast) (Fig 28). Movement along NW-SE trending fractures dominantly sinistral oblique-slip, but dextral and pure normal-slip (down to the southwest) is also recorded (Fig 28).

In addition to the study of slickensides, a cm-scale offset of a quartz vein by approximately E-W striking faults dipping to the south (Fig. 29). The apparent master fault lies at the contact of gabbro and a heavily fractured (fault breccia?) pegmatite. The quartz vein is offset by several minor fractures, creating an apparent reverse drag effect towards the pegmatite. Local reverse dip-slip movement is also suggested at one of the minor fractures (Fig. 29).

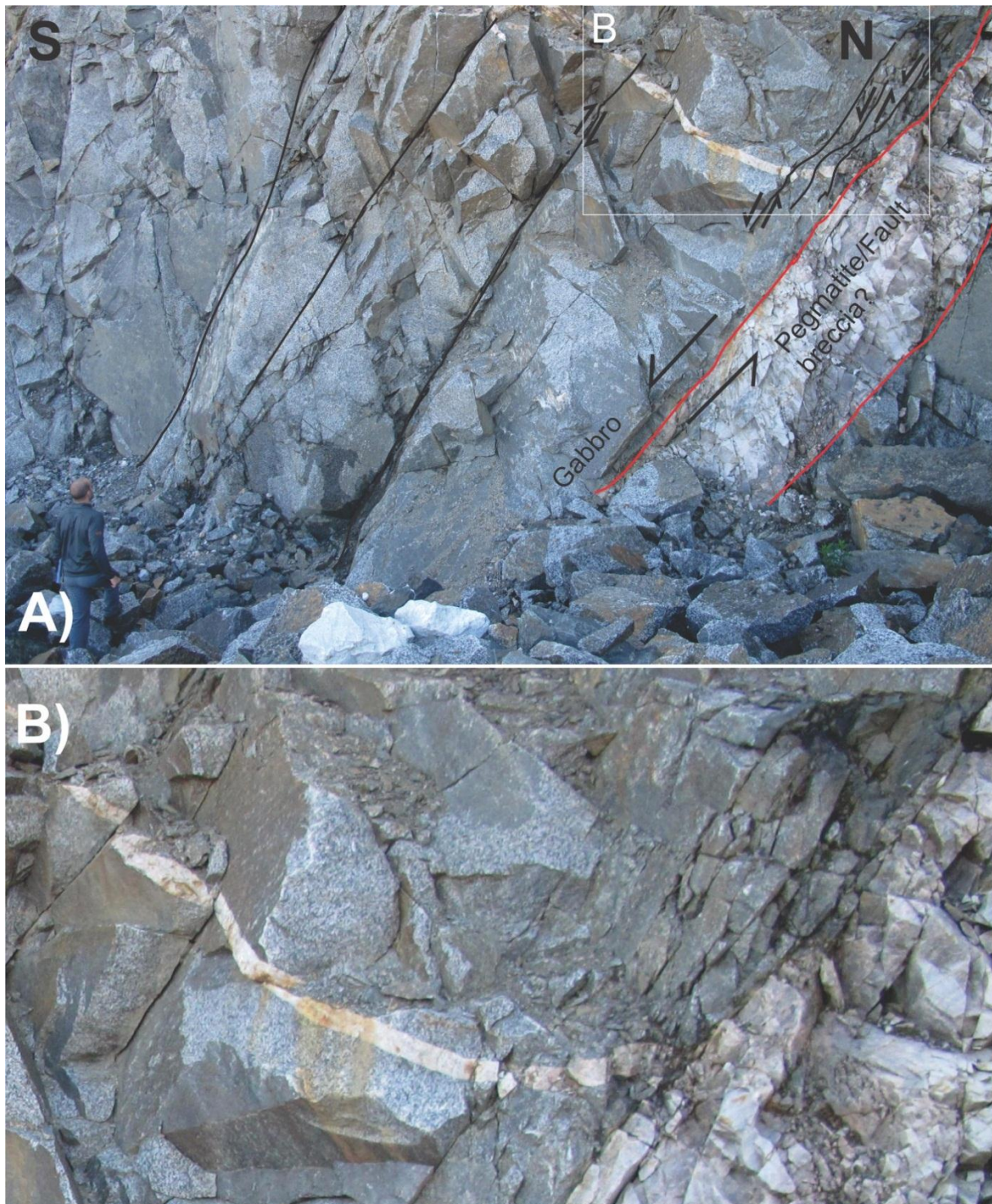


Figure 29 A) Possible cm-scale offset of quartz vein along approximately E-W striking faults in Gabbro. The main fault is located within the lithological boundary between the gabbro and a heavily fractured granitic pegmatite. Fracture frequency clearly increases towards the lithological boundary. B) is zoomed in on the frame in A) to better illuminate the possible faults. Photo: prof. Steffen Bergh.

2.4.1.4 Pre-existing fabrics in the basement rocks

The foliation of the rocks in the Sundsvoll quarry was not studied in detail. However, many of the most prominent faults and fractures in the quarry seem to be located within the lithological boundary between gabbro and granitic rocks.

2.4.1.5 Summary and preliminary interpretations

The local lithology in the Sundsvoll quarry is dominated by Archean gabbros, rich in hornblende and amphibole, and Early Proterozoic tonalitic granite and granitic pegmatites that contain a complex network of brittle faults and fractures (Fig. 24 b). Remote sensing images indicated N-S to NE-SW striking faults/fractures to be the dominant sets (Figs. 9 & 24), but sets of NW-SE and E-W striking faults/fractures appear to be just as common. The larger fractures are sometimes characterized by a central layer of dark material initially believed to be fault gouge, but closer inspection revealed that the material was too sandy to be dated.

Slickensides were identified over the whole quarry, and the brittle deformation has consequently been distributed over a significant area. Investigations of kinematic indicators has revealed a variety of movement directions, with N-S striking faults being dominantly sinistral strike-slip and E-W striking fractures tending to be dominantly dextral strike slip (Fig. 28). However, it must also be noted that almost all the fracture/fault directions has a subsidiary dip-slip normal component (Fig. 28). Moreover, the cm-scale offset of a quartz vein by c. E-W striking faults dipping to the south, create an apparent reverse drag effect, indicating normal dip-slip movements (Fig. 28).

Due to the complex cross-cut and merging relationship of the different fractures it has been difficult to estimate their relative age, although the bending of E-W striking fractures toward NNE-SSW striking fractures may indicate that the NNE-SSW are oldest.

The most prominent fractures seem to be concentrated along the lithological boundaries between the amphibole rich gabbro and the granitic pegmatites (Figs. 26 & 29). It is therefore suggested that these boundaries have acted as zones of weakness, and thus influenced the formation of brittle fractures. Pegmatites have intruded the gabbro from several directions, meaning that potential zones of weakness exist in a number of orientations. Accordingly, the diversity in brittle faults/fracture trends observed in the quarry (Fig. 24 b) may be attributed to old zones of weakness in the bedrock.

2.4.2 Sundsvoll shoreline

2.4.2.1 Large scale field relations and host rock characteristics

The Sundsvoll shoreline is located just 100 meters east of the quarry (Fig. 24) and also consists of hornblende and amphibole rich gabbro with high content of iron oxides and sulfides, sometimes giving it a yellow character (Fig. 30). Granitic pegmatites also occur, but are not as abundant as in the quarry. The shoreline makes it possible to study the fractures described in the quarry in map view, and may thus reveal information about relative age that was not possible to retrieve from the quarry. However, the ratio between fault/fracture sets differs from that of the quarry, with NNE-SSW to NE-SW striking fractures being very dominant overall (Fig. 30 b).

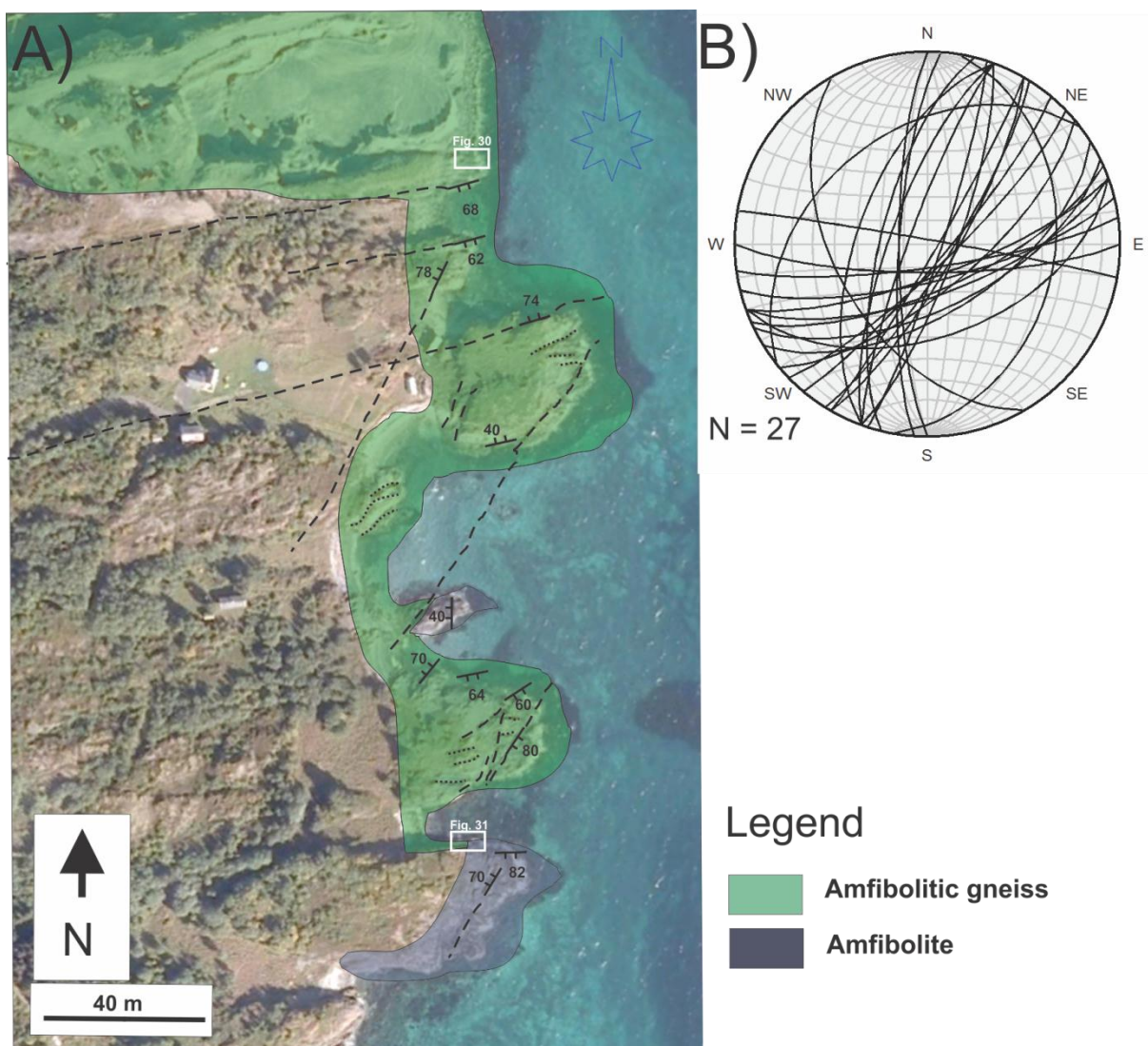


Figure 30 A) Structural and lithological map of the Sundsvoll shoreline. The shoreline is dominated by amphibolitic gneiss with a ductile foliation striking NE-SW to E-W. The bedrock is cut by dominantly NE-SW to ENE-WSW striking fractures. For structural legend, see Common legend in Figure 12.

2.4.2.2 Description of brittle fractures and associated structures in the fault zone

The NNE-SSW striking fractures, dip steeply to the east and west, while the NE-SW striking fractures dip steeply to the southeast and the northwest (Fig. 30). These, steep bisecting brittle fractures make up rhombic networks of multiple cross-cutting, mostly rectilinear fractures (Fig. 31). The orientations of 60 fractures were measured and plotted in a rose chart (Fig. 31 c), illustrating that, locally, the main fracture directions are NNE-SSW and ENE-WSW with subsidiary fractures striking N-S to NNW-SSE. The main fractures create a rhombic pattern and (mostly) have a planar geometry, with a bisecting horizontal axis oriented c. NE-SW. At the picture scale, the main fractures seem continuous up to two meters, but at closer inspections the individual fractures can be seen to display both right-stepping and left-stepping patterns (Fig. 31), and bend towards each other. NW-SE trending fractures parallel to the bisecting horizontal axis terminate against both NNE-SSW and ENE-WSW striking fractures, and sometimes create geometries similar to that of imbrication fans. Further south, NNE-SSW striking fractures bend into E-W striking fractures (Fig. 32).

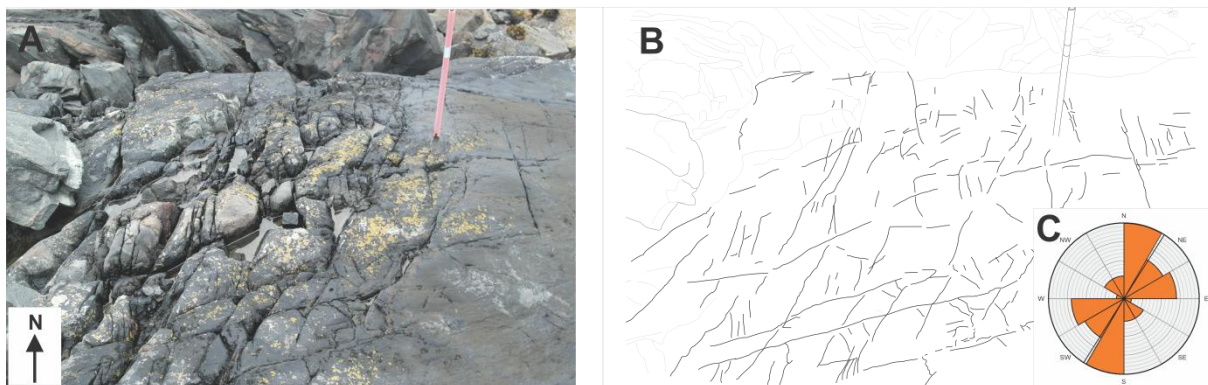


Figure 31 A) Network of steep, cross-cutting NNE-SSW and ENE-WSW striking fractures, creating a rhombic pattern. B) Sketch of the picture, better illustrating the geometry of the fracture zone. C) Rose diagram of 120 measured fractures from the fracture zone, illustrating dominant fracture directions. For location, see Figure 30.

2.4.2.3 Description of kinematic data

No direct kinematic indicators such as slickensides or brittle offsets were observed along the coast of Sundsvoll. However, indirect information can be retrieved from looking at the orientation and geometry of the brittle fractures (see chapter 2.4.2.5).

2.4.2.4 Pre-existing fabrics in the basement rocks

The rocks in the shoreline appeared to be homogenous, and fractures did not seem concentrated along lithological boundaries as was observed in the quarry (see chapter 2.4.1.4).



Figure 32 NNE-SSW striking fractures (red) bend into parallelism with ENE-WSW striking fractures (black) at the Sundsvoll shoreline. See Figure 30 for location.

2.4.2.5 Summary and preliminary interpretations

The rocks at the Sundsvoll shoreline consists of a sulfide rich gabbro intruded by granitic pegmatites, and contain steeply dipping fractures dominantly striking NNE-SSW to NW-SE and ENE-WSW. The bisecting nature of the NNE-SSE and ENE-WSW striking fractures is consistent and suggest that these fractures formed synchronously, either as conjugate shear fractures related to pure shear deformation (Mode II of Kulander et al. (1979); see chapter 4.1 this work) and/or as oblique Riedel shear fractures (R and R') in a simple shear regime e.g. adjacent to a larger fault zone (Smith & Durney, 1992; Crider, 2001; Katz et al., 2004). The location lacks direct shear indicators, but the systematic orientation and merging of connected branches between individual fractures (Fig. 31) works as incidental evidence of a shear fracture (Mode II) origin. According to the Anderson theory of faulting, conjugate shear

fractures initiate due to rock failure with the acute bisecting axis parallel to the shortest strain axis (or maximum σ_1 stress axis) (Anderson, 1951; Hobbs et al., 1976). Thus, one interpretation could be that the fractures are conjugate and formed due to shearing with a bisecting angle oriented ca. NE-SW (i.e. the principal σ_1 axis). Interactions between fractures may have caused local variations in the stress orientations, thus producing slight variations in fracture orientations. Due to the bisecting angle, the fractures could have been interpreted as an echelon R shears linked together by P shears at higher displacements (Woodcock & Fischer, 1986), but this is unlikely due to the cross-cutting nature of the fractures. The fractures are also similar to a fundamental joint system (Mandl, 2005), that consists of an older systematic set of joints and a younger, orthogonal non-systematic set. A third possibility is therefore that the fractures actually are tension joints formed at different times at different paleostress orientations. It would then be expected that the youngest set displayed a more complex geometry than the oldest, but this is not observed (Fig. 31). Given the intense shearing that was observed in the quarry just 100 meters away, formation as conjugate shear fractures thus remains the most likely interpretation, although movement probably was in the mm-scale by the shoreline.

The rocks along the shoreline seem to be homogenous and brittle faults fractures did not seem to concentrate in the lithological boundaries as was observed in the Sundsvoll quarry (chapter 2.4.1.4). As a result, pre-existing fabrics did most likely not influence the formation of brittle faults and fractures at the Sundsvoll shoreline.

2.4.3 Gammelhamn quarry

2.4.3.1 Field relations and host rock characteristics

Gammelhamn is a village situated on the southeastern side of the rhombic bay on Bjarkøya (Fig. 24). A small quarry is located here, with a homogeneous lithology consisting of unfoliated granite/granodiorite. Terrain models (Figs. 9 & 20) show the topography to be governed by NE-SW and E-W striking lineations, sub-parallel to the strike of the Stonglandseidet fault zone (Koehl, 2013). The Stonglandseidet fault zone is believed to continue from Stonglandet through the E-W striking escarpment separating Bjarkøya from Helløya (Zwaan & Grogan, 1998). However, as the quarry is located directly southeast of Stonglandet, it was interesting to see if the fault zone could rather be exposed here.



Figure 33 A) Overview of the Gammelhamn quarry showing the host rock intensely fractured by NNE-SSW and E-W to ENE-WSW striking fractures. B) A closer look at two steep, chlorite-coated NNE-SSW and E-W striking fracture surfaces with dextral shear-sense. For structural legend, see Common legend in Figure 12.

2.4.3.2 Description of brittle fractures in the basement rocks

The two most prominent sets of fractures identified at the Gammelhamn quarry, are made of high-frequency NNE-SSW striking fractures that dip steeply to the NW or the SE, and steep, high-frequency, E-W to ENE-WSW striking fractures dipping N or S (Figs. 24 c & 33). Both sets are characterized by precipitations of chlorite, and appear to crosscut, but not offset, each other. Occasionally they also merge into each other. In cross-section, the fracture surfaces are commonly curved, causing the dip angle to vary between steep and moderate on the same fracture. Possible fault gouge was also identified in the central parts of some of the faults.

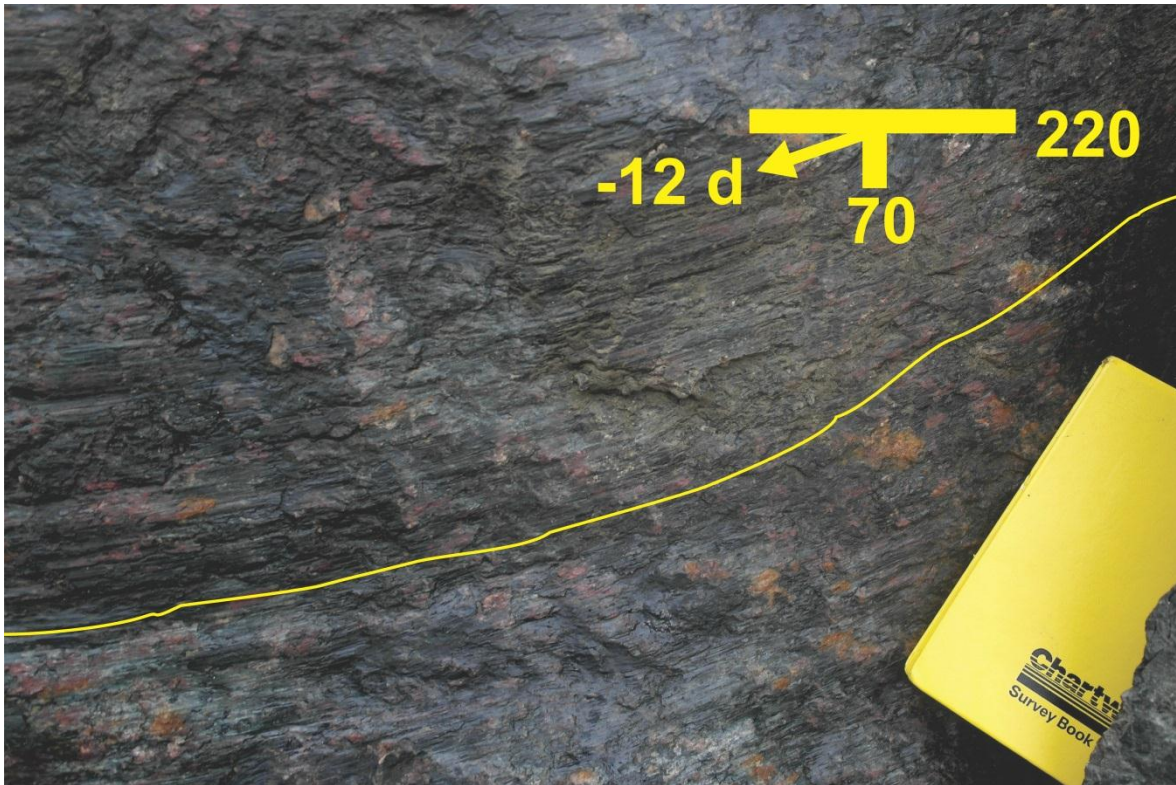


Figure 34 Dextral slip along chlorite-coated ENE-WSW striking fracture in the Gammelhamn quarry. For structural legend, see Common legend in Figure 12.

2.4.3.3 Description of kinematic data

Slickenside mineral fibers have been observed on numerous chlorite-coated (Fig 33 b & 34) fractures from both the dominating sets. The slickensides generally plunge at a gentler angle than the fracture surfaces, indicating mostly dextral strike-slip motion, perhaps also with a minor dip-slip normal and/or sinistral-slip components (Fig 33 b, 34 & 35).

Slip-linear data, Gammelhamn

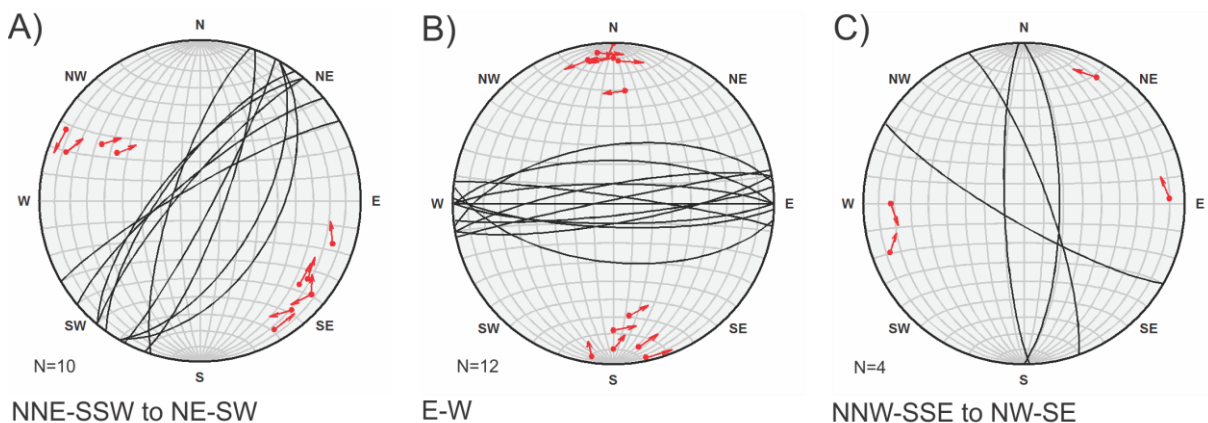


Figure 35 Stereonets displaying the slickenside data recorded in the Gammelhamn quarry. A) NNE-SSW to NE-SW striking fractures are dominantly oblique-slip with both dextral and sinistral components. B) E-W striking fractures are oblique-slip, with a dominant dextral-slip component. C) Movement along NNW-SSE to NW-SE striking fractures is almost pure dextral or sinistral.

2.4.3.4 Pre-existing fabrics in the basement rocks

The granite in the quarry is not particularly foliated (Figs. 33 b & 34), and no other pre-existing fabrics were observed in the quarry.

2.4.3.5 Summary and preliminary interpretations

The homogenous granite/granodiorite in the Gammelhamn quarry is highly cracked by NNE-SSW and ENE-WSW striking fractures coated with chlorite and, to a smaller extent, hematite. Rather than cross cutting each other, the two fracture sets seem to merge into each other and bend. Chlorite precipitations and similarly plunging and trending slickensides on both fracture sets further indicate a synchronous evolution. The slickensides indicate dominantly dextral strike-slip movements, but with components of dip-slip normal and sinistral-slip movements.

The same fracture sets were observed by (Koehl, 2013) at Stonglandseidet in his description of the Stonglandseidet fault zone, but due to a lack of slickensided surfaces he was not able to determine the definite shear sense of the fault zone. Nevertheless, clockwise curving geometries (in map view) of NNE-SSW trending fractures toward ENE-WSW trending fractures and ENE-WSE and NNE-SSW trending fractures toward more NW-SE trending fractures probably indicate dextral strike-slip movement (Koehl, 2013), similar to what has been inferred for the shear fractures of Gammelhamn. At Stonglandet the core of the Stonglandseidet fault zone is characterized by a potentially up to 150 meters wide, calcite-rich cataclastic zone (Koehl, 2013). Neither cataclasites nor calcite precipitations were identified in the Gammelhamn quarry, and although this does not rule out a connection to the Stonglandseidet fault zone, it at least proves that the deformation was of a significantly lower character.

2.5 Skrolsvik, Senja

2.5.1 Field relations and host rock characteristics

Skrolsvik on Senja (Figs. 2, 9 & 36) is located close to the eastern continuation of the Stonglandseidet fault zone (Forslund, 1988; Olesen et al., 1997; Zwaan & Grogan, 1998) and provide well exposed outcrops of quartz dioritic gneiss with reddish granitic pegmatites and quartz veins. The diorite is largely homogenous, but foliation is observed to have developed in the Skrolsvik quarry, where the rock can be studied in cross-section. At the Senjehesten peninsula, a lithological boundary between diorite and granitic gneiss appears to follow the shoreline, and the foliation in the gneiss apparently follows the diorite-gneiss boundary (Fig. 40).

The Stonglandseidet fault zone was previously mentioned by Tveten and Zwaan (1993) and Olesen et al. (1993); (1997), and was described by Koehl (2013) as an ENE-WSW striking and SE dipping normal fault. The fault core is characterized by a calcite-rich cataclastic zone up to 150 m wide, turning into highly fractured proto-cataclastic granite in the hanging wall which is progressively less deformed towards the south, defining a ca. 500 wide damage zone (Koehl, 2013). A similar decrease in fracture density is observed northwards from Skrolsvik, and what was thought to be spectacular faults from DEM studies proved to be N-S striking foliation and NE-SV striking felsic pegmatite veins, and the field work therefore focused on locations closer to the fault zone.

The field work at Skrolsvik was conducted in a small quarry, the shoreline beneath this quarry and the Senjehesten peninsula (Fig 36).

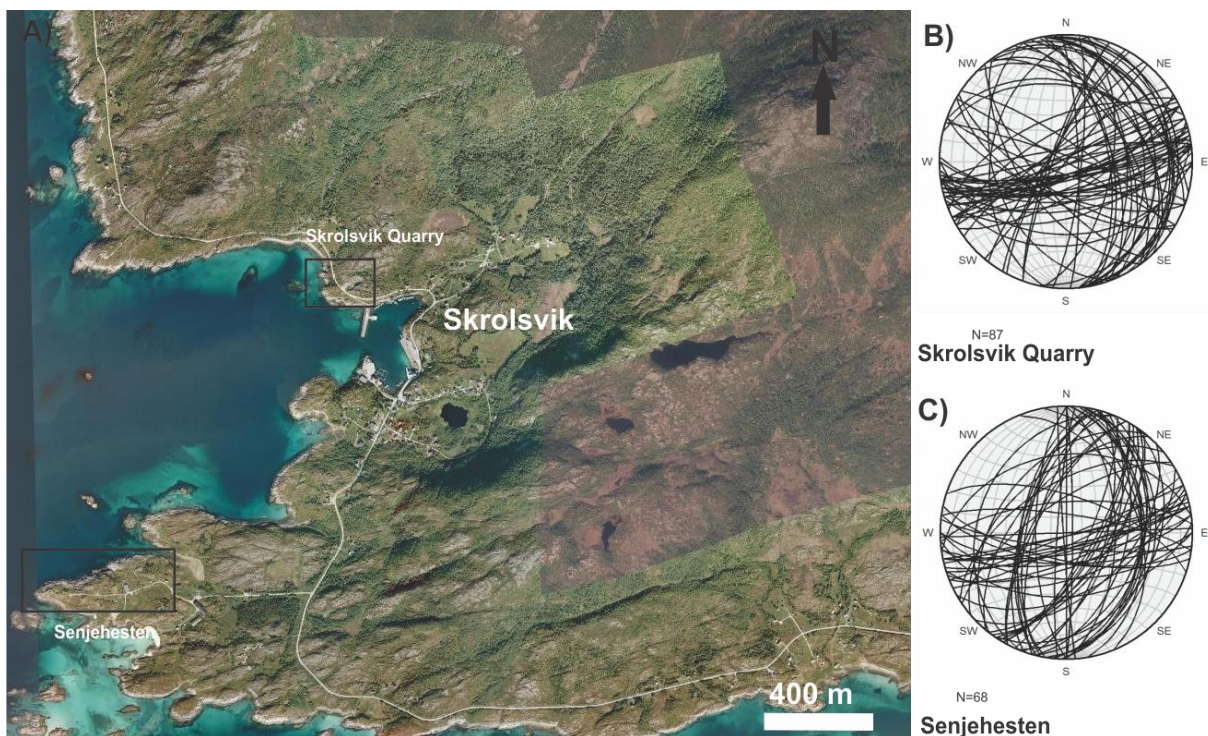


Figure 36 A) Satellite photo of Skrolsvik, showing large scale lineament patterns and fieldwork locations. B) and C) Lower-hemisphere Schmidt stereonet displaying fracture orientation data from the Skrolsvik quarry and the Senjehesten peninsula, respectively.

2.5.2 Skrolsvik quarry

2.5.2.1 Description of brittle fractures in the basement rock

The fractures in the Skrolsvik quarry display significant variation in dip and orientation, but can roughly be divided into three dominant groups: Steeply dipping, NE-SW and ENE-WSW striking fractures and more gently dipping, NNW-SSE striking fractures (Figs. 36 b). The fractures cross-cut each other and the moderately dipping gneiss foliation (Fig. 37). Some of the fracture planes are coated with fibrous epidote that reveals their kinematic character.

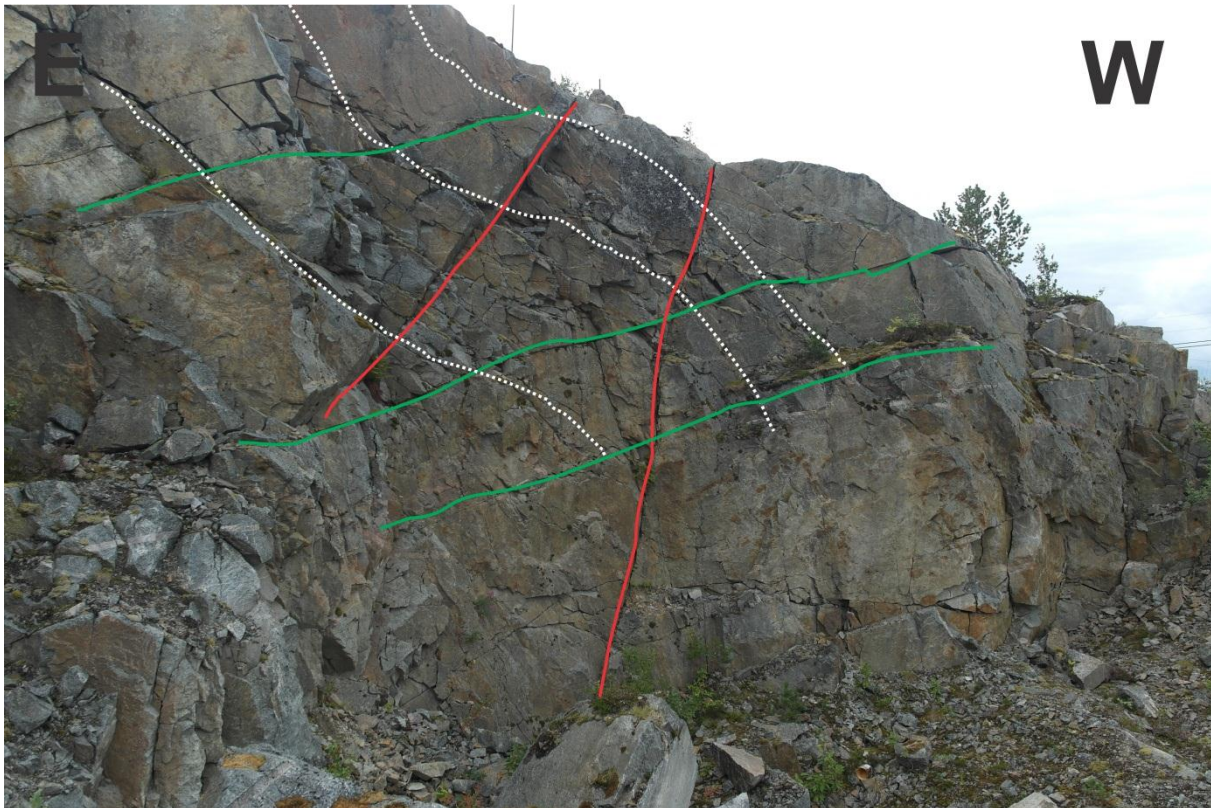


Figure 37 E-W cross-section in Skrolsvik quarry, showing steep NNE-SSW and gently NW-SE striking fractures cutting (red and green, respectively), but not offsetting foliation (dotted white).

Along the shoreline just beneath the quarry, the relationship between the fractures closely resembles the quarry. Bisecting fractures similar to the ones observed on Bjarkøya were also discovered beneath the quarry in a c. one meter wide fracture zone (Fig. 38). 71 measurements of orientations were taken from the fracture zone and plotted in a rose chart (Fig. 38 c). The most abundant fractures are definitely those striking ENE-WSW, but a set of NNE-SSW striking fractures are also well developed, despite occurring with significantly lower frequency (Fig. 38 c). Minor fractures were observed to trend in several directions, e.g. NW-SE and NE-SW. The ENE-WSW and NNE-SSW fractures are oriented at almost 60° to each other, creating a rhombic pattern in map-view (Fig. 38). The fractures mostly have a planar geometry, with a bisecting horizontal axis oriented ca. NE-SW and seem fairly continuous on a m-scale. The E-W striking fractures are a bit more complex, with sets that in isolation may define an echelon gash fractures and/or relaying and left and right stepping fractures creating horsetail- and/or duplex-shaped features (Fig. 38).

In another c. one meter wide fracture zone, NW-SE striking fractures were observed to bend anti-clockwise towards ENE-WSW to E-W striking fractures that show both right- and left-stepping geometry (Fig. 39). 166 strike measurements were taken from this fracture zone and plotted in a rose diagram, that turned out to be pretty similar to the one from the first fracture zone (Figs. 38 c & 39 c).

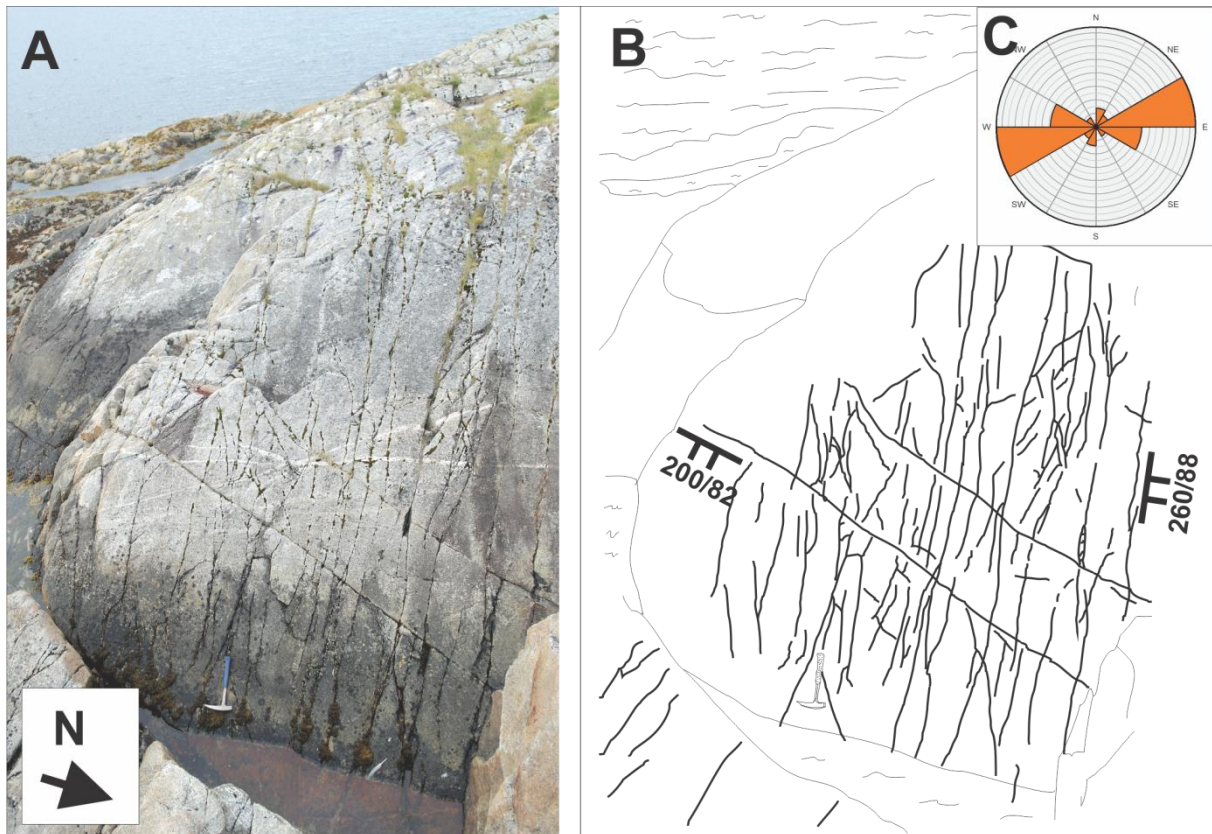


Figure 38 A) Picture of bisecting NNE-SSW and E-W striking fractures beneath the Skrolsvik quarry. B) Sketch of the picture, better illustrating the geometry of the fracture zone. C) Rose plot of 142 measured fractures in the fracture zone, illustrating the dominating fracture directions. For structural legend, see Common legend in Figure 12.

2.5.2.2 Description of kinematic data

A few surfaces in the Skrolsvik Quarry contained good slickensides that show dextral oblique-slip to normal dip-slip along NE-SW striking fracture planes (Fig. 40 a). A single measurement indicates dextral-oblique to normal-slip along E-W striking fractures (Fig. 40 b), with normal-oblique movements were also recorded from NNW-SSE striking fractures (Fig. 40 c).

The outcrop by the shore lacks direct kinematic indicators, but the systematic orientation and merging of connected branches between individual fractures (Figs. 38 & 39), works as incidental evidence of a shear fracture origin. When only looking at the geometry, it is likely that they formed as conjugate shear fractures related to pure shear deformation (Mode II of Kulander et al. (1979), see chapter 4.1 this study) and/or as oblique Riedel shear fractures (R and R') with dextral and sinistral strike-slip movements in a simple shear regime, e.g. adjacent to a larger fault zone (Smith & Durney, 1992; Crider, 2001; Katz et al., 2004).

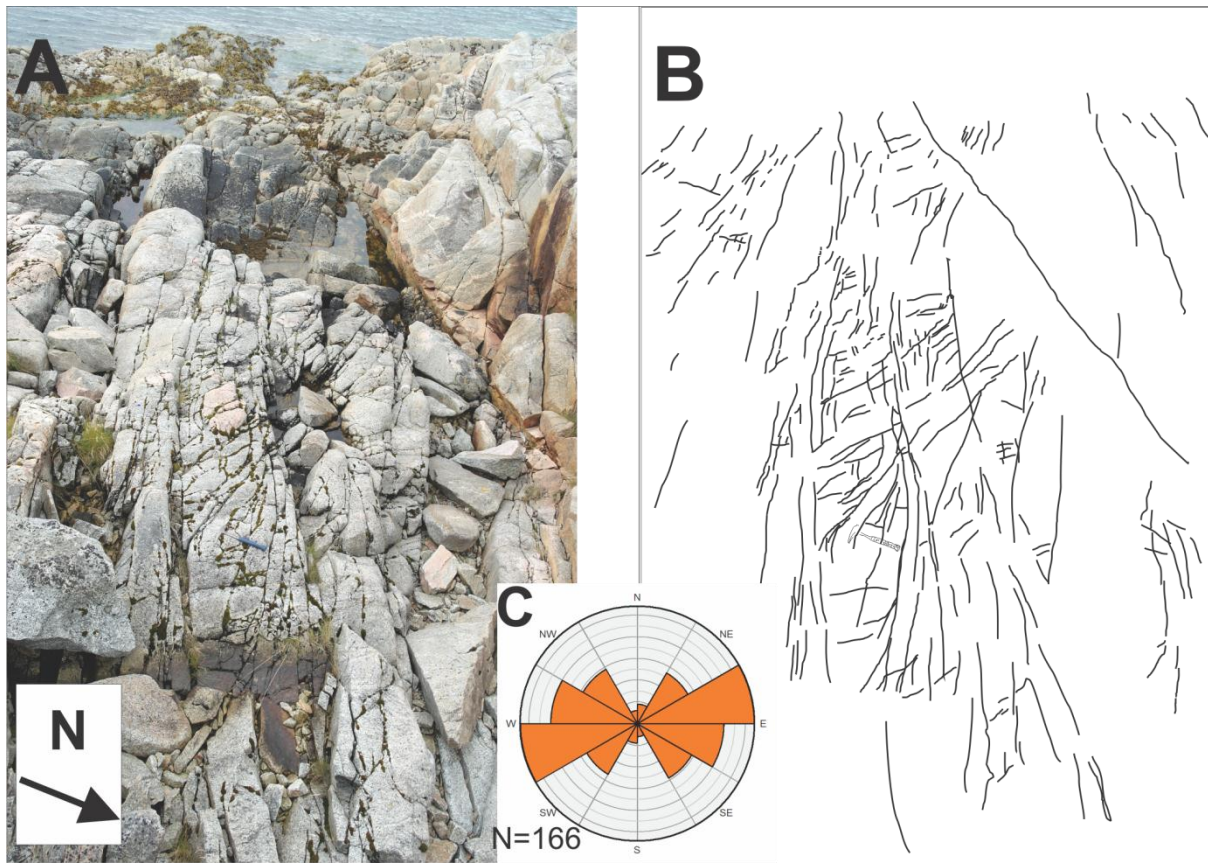


Figure 39 A) Fracture zone beneath the Skrolsvik quarry. NW-SE striking fractures seemingly bend into parallelism with E-W striking fractures. B) Sketch of the picture, better illustrating the geometry of the fracture zone. C) Rose plot of 166 fracture measurements from the fracture zone, illustrating the dominating fracture directions.

Slip-linear data, Skrolsvik

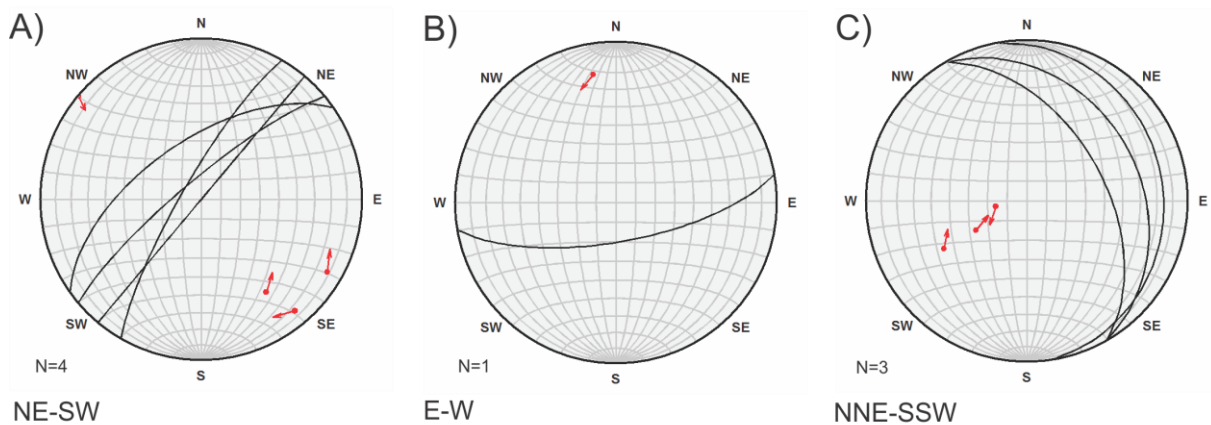


Figure 40 Stereo nets displaying the slickenside data recorded in the Skrolsvik quarry. A) NE-SW striking show dextral/sinistral oblique movements. B) The single measurement from E-W striking fractures shows movement to be almost pure dip-slip normal, but with a small component of dextral shear. C) NNE-SSW striking fractures show dominantly dip-slip normal, but also dip-slip reverse.

2.5.2.3 Pre-existing fabrics along the fault zone

Older ductile fabrics were observed around Skrolsvik, including in the Skrolsvik quarry, where a NE-SW striking foliation dips moderately to the northwest. The foliation is crosscut, but not offset, by NNW-SSW and NE-SW striking fractures, dipping to the east and northeast, respectively (Fig. 37).

2.5.2.4 Summary and preliminary interpretations

The bedrock in the Skrolsvik quarry is made up by diorite with a NE-SW striking foliation dipping moderately to the northwest. It is intensively fractured by dominantly NE-SW to ENE-WSW striking fractures dipping steeply to the NW/SW and NNW/SSE, respectively. Fractures striking NW-SE and NNE-SSW and dipping moderately to gently towards the ENE or NE, are also common (Fig. 36).

Two studied fracture zones however, show different and more detailed interrelations between the fracture sets (Figs. 38 & 39). Due to the lack of direct kinematic indicators along the shoreline, the fractures can be interpreted either as extensional joints or shear fractures. The geometry of the two fracture sets of Figure 38 are similar to a fundamental joint system (Mandl, 2005; see chapter 2.3.2.5 this work). In such a model, the more straight and continuous NNE-SSW striking set would be interpreted as the oldest and the more disturbed ENE-WSW striking set as the youngest. Extensional joints form normal to the direction of greatest tensile stress σ_3 (Mandl, 2005) meaning that the formation of the orthogonal set of non-systematic joints requires a rotation of the principal stress direction from approximately WNW-ESE to NNW-SSE. Given that the angle between the fracture sets is between 60-70 degrees rather than orthogonal, it remains a possibility that the two sets formed synchronously, maybe as conjugate shear fractures related to pure shear deformation (Mode II of Kulander et al. (1979), see chapter 4.1 this study) and/or as oblique Riedel shear fractures (R and R') in a simple shear regime e.g. adjacent to a larger fault zone like the Stonglandseidet Fault Zone (Smith & Durney, 1992; Crider, 2001; Katz et al., 2004).

The second fracture zone (Fig. 39) displays a branching and merging of ENE-WSW and NW-SE striking fractures, as the NW-SE striking set is rotated anti-clockwise towards the ENE-WSW striking set, that shows both right- and left-stepping geometry. Given this relationship, it seems likely that the fractures either evolved as a result of sinistral slip along a younger fracture set (ENE-WSW) and following anti-clockwise rotation of an older fracture set (NW-SE), or by anti-clockwise rotation of the younger NW-SE striking set caused by local stress perturbations along potentially dextral older/synchronous ENE-WSW striking fractures (Dyer, 1988; Hansen & Bergh, 2012; Koehl, 2013; Fig. 49 this work). Note that shearing along ENE-WSW fractures is not a requirement to bend the NW-SE striking fractures.

The limited kinematic data in the quarry also indicate dextral oblique-slip to be the dominant slip direction, and does, along with the shoreline interpretations, fit well with a dextral Stonglandseidet Fault Zone (Koehl, 2013). Normal-slip movements are also recorded from NW-SE striking faults.

Because of a lack of markers, it is hard to determine the offset of the faults, but as there are no signs of intense deformation, e.g. cataclasites or fault gouge, slip probably was in the mm to cm scale both in the quarry and along the shoreline.

Fractures apparently crosscut the ductile foliation in the diorite (Fig. 37), and the foliation can consequently not be directly related to the formation of the fractures.

2.5.3 Senjehesten peninsula

2.5.3.1 Description of brittle fractures and associated structures in the fault zone

The fractures at the Senjehesten peninsula (Fig. 36 a) are dominantly N-S to NNE-SSW and ENE-WSW striking, sometimes with thin coatings of hematite (Figs. 36 c, 41 & 42). While the ENE-WSW striking fractures generally dip steeply to the north or south, the N-S to NNE-SSW striking fractures show moderate dips both to the E/SE and W/NW at an angle close to 60° and might thus represent a conjugate fracture set (Figs. 36 c & 43).

A c. 50 cm wide fracture zone was chosen for more detailed study. It does not reflect the overall fracture pattern of the Senjehesten peninsula (Figs. 41 & 42): The orientations of 53 fractures from this zone were measured and plotted in a rose chart, illustrating a significant dominance of WNW-ESE striking fractures and lesser portions of ENE-WSW and NW-SE striking fractures (Fig 42 c). Coatings of hematite are observed on either of the fracture sets, and the WNW-ESE striking fractures are connected by ENE-WSW striking fractures, defining an apparent right-stepping geometry, sometimes creating duplex-shaped fracture sets that are well displayed in horizontal views (Fig. 42). The fracture zone propagates through a pegmatite vein, but no offset is visible on the scale of observation.

2.5.3.2 Description of kinematic data

A potential conjugate fracture set was observed at the Senjehesten peninsula and indicate normal dip-slip to the east and west, forming horst-graben like structures (Fig. 43). A pegmatite vein is offset a couple of cm's down to the east, indicating normal dip-slip along a N-S striking fracture dipping to the east (Fig. 43).

Although somewhat chaotic, it may be possible to derive the shear sense of the anastomosing fractures (Fig. 42) from their interaction with one another. Eig and Bergh (2011) presented three possible kinematic mechanisms that may have produced similar fracture sets at Moskenes, western Lofoten: (i) fracture propagation, branching from a master strike-slip fault, where the resulting duplex may be releasing or restraining due to the nature

of bending (Woodcock & Fischer, 1986; Woodcock & Schubert, 1994; Morley, 2004; Cunningham, 2007), (ii) interplay between a main stepping fracture set and counter-stepping splays or relays (Smith, 1996), and (iii) linkage of early-stage or precursory en echelon fractures due to further propagation and relay fracture generation (Woodcock & Fischer, 1986; Woodcock & Schubert, 1994; Crider & Peacock, 2004).



Figure 41 *Lithological and structural map of the Senjehesten peninsula. The bedrock consists of granitic gneiss and diorite that are cut by NE-SW and E-W striking fractures that create a rhombic pattern. The diorite-gneiss boundary seems to be folded along the peninsula. While NE-SW striking fractures cut through this boundary, the E-W striking fractures seemingly bend into parallelism with it. For structural legend, see Common legend in Figure 12.*

2.5.3.3 Pre-existing fabrics along the fault zone

The foliation appears to be folded parallel to the shoreline. The NE-SW trending fractures were observed to propagate through the foliation, while the E-W trending fractures bends into parallelism with the diorite-gneiss boundary (Fig. 41).

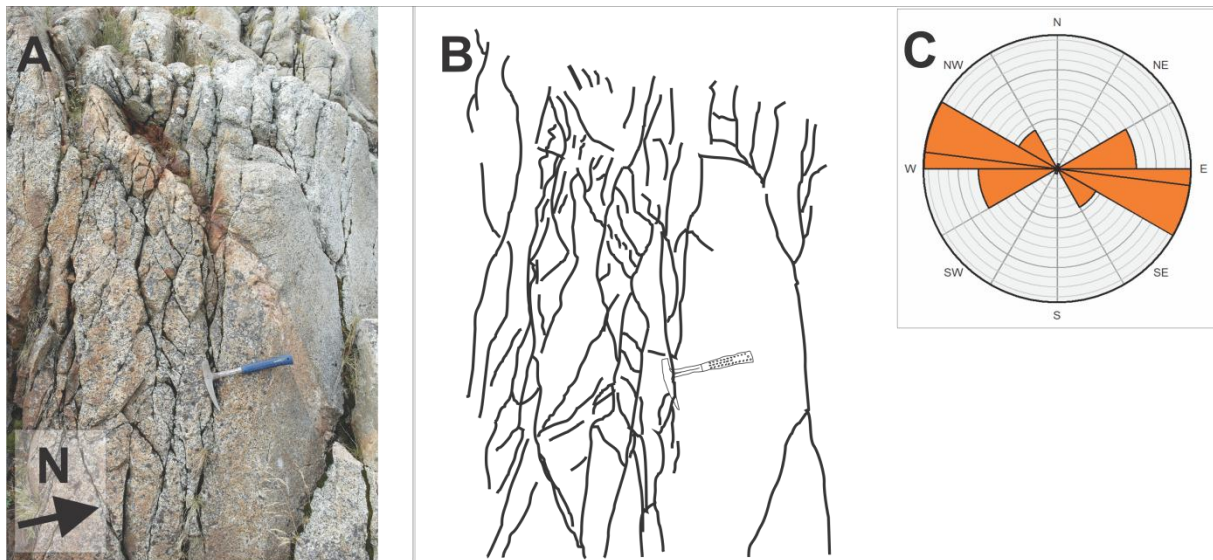


Figure 42 A) Anastomosing fractures at Senjehesten, striking approximately E-W and WNW-ESE. B) Sketch of the picture, better illustrating the geometry of the fracture zone. C) Rose plot of 106 fracture measurements from the fracture zone, illuminating the dominating fracture directions.

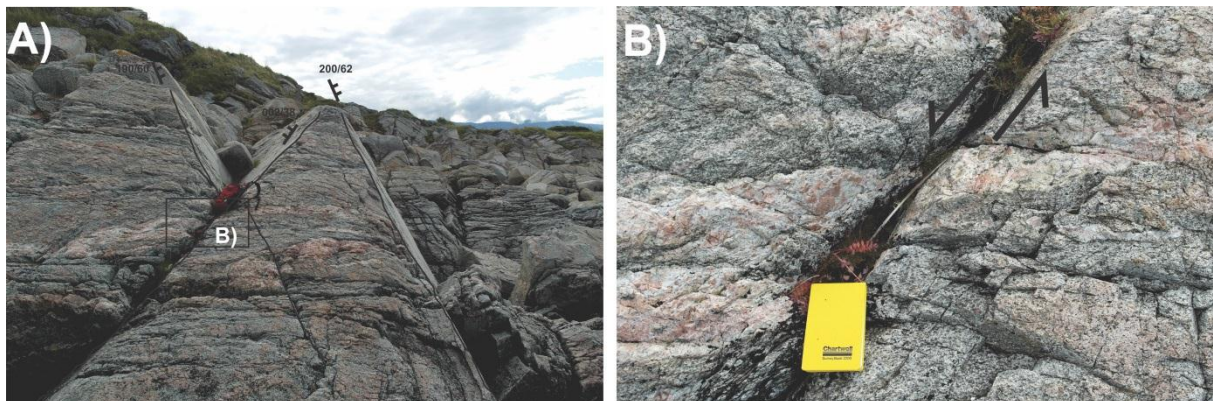


Figure 43 A) Possibly NNE-SSW striking, east/west dipping conjugate faults at Senjehesten offsetting a pegmatite vein down-to-the-east. B) Close-up picture of the east dipping fault displacing the pegmatite. For structural legend, see Common legend in Figure 12.

2.5.3.4 Summary and preliminary interpretations

The bedrock at Senjehesten consists of a diorite intruded by granitic pegmatites and a granitic gneiss (Fig. 41). The diorite-gneiss boundary follows the shoreline and thus appears to be folded (Fig. 41). DEM studies and fieldwork (Figs. 9, 36 & 41) have revealed a well-defined network of cross-cutting NNE-SSW to NE-SW and E-W striking fractures with precipitations of hematite, creating a rhombic fracture pattern in the area. This fracture pattern is, however, not always observed on smaller scales, as shown by a c. 50 cm wide fracture zone consisting of anastomosing, sub-vertical fractures striking WNW-ESE to NW-SE and ENE-WSW. Such fracture geometries can often be used to determine the shear sense along the fractures (Eig & Bergh, 2011), however, it is difficult to determine the exact origins of this fracture zone. Although it remains ambiguous, the complex nature of the fractures can likely be attributed to strike-slip movements (chapter 2.5.3.2).

The apparent down-to-the-east displacement of a pegmatite vein by a NNE-SSW striking fault (Fig. 43), is a more precise kinematic indicator - illustrating that normal faulting has taken place at Senjehesten. Together with an oppositely dipping fault/fracture of the same orientation (Fig. 43), this fault makes an apparent horst-graben system somewhat similar to the Andøya horst observed on the seismic data (Fig. 46).

The foliation and the diorite-gneiss boundary appear to be folded parallel to the shoreline. While the NE-SW trending fractures were observed to propagate through both the foliation and the lithological boundary, the E-W trending fractures bend into parallelism with the diorite-gneiss boundary (Fig. 41). Consequently, it is possible that the lithological boundary and/or ductile foliation acted as zones of weakness, and that the E-W striking fractures followed this zone rather than propagating through it.

3 Description of offshore brittle structures

3.1 Bathymetry data

Due to the great distance between the datasets, faults and fractures mapped onshore cannot be directly linked to faults mapped from seismic data offshore. Fortunately digital elevation models of bathymetry and onshore topography (see chapter 2.2) along with magnetic anomaly data (chapter 3.2), covering both offshore and onshore areas, make such a fault correlation possible. A key observation to verify the bathymetry as a valid correlation tool on the shallow shelf is where bathymetric lineaments (Fig. 9) can be traced onshore to known onshore fault outcrops, e.g. the Stonglandseidet fault zone, but it is even better when a seismic line cross-cuts an interpreted lineament, validating that it is truly a fault. Unfortunately, due to the limited seismic coverage in Andfjorden, such relationships rarely occur.

The seafloor/bathymetry floor has been studied in the inner and outer Andfjorden between Andøya and Senja (Fig. 9). The emphasis has been to separate structural elements from other submarine landforms, of mainly glacial origin, and to correlate those elements with structures observed in seismic data and onshore. The interpretation has been done on 50 meters grid from MAREANO (Fig. 9). The morphology of the area was thoroughly mapped by Plassen (2009) and Rydningen et al. (2013), and the interpretations in this chapter will thus be based on these papers.

3.1.1 General seafloor morphology

The bedrock of the seafloor in northwestern Andfjorden is thought to consist of sedimentary rocks from the Jurassic and the Cretaceous. Because of their relative soft and porous nature, the rocks were susceptible to erosion, and the Weichselian ice sheet thus created a rather flat and even seafloor that is now covered by glacial sediments with landforms such as streamlines, drumlins and moraines (Plassen, 2009; Rydningen et al., 2013). The glacial cover prohibits confident interpretation and mapping of brittle bedrock-lineaments, which clearly are far more visible onshore and in the inner part of the fjord, where the glacial cover is very thin (Fig. 9).

The transition from the outer to the inner fjord coincides with the change from Mesozoic sedimentary rocks to crystalline bedrock of Precambrian age (e.g. Plassen, 2009; Rydningen et al., 2013) The boundary makes a well-defined NNE-SSW to ENE-WSW trending lineament that is also easily observed on the seismic profile LO88R0713, but it is not necessarily as a fault (Fig. 47, see chapter 3.3).

The morphology of the inner shelf has previously been termed as a submarine archipelago (Plassen, 2009). The bathymetric data shows a large degree of variation,

frequently changing between protruding rock faces with a thin or patchy sediment cover and deeper depressions, usually defined by NE-SW or ENE-WSW striking escarpments, with larger sediment accumulations. There is also a small glacial trough between Skrolsvik on Senja and Bjarkøya, which contains drumlin and flow line structures similar to those observed in the outer fjord (Fig. 9). The trough is delimited by a significant NNE-SSW striking escarpment in the west and by a less defined (perhaps due to the sediment cover?) ENE-WSW striking escarpment in the south.

3.1.2 Lineations - Regional trends

The three sets of lineaments observed onshore (chapter 3.2; Fig. 9) were also observed on the bathymetric data (Fig. 9): (i) NNE-SSW to NE-SW, (ii) ENE-WSW to E-W and (iii) NW-SE. The lineaments are dominantly straight and show left- or right-stepping and relay geometry where the individual lineaments die out. Curved traces are even more prominent on the bathymetry, especially in inner Andfjorden, just north of Bjarkøya, where major NNE-SSW striking lineaments bend into parallelism with ENE-WSW striking ones (Figs. 9 b & c). The second form of curvature, where NNE-SSW striking lineaments appear to bend sharply towards the east, is also observed on bathymetry on the shelf north of Andøya (Fig. 9). Another important observation is the prominent ENE-WSW oriented lineament east and west of Stonglandet. Interestingly, this lineament can be traced onshore where it overlaps with the onshore part of the Stonglandseidet Fault Zone. Again, the NW-SE striking lineaments are the least developed, although the set can locally be observed to dominate the seabed relief in the inner parts of Andfjorden. Distinct features such as Toppsundet between Grytøya and Hinnøya, Kasfjorden on Hinnøya and Straumen on Andørja are all NW-SE trending, but do not appear as distinct scarps on the bathymetric data (Fig. 9).

3.2 Magnetic anomaly data

3.2.1 General description

The total magnetic field (TMF) of the study area is displayed in Figure 44. There is evidently a large variation in the TMF, and the area can be divided into zones based on the most prominent positive and negative magnetic anomalies (Fig. 44).

It is clear that most of the high-amplitude anomalies are located in the islands of Langøya, Andøya, Senja and Kvaløya. The inner areas are magnetically quiet except for a significant positive anomaly in the southeast. A pronounced low is also observed in the area north of Andøya and Senja, and seems to continue into Andfjorden where the susceptibility gradually increases southwards to prominent positive anomalies crossing the fjord (Fig. 44).

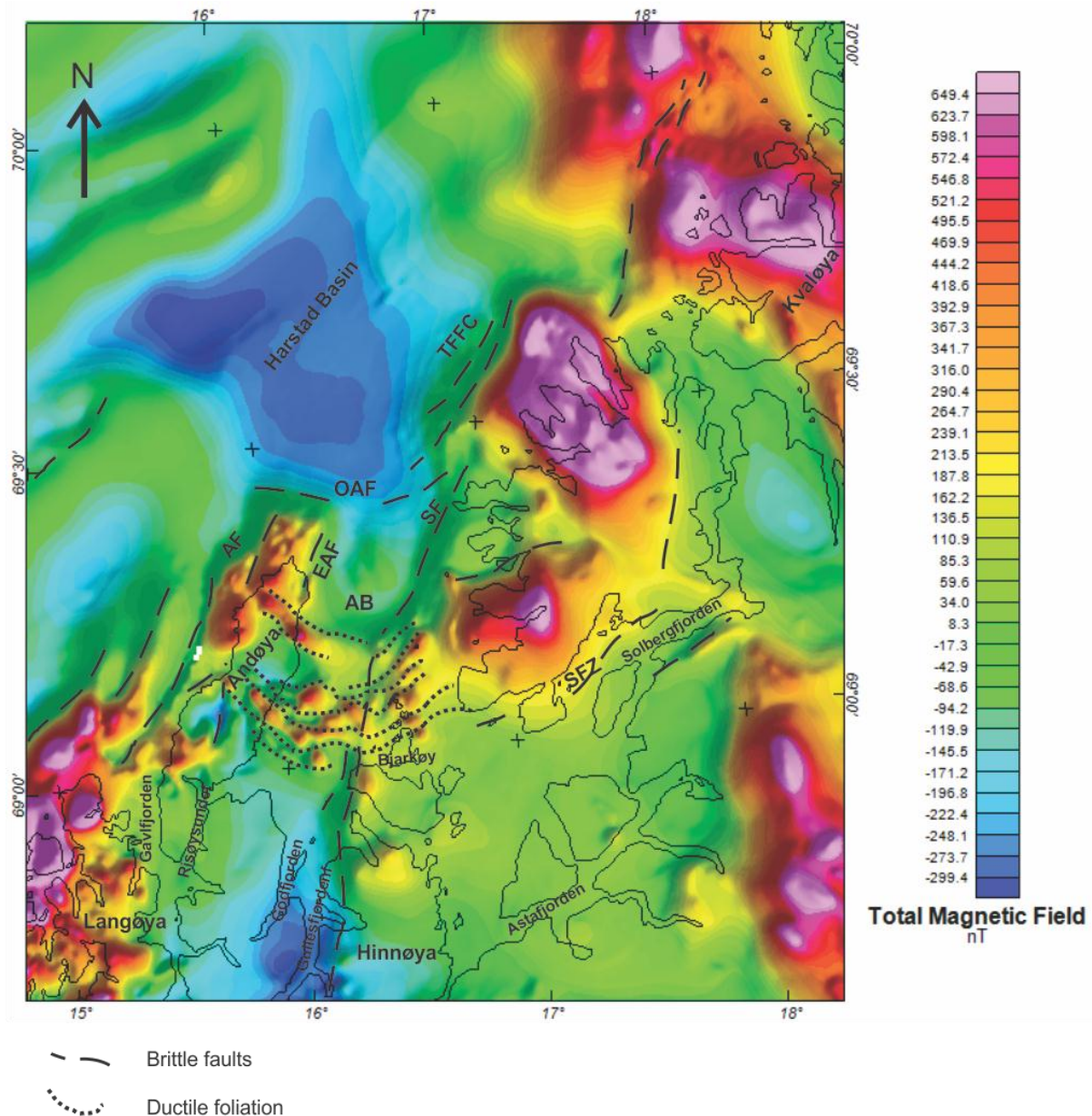


Figure 44 Total magnetic field of the study area (from NGU) and interpreted lineaments. Abbreviations are given in Table 1.

3.2.2 Lineaments

Defined either by a steep TMF gradient or continuous high or low values, the magnetic anomaly data also shows conspicuous lineaments that can be traced for several kilometers. Based on their direction, the lineaments can be divided into three groups: (i) A set of NNE-SSW trending lineaments that can be traced in a seemingly right- and left-stepping pattern from offshore Kvaløya, along western Senja into Andfjorden and possibly also into Gullesfjorden (Fig. 44). Narrow, parallel positive and negative NNE-SSW trending lineaments are also visible northwest of Andøya, where they can be traced onshore to Langøya (Fig. 44). (ii) A less conspicuous set of ENE-WSW to E-W trending lineaments. The lineaments define transitions from highly to less magnetic areas, and appear to be best developed east of the major NNE-SSW striking lineament traceable from Gullesfjorden to western Kvaløya (Fig.44).

(iii) A set of lineaments bending from NE-SW to WNW-ESE, that appear as parallel positive and negative anomalies in the inner part of Andfjorden. The lineaments can confidently be traced from onshore Andøya to the eastern part of Andfjorden and possibly all the way to Senja (Fig. 44).

The first set of lineaments is oriented parallel to major fjords such as Andfjorden, Gullesfjorden and Gavlfjorden (Figs. 2, 9 & 44), while the second set is oriented similar to smaller fjords such as Sifjorden on eastern Senja, but also larger features like Solbergfjorden (Figs. 2, 9 & 44). The second and third sets have similar orientations, but the third set bends in a way that is not observed anywhere else but in the section from Andøya across the inner Andfjorden to Senja (Fig. 44). It is therefore likely that the third set is unrelated to the second set, and originated as a separate and, possibly, local feature.

3.2.3 Relation to lithology

To interpret these observations, the magnetic anomaly data has been used in conjunction with several geological maps: Svolvær 1:250000 (Tveten, 1978), Narvik 1:250000 (Gustavson, 1974), Andøya 1:250000 (Henningsen & Tveten, 1998), Tromsø 1:250000 (Zwaan & Grogan, 1998). From these maps, it becomes clear that the most prominent positive anomalies in the outer islands can be attributed to granulite facies gneisses (Henningsen & Tveten, 1998; Zwaan & Grogan, 1998), while the high amplitude in the southeast probably is related to susceptible intrusives (amphibolite/meta-gabbro) within the Caledonian sequence (Gustavson, 1974). The Caledonian Nappes of Troms are otherwise practically non-magnetic (Olesen et al., 1997), as visualized by the magnetically quiet area in Figure 44.

The largest negative anomaly in the area is related to the southern segment of the Harstad Basin, where susceptible basement is down faulted and covered by a several kilometers thick sedimentary rock sequence (e.g. Brekke & Riis, 1987; Kløvjan, 1988; Gabrielsen et al., 1990; Olesen et al., 1997; Hansen et al., 2012; Indrevær et al., 2014). Directly south of the Harstad Basin, between Andøya and Senja, the magnetic low likely reflects the geometry of the Mesozoic Andfjorden basin (Fig. 44). The anomaly is clearly related to the Harstad Basin-anomaly, but the weaker signal indicates a significantly thinner sediment sequence in Andfjorden compared to the Harstad Basin. The broad, elongated NE-SW trending high and low anomalies southwest of the Harstad Basin (Fig. 44) are likely a continuation of the basin or related basins and/or basement ridges, while the northwestern most anomalies probably mark the onset of oceanic crust (Olesen et al., 1997)

The NE-SW to WNW ESE trending highs and lows crossing Andfjorden (Fig. 44) seem to be an offshore continuation of Proterozoic supracrustal rocks (Skogvoll Group) on Andøya (Olesen et al., 1997; Henningsen & Tveten, 1998). The positive anomalies likely

originate from lenses of almost pure magnetite, and the alternation between highs and lows seems to be parallel to foliation measurements onshore (Henningsen & Tveten 1998). The gabbro massif, which was observed in the Skarsteinsdalen Quarry and separate the two grabens in the Mesozoic basin onshore Andøya (Figs. 3 & 4), is clearly also traceable into the fjord (Fig. 44). However, it is difficult to say whether it continuous across to Senja or terminates against the conspicuous NNE-SSW striking lineaments of the eastern fjord, presumably defining the eastern boundary between sedimentary rocks and crystalline basement (Zwaan & Grogan, 1998; Figs. 2, 9 & 44 this work).

3.2.4 Relation to faults

The magnetic anomaly pattern also seems to coincide well with known faults (Figs. 1, 2 & 44). Lineaments of the first set with high TMF gradient and/or continuously low or high susceptibility appear to overlap with the traces of faults such as the Andøya fault (Henningsen & Tveten, 1998; Hansen et al., 2012), west of Andøya and the Senja fault (Zwaan & Grogan, 1998; Hansen et al., 2012) in eastern Andfjorden. The Senja fault is part of a lineament that can be traced from Gullsfjorden to west of Kvaløya (Fig. 44). This lineament can probably be linked to the Troms-Finnmark Fault Complex that defines the boundary between Mesozoic rocks and crystalline basement in Andfjorden and on the margin west of Senja and Kvaløya (Indrevær et al., 2014). The nature of the southern segment of this lineament (from inner Andfjorden to Gullsfjorden) is a bit more uncertain: It may either be a southern continuation of the Troms-Finnmark Fault Complex (Indrevær et al., 2014) or represent a Caledonian thrust (Gustavson, 1974; Olesen et al., 1997). If the latter is true, the Troms-Finnmark Fault Complex might die out in Andfjorden or step to the western side of Andøya where it continues as the Andøya fault.

The second set can also be related to faults. East of the Troms-Finnmark Fault Complex ENE-WSW to E-W trending lineaments can associated with the Sifjorden fault zone (Gagama, 2005), that defines the northern termination of the positive anomaly in southwestern Senja, and the Stonglandseidet and Grasmyskogen fault zones (Koehl, 2013) believed to define the boundary between the Precambrian basement and Caledonian nappes in eastern Senja and Solbergfjorden (Tveten & Zwaan, 1993; Olesen et al., 1997).

As mentioned, the third set is presumably linked to ductile foliation in Proterozoic supracrustal rocks, but this does not exclude the possibility that the lineations actually are caused by a dense population of faults: This rock unit may border to the Mesozoic rocks of the Andfjorden basin, and the lineations may represent a tectonic boundary between the two lithologies. The boundaries of the Andfjorden basin will be further discussed in chapters 3.3 and 4.

3.3 Seismic data

3.3.1 Introduction

This part of the thesis is a geological investigation based on interpretation of seismic data from the outer Andfjorden and southern Troms II continental margin (Fig. 45) with emphasis on faults, their relation to basin and ridge features, and the structural evolution of the area.

3.3.2 Database

The seismic database used in this investigation consists of conventional 2D lines collected by NPD, WesternGeco, Norsk Hydro. The most important seismic sections chosen for this study, are LO88R0711, LO88R0713 and LO88R0752 collected by Hydro in the Andfjorden area in 1988 and reprocessed by StatoilHydro in 2007 (Fig. 45). These three sections are thoroughly investigated with emphasis on the main faults, their geometry and orientation, and relationship to the evolution of the Andfjorden and Harstad Basins.

3.3.3 Seismic stratigraphy and key horizons

Limited well data from the studied areas offshore hinders a complete stratigraphic analysis, in part because the complex structuring and quality of the data makes it difficult, and partly because it is beyond the scope of this study.

The offshore descriptions of the stratigraphy relevant for this study, is based on interpretation of seismic data and a few drilled well logs. The shallow drill cores 7018/4-U-2, 7018/5-U-1, - U-2, -U-6 and 7018/7-U-1 in the Troms III area as well as the 6814/04-U-1 and -U-2 cores from the Nordland VII area provide some stratigraphic information valuable to the geological understanding of Troms II and Andfjorden. However, correlation of well data to the seismic profiles has been difficult due to the limited spacing (in Andfjorden) and quality of the seismic section. Tormod Henningsen's (pers.com. 2014) interpretation of the Top Basement horizon has been used to date the lowermost reflector in Andfjorden, southern Troms II and northeastern Nordland VII. Henningsen's (pers.com. 2014) interpretation is based on picks from IKU wells in Nordland VI and two seismic lines without well information, but where it is possible to interpret reflectors lapping onto what *must* be the basement. This reflector outlines well the general geometry of the basement configuration of the area, and is in accordance with gravimetric bouguer anomalies (Henningsen, pers. com., 2014). The interpreted horizons in the overlying strata are those relative continuous over larger areas and with the clearest seismic character, compared to the more diffuse reflections of e.g. basement strata. These were not necessarily located at the same stratigraphic level on each seismic section, but, for simplicity, the interpreted horizons on key profiles were correlated, separating the strata into three main sequences based on lithostratigraphic and sequence

stratigraphic correlation between cored successions at Troms III, Nordland VII and Andøya (Smelror et al., 2001; Bøe et al., 2010; Fig. 7 this work):

Sequence 1: Crystalline, Precambrian rocks

Sequence 2: Jurassic strata

Sequence 3: Cretaceous strata

Based on a well-defined unconformity observed in section LO88R0752, the Cretaceous strata was locally subdivided into Lower/Mid and Upper Cretaceous (Fig. 46). The seismic reflectors mapped in this study are listed in Table 3.

Table 3 Seismic reflectors mapped in this study

Reflection	Abb	Properties	Well ties in study area
Reflector 1 - top Basement	R1	Strong continuous reflector separating overlying stratified units from an underlying transparent or chaotic unit	6710/03-U-03 6814/04-U-02
Reflector 2 - Base Cretaceous	R2	Semi-continuous reflector occurring across the study area.	6710/03-U-01 6814/04-U-02
Reflector 3 - Base Upper Cretaceous	R3	Local, high amplitude reflector, represented by an angular unconformity, gradually onlapped by younger seismic units	6711/04-U-01

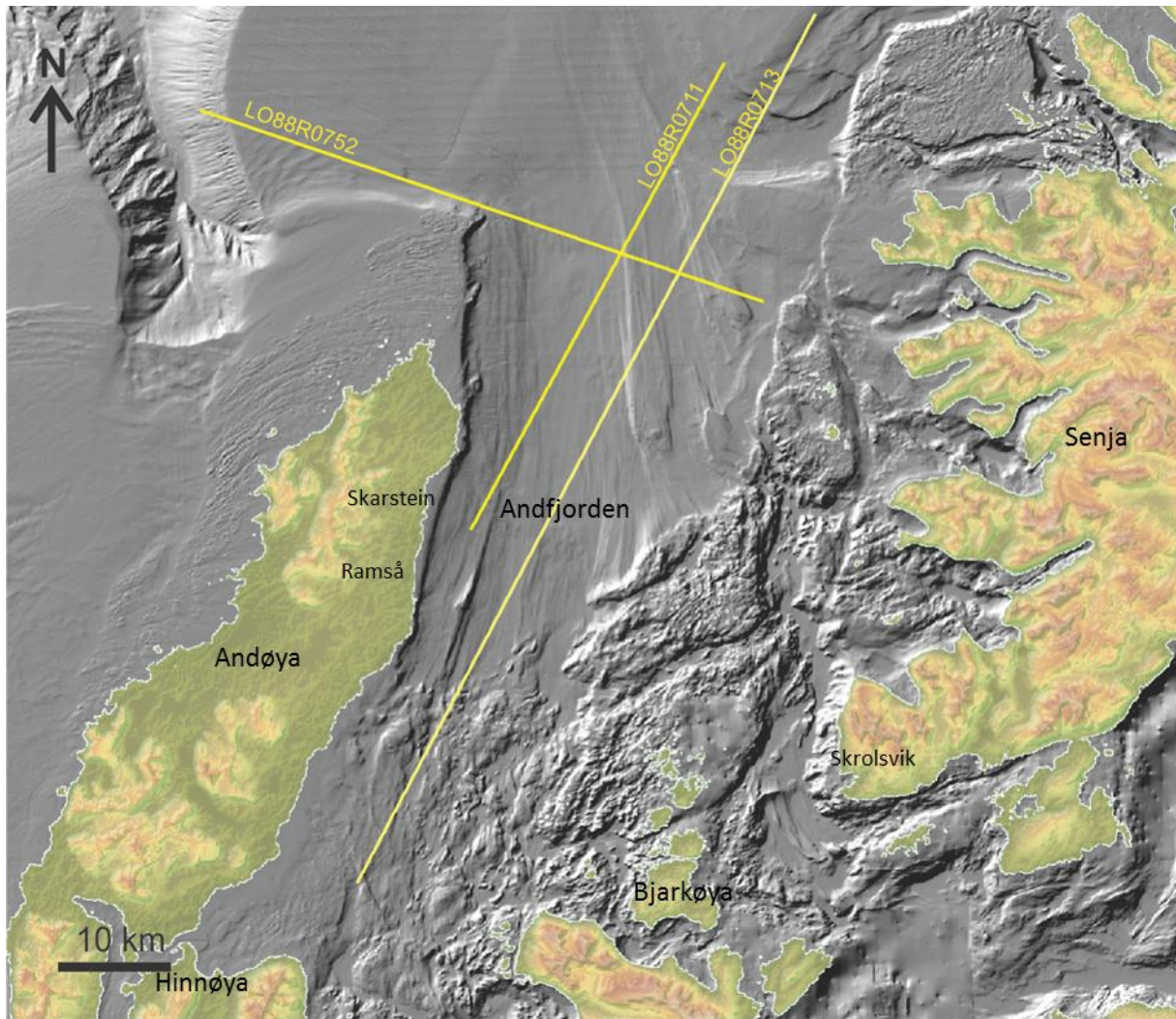


Figure 45 Seismic lines in Andfjorden interpreted for this work.

3.3.4 Seismic interpretation

3.3.4.1 Seismic section L088R0752

This WNW-ESE oriented section is located in outer Andfjorden and displays the Andfjorden basin and the Harstad Basin separated by the offshore continuation of the Andøya horst (Fig. 46). Since the section crosses the trend of the Andfjorden basin, it is significant to understand the structural configuration of the basin with its eastern and western boundary faults.

The section is roughly divided into three sequences bounded by the seismic reflectors 1 and 2. The full architecture of the Harstad Basin is not revealed in this section, but in the Andfjorden basin the sequences seem to be contained in two half-grabens (Fig. 46). Reflector 1 is the deepest and most continuous in both basins, and separates Sequence 1 from Sequence 2. Sequence 1 is characterized by a very chaotic seismic signal, and it is not possible to observe any stratification. Sequence 1 is therefore interpreted to consist of Precambrian crystalline basement rocks, and Reflector 1 thus defines the base of the

Andfjorden basin. Sequence 2, however, appears to be well-stratified, and has a fairly constant thickness in the two basins. It consists of parallel medium to low frequency seismic reflectors generally dipping to the east, that are offset by several west dipping planar faults, displacing Reflector 1 by as much as 0.5 s in Andfjorden and c. 3.0 s in the Harstad Basin. The sequence may lap on to the Andøya horst, but it is also possible that it is separated from the horst by east dipping curved faults, as indicated in figure 46. Sequence 2 represents the oldest sedimentary rocks in the Andfjorden basin, and can likely be correlated with the Mid-Jurassic fining upwards sequences onshore Andøya ((Dalland, 1974, 1975, 1979, 1981). It is also possible that the lower part of Sequence 2, consists of rocks related to the enigmatic Holen Fm onshore (see chapter 1.2.4), but this cannot be confirmed with the present data set.

Sequence 3 is significantly thicker than Sequence 2, ranging from about 2.0 s TWT in the Andfjorden basin to c. 3. s TWT in the Harstad Basin. The two sequences are separated from each other by Reflector 2, which is fairly continuous, but not as distinct as Reflector 1. The internal reflectors of Sequence 3 dip mostly to the east, and are seemingly parallel to those in Sequence 2. However, the dip seems to decrease upwards in the stratigraphy, and the upper part of the sequence consists of parallel, almost horizontal seismic reflectors that lap onto an erosional unconformity - Reflector 3. Internal variations like onlap, truncations and wedge shaped bodies are also common, especially in the Harstad Basin and the eastern part of the Andfjorden basin (Fig. 46).

The faults evidently also affect Sequence 3, creating numerous rotated fault blocks that divide the Andfjorden Basin into several terraces and sub-basins. A pronounced increase in thickness is observed towards NW dipping faults, with gradual westward onlap onto Reflector 2.

Faults mostly affect the lower and middle part of the sequence, and seemingly die out in the upper part. This is evident from the eastern part of the Andfjorden basin, where all the west dipping faults are truncated by the same reflector (Fig. 46). Sequence 3 is the upper unit of sedimentary rocks and can likely be correlated with the Early Cretaceous fining-upwards sequence onshore Andøya (Fig. 7). However, a well-defined unconformity is observed in the upper sequence in the western Andfjorden basin. Reflectors gradually lap on to the unconformity, and are interpreted to represent Upper Cretaceous rocks, a unit that is not present in the basin onshore Andøya.

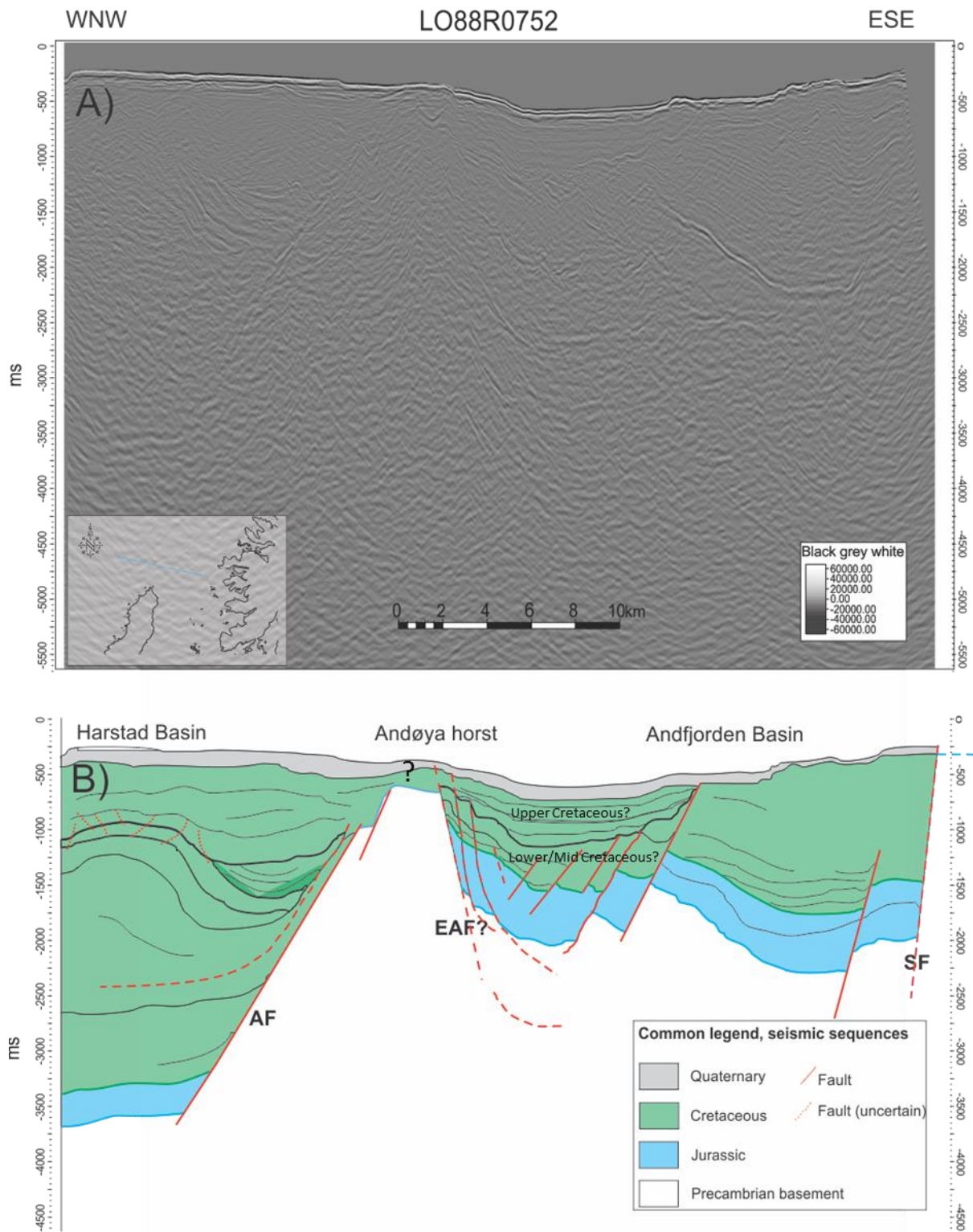


Figure 46 A) Uninterpreted seismic section LO88R0752, blue line in the index map. B) Interpretation of seismic section LO88R0752. Jurassic and Cretaceous sedimentary rocks and unconsolidated Quaternary sediments overlie Precambrian crystalline basement rocks. The Harstad (west) and Andfjorden (east) basins are separated by the offshore continuation of the Andøya basement horst (may continue up to the seafloor). Andfjorden is characterized by dominantly W dipping faults. Abbreviations are given in Table 2.

Seven NW dipping faults are identified inside the Andfjorden part of the profile. The faults can be traced from the basement upward until they terminate in the lower to middle part of Sequence 3 (Fig. 46). The faults appear as diffuse, narrow zones, cross-cutting internal

basin strata and seemingly offsetting the reflectors in a normal manner (Fig. 46). They are steep planar, creating a domino style pattern of rotated fault blocks, dividing the Andfjorden basin into several terraces and sub-basins. Notably, the basin-internal basement ridges all seem to be linked to the footwall of such NW-dipping faults. The off-set character indicates they are normal faults with hanging-wall movement down-to the NW. The westernmost of the NW dipping faults (The Senja fault) is not observed on the seismic data, but must exist somewhere close to the eastern limit of the section, as it marks the boundary between the Andfjorden basin and the basement rocks of Senja further east (Zwaan & Grogan, 1998).

The western termination of the Andfjorden basin against the basement rocks on Andøya is more ambiguous. The sedimentary strata may lap conformably onto the basement rocks, but may as well be cut by a major, steep SE dipping (listric?) fault, which offsets the top Reflector 1 by almost 2 s TWT (Fig. 46). The dip of the fault apparently decreases with depth, yielding listric geometry. Three more SE dipping faults are inferred just east of this master fault, synthetic and seemingly sharing a similar geometry, but with significantly less offset. These faults are not as apparent as the NW dipping faults, but are postulated based on the wavy geometry of the sedimentary strata in this area.

The basement high in the central part of the studied section (Fig. 46) is believed to be the offshore continuation of the Andøya basement horst, and its western boundary is characterized by another NW dipping master fault, which down-drops Reflector 1 to almost 4 s TWT (Fig. 46). Planar disturbances in the seismic signal can be observed in the basement, possibly representing planar to listric fault traces and/or a moderately dipping detachment zone in the continuation of this master fault. Another detachment fault zone is postulated within the Sequence 3 west of Andøya, as it underlies a huge upwelling of strata that increases the thickness of Sequence 3 by at least 0.2 s TWT and where the strata dip southeastward toward the fault zone. The overall structure resembles a roll-over anticline, with associated synclines and possibly also a wedge-shaped graben against the Andøya horst (cf. Gibbs, 1984). This overall anticline structure also affects the overlying by a number of planar normal faults at its top, indicated by numerous small offsets. These faults do not sole out into a detachment, but die out downwards, penetrating 0.2 to 0.8 s TWT beneath the fold's crest.

3.3.4.2 Section L088R0713

This NE-SW oriented section traverses the entire Andfjorden basin and continues northwards into the Harstad Basin, providing important information about the northern and southern termination of the Andfjorden basin (Fig. 47).

Individual reflectors, strata configurations, ridges, basins and associated faults and structures are more difficult to detect than in the section L088R0752. However, the same

rock sequences are observed in this section, and are identified by the same criteria as in section LO88R0752. Sequence 1 outcrops on the seafloor in the southwest and dips in a stepwise manner to the north east, until it becomes almost horizontal to slightly concave upward in the outermost part of the fjord (Fig. 47). At the northern termination of the Andfjorden basin, in the transition to the Harstad Basin, Reflector 1 is abruptly down dropped to about 3 s TWT and deeper.

Sequence 2 consists of undulating, parallel, high frequency seismic reflectors with a generally weaker signal than in section LO88R0752 (Fig. 46). It laps conformably onto Reflector 1 in the southwest, and increases in thickness towards the northeast, up to a maximum of 0.4 s TWT in the Harstad Basin

Sequence 3 also appears to lap onto Reflector 1 in the southwest, and consists of several well-displayed internal reflectors dipping to the NE. In the Andfjorden basin these are parallel with a wavy character, and have an apparent onlap relationship. The sequence increases in thickness towards the northeast, but interpretation and tracing of seismic reflectors into the Harstad Basin is problematic, as the signal here is much more chaotic, and also disturbed by a seabed multiple masking the dip of true reflectors. Nonetheless, it is evident that Sequence 3 experiences a massive and sudden thickness increase upon entering the Harstad Basin. While Sequence 3 might extend all the way to the seafloor, it seems as the upper reflectors are truncated against an unconformity, and that there is an overlying cover of unconsolidated (glacial?) sediments. A transparent unit southwest of the basement high, image this cover which rest directly on Reflector 1, but it is also possible that the unit is made up of rocks belonging to Sequence 2 or 3.

When present, faults are recognized as zones of disturbed and offset seismic signals rather than distinct seismic reflectors. Sequence 2 and 3 conformably lap onto Sequence 1 and does not seem to be affected by faults except for a major off-set of strata (c. 1 s TWT) by a NE-dipping fault in the northern termination of the Andfjorden basin. The offset character indicates that it is a normal fault, with hanging-wall movement down to the NE. As the west dipping faults in section LO88R0752, this fault seems to die out in the lower to middle part of Sequence 3. Two minor synthetic faults are interpreted south east of this fault, and are identified by apparent offsets of Reflector 1.

The stepwise shape of Reflector 1 allows for three low angled listric faults dipping to the NE to be postulated (Fig. 47). These potential faults may merge at a detachment zone that continues into the basement below the Harstad Basin, where the steep terminate against it or merge into it. If these faults actually exist, the relationship between Sequence 1 and sequences 2 and 3 is tectonic rather than passive onlapping of the strata

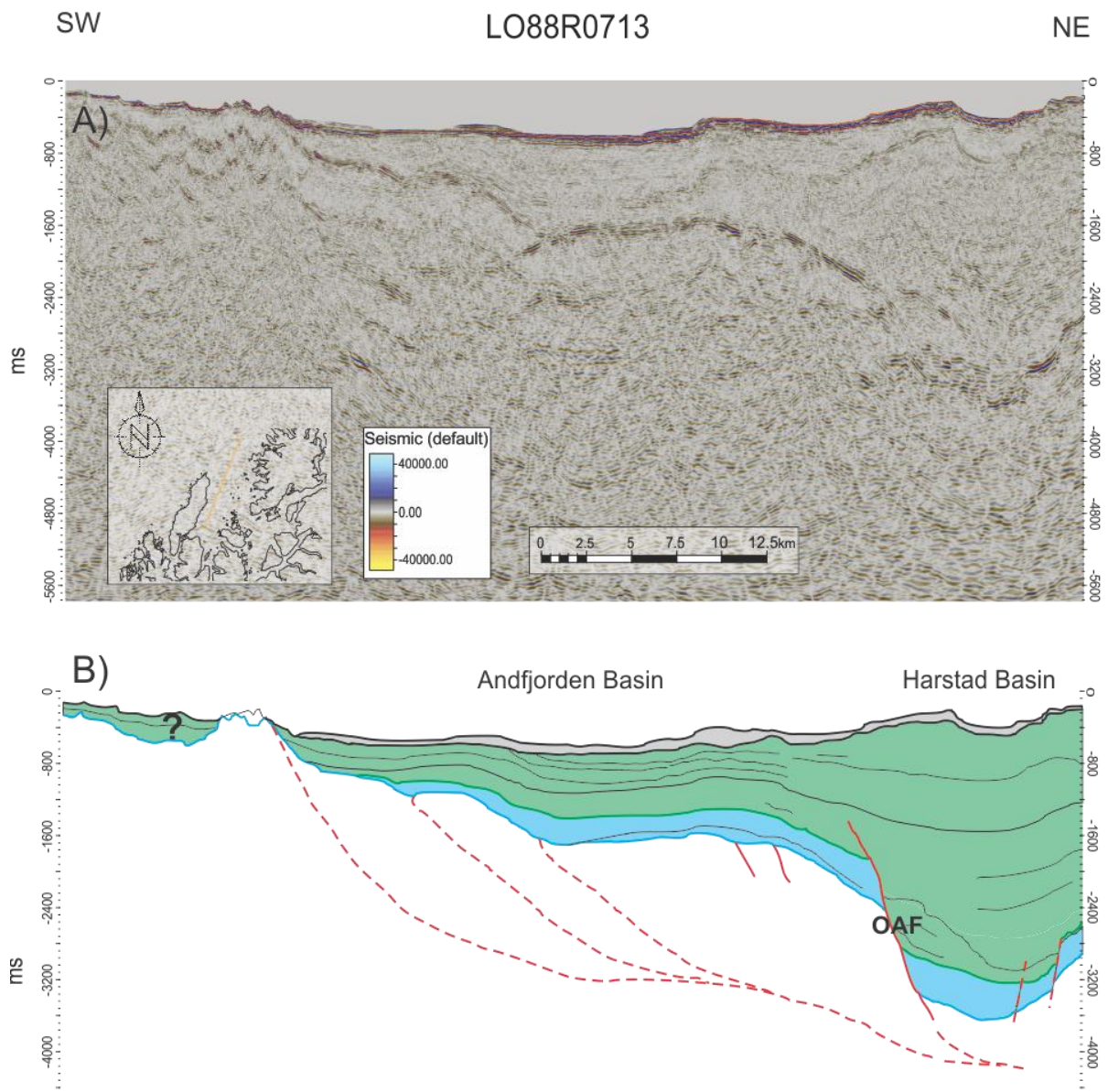


Figure 47 A) Uninterpreted seismic section LO88R0713, yellow line in the index map. B) Interpretation of seismic section LO88R0752. Jurassic and Cretaceous sedimentary rocks and unconsolidated Quaternary sediments overlie Precambrian crystalline basement rocks. The thickness of the Andfjorden basin (south) gradually increases towards the north. A significant increase of the Cretaceous strata is observed towards the Outer Andfjorden fault defining the boundary between the Andfjorden and Harstad basins. For legend, see Figure 46. Abbreviations are given in Table 1.

3.3.4.3 Section LO88R0711

LO88R0711 is also oriented NNE-SSW, but is located a few kilometers closer to Andøya than LO88R0713 and does not extend as far into Andfjorden (Fig. 48). Faults are also generally easier to detect, providing valuable information about the internal structure of the Andfjorden basin.

The seismic signal is generally weak, but two relatively well-defined reflectors (Reflectors 1 and 2) define the same stratigraphy as for the two previous sections. Sequences 2 and 3 are semi-parallel and overly the chaotic Sequence 1. As in section

LO88R0713, the sequences dip to the northeast, and are almost flat lying to concave upwards in the central part of the section, and both truncations and onlap relationships are observed within the upper sequence (Figs. 47 & 48). The central part seems to be downfaulted along a NE dipping fault in the southwest, and a SW dipping fault c. ten kilometers to the northeast, creating a seemingly dome-shaped graben. The southwestern fault appears as a steeply dipping individual reflection within Sequence 2 and in the upper part of Sequence 1, and is interpreted to continue well into Sequence 3, where it is characterized by a steep, narrow zone with noise and diffuse reflectors. The northeastern fault however, is identified by a distinct break in Reflector 1, which is offset c. 0.3 s TWT down-to-the-southwest. The throw of the southwestern fault is significantly less, as Reflector 1 and 2 are down faulted c. 0.1 s TWT down-to-the-northeast.

Just two or three kilometers northeast of the dome-shaped graben, a major NE-dipping fault defines the northern termination of the Andfjorden Basin. Movement appears to be down-to-the-northeast, as Reflector 2 is down dropped c. 2 s TWT. Reflector 1 however, dips steeply parallel with the fault and is apparently offset from c. 1.5 s TWT downwards to c. 3 s TWT over a distance of less than four kilometers. The fault seems to extend well into Sequence 3, and possibly up to the seafloor. Downwards, it achieves a more listric geometry, and merges into near-flat lying Sequence 1-seated bowl-shaped reflections that may be expressions of a detachment. A major synthetic fault is observed within Sequence 3 northeast of the boundary fault. It is identified by the offset and wavy geometry of two internal reflectors, that create apparent roll-over structures similar to the one observed in section LO88R0752 (Figs. 46 & 48). Apparent anticlines and drag effects are also observed along the northeastern boundary fault of the graben.

The uppermost seismic reflectors in Sequence 3 of the Harstad Basin, display an irregular, wavy geometry, creating units that pinch out towards the northeast. These bodies may be sedimentary wedges deposited in small basins created by rotated fault blocks internally in Sequence 3.

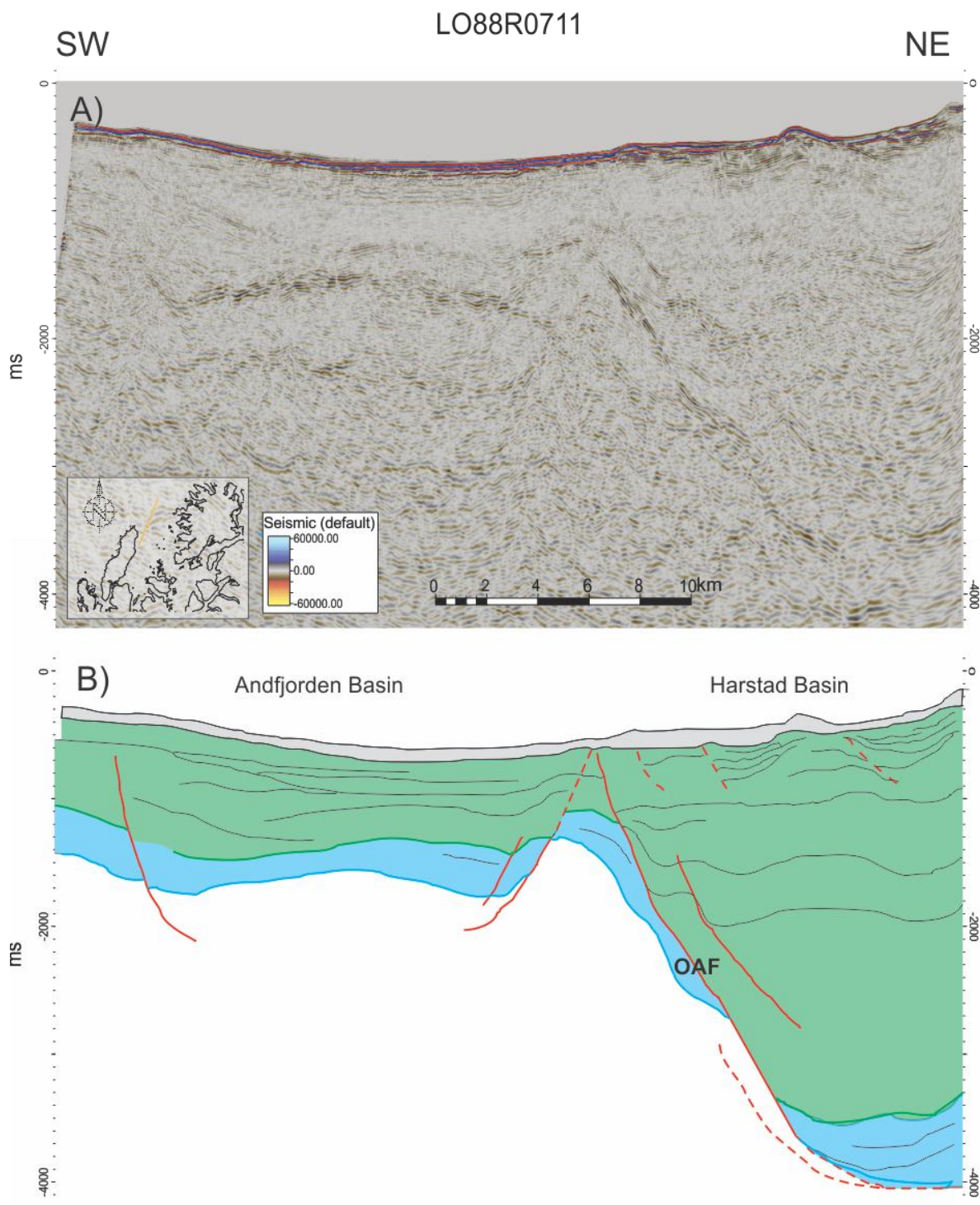


Figure 48 A) Uninterpreted version of the seismic section LO88R071, yellow line in the index map. B) Interpretation of the seismic section LO88R0752. Jurassic and Cretaceous sedimentary rocks and unconsolidated Quaternary sediments overlie Precambrian crystalline basement rocks. The thickness of the Cretaceous sequence increases dramatically against the Outer Andfjorden fault defining the boundary between the Andfjorden and Harstad basins. For legend, see Figure 46. Abbreviations are given in Table 1.

3.3.5 Summary and preliminary interpretations

Based on the interpreted seismic data, two sequences of sedimentary rocks have been defined: (i) A Mid Mesozoic (Jurassic?) sequence that displays a fairly constant thickness throughout the study area, and (ii) an Upper Mesozoic (Cretaceous?) sequence that

experiences a gradual thickness increase from the inner to the outer Andfjorden basin, and pronounced growth towards basin bounding faults striking c. NNE-SSW and c. E-W. These faults are part of the two main fault populations detected in the area. The NNE-SSW set dominantly dips to the west, while the E-W striking set dips both north and south.

A sandy limestone unit (the Holen Formation) overlying weathered basement in boreholes I, II and V on Andøya (Dalland 1974) may be the offshore expression of Sequence 2. However, since the great lithological contrast to overlying Mid Jurassic sandstones does not show up as a significant seismic reflection within the pre-Cretaceous sequence, this may indicate that the Holen Formation is absent in the offshore portion of the Andfjorden basin. The sandy limestone obtained in boreholes I, II and V may then represent basement marbles, perhaps from the marble rich Vet Formation in the Proterozoic Skogvoll Group (Midbøe, pers com 2013). Another possibility is that the boundary thought to represent an unconformity between Lower/Mid Cretaceous and Upper Cretaceous rocks in Andfjorden (Fig. 46) rather represents the base Cretaceous. If this is true, the majority of the sedimentary strata in the Andfjorden basin is Jurassic or even older, perhaps Permian or Triassic, and possibly related to the well-documented Permian rift event in the West Troms Basement Complex (cf. Olesen et al., 1997; Davids et al., 2013). Based on lithostratigraphic correlations between Nordland VII, Andøya and Troms II (Smelror et al., 2001; Bøe et al., 2010; Fig. 7 this work) this theory remains unlikely, and this study will therefore continue to operate with the sedimentary sequences defined earlier. However, Brekke and Riis (1987) argued for Permian rocks in Andfjorden, and this cannot be completely ruled out without a core of the succession.

In order to infer the relative timing of these basin-boundary faults, various criteria can be used, such as integrating seismic architecture relative to sedimentation (pre-, syn-, post-rift), lateral thickness variations adjacent to growth/syn-depositional faulting offshore (cf. Hansen et al., 2012), in conjunction with onshore cross-cutting relationships between different fault populations (cf. Bergh et al., 2007). Since cross-cut relationships observed onshore are not conclusive alone, the timing of offshore faults is solely based on the two former seismic criteria. The correlation of the seismic sequences to the stratigraphy of the Mesozoic basin onshore Andøya and drill cores from Nordland VI, VII and Troms II (Fig. 7), yields constraints to the relative timing of the faults.

The two major fault sets, dipping WSW and N, respectively, both extend from the Precambrian basement upwards, through the Jurassic rocks before they die out somewhere within the Cretaceous strata. The upper terminations of the faults are often hard to detect; sometimes due to the quality of the seismic data, but more importantly because of the varying thickness of the Cretaceous sequence and the lack of traceable reflectors that can be used for correlation. The lack of pronounced thickness variations in the Jurassic

sequence may indicate that sedimentation took place before faulting was initiated, or during the *rift initiation* stage, where the rate of fault displacement is relatively low and sedimentation keeps pace with subsidence (e.g. Prosser, 1993; Hansen et al., 2012). On the other hand, the conspicuous growth of the Cretaceous strata towards major faults (Figs. 46, 47 & 48) is evidence of a blatant increase in the rate of fault displacement, i.e. when the rate of subsidence outpaces sedimentation rates (Hansen et al., 2012). The increased rate of faulting may have caused the formation of syn-rift structures, including the many intrabasinal highs and sub-basins within the Andfjorden basin (Fig. 46). The major NNE-SSW (Fig. 46) and E-W (Figs. 47 & 48) striking faults confined to the Cretaceous sequence then likely developed as response to the great accumulation of sediments (cf. Gibbs, 1984), resulting in the formation of the major roll-over anticline and the wedge-shaped graben in the Harstad Basin northwest of Andøya (Fig. 46). A secondary result of the subsidence of a continental margin with synchronous accumulation of sediments is that a new, upper set of listric faults will be generated (Gibbs, 1984). Growth of the anticline may then have induced gravitational instability within the syn-kinematic sediments and development of a range of shallow, gravity-driven failure mechanism, although outer arc bending of a fold or crestal collapse in response to localized extension over the outer arc of the culmination (Morley, 2007). The gradual thickness increase of the Cretaceous unit from the inner to outer Andfjorden basin (Fig. 43), indicate that subsidence was greater in the outer fjord, and that this probably occurred synchronously with the faulting, and might even be explained by variable slip along the Senja fault that defines the eastern border of the Andfjorden basin (Fig. 46).

Faults do not extend through the entire sequence, and in seismic section LO88R0752, the faults in the western Andfjorden basin all terminate at a well-defined angular unconformity, that may also be traced westwards into the Harstad Basin (Fig. 46). Reflectors in this upper sequence gradually lap onto the unconformity, and are interpreted to represent the Upper Cretaceous. The unconformity is thus interpreted to define the boundary between the syn-rift Lower Cretaceous rocks from post-rift Upper Cretaceous rocks. Upper Cretaceous rocks are not identified on Andøya, but a similar relationship between Lower and Upper Cretaceous rocks was described from the Nordland VI area by (Hansen et al., 2012).

In its most simple form, the architecture of the Andfjorden basin seem to represent that of a half-graben, bounded by the major west-dipping Senja fault (Hansen et al., 2012) in the east and with a gradual onlap towards Andøya basement horst in the west (Fig. 46). The sedimentary rocks also seem to lap onto basement in the inner basin, and the thickness increase within the sequences towards the northeast, can probably be explained by differential slip along the Senja fault. The boundary to the Harstad Basin is defined by a major E-W striking fault, the Outer Andfjorden fault (Figs. 47 & 48). It is also possible that the western boundary of the basin is bounded by major east-dipping faults, making the basin a

full graben, but the nature (and even the existence) of these faults is uncertain. Several faults synthetic to the Senja fault, and synthetic and antithetic to the Outer Andfjorden fault, further subdivide the basin into several-sub-basins and ridges (Figs. 46, 47 & 48) making the internal structure of the basin more complex than the simple half-graben model.

4 Discussion

The aim of this project has been to correlate onshore and offshore brittle faults and fractures related to the Andfjorden basin by combining detailed structural fieldwork with interpretations of modern techniques such as DEM data, bathymetry data, magnetic anomaly data and seismic data. This correlation will be used to discuss the structural development of the Mesozoic basins onshore Andøya and in Andfjorden, and further, to discuss fault timing and kinematics and the implications of these findings to the overall margin evolution.

The field localities have been described individually, and by using the brittle fault and fracture characteristics in conjunction with kinematic data, it has been possible to propose a relative timing constraint between the different fracture sets. Correlating the stratigraphy from wells to the seismic stratigraphy also made it possible to infer the absolute age of faulting relative to sedimentation in the Andfjorden basin. In combination, this has been used to develop a model for the evolution of the Mesozoic basins onshore Andøya and in Andfjorden.

4.1 Discussion of onshore structures relative to the Andfjorden basin

Detailed studies of faults and associated fractures have been performed at several locations in and around Andfjorden, with aims of identifying major boundary faults to the Mesozoic sedimentary basins onshore Andøya and in Andfjorden. However, most of the localities did not showcase such faults, but typically displayed higher frequencies of fracture zones of varying width and intensity. The dominant fault-fracture sets, strike NNE-SSW to NE-SW, ENE-WSW to E-W and approximately NW-SE, and a number of them were studied in both map-view and cross-sections (see chapter 2.3).

The bedrock of the onshore studied areas is mostly Precambrian TTG-gneisses and magmatic and intrusive rocks such as gabbros and dolerite. Generally, brittle faults and fractures are oblique to the foliation of the basement gneisses. Sometimes, however, bedrock inhomogeneities such as lithological boundaries and foliations appear to influence the networks of brittle faults/fractures, e.g. the bending of E-W striking fractures into parallelism with the NE-SW striking diorite-gneiss boundary at Senjehesten (Fig. 41), steep NW-SE striking fractures sub-parallel to the foliation at Skarstein and Fiskekenes (Figs. 15 & 20), increase in fault/fracture frequency towards lithological boundaries in the Sundsvoll quarry (chapter 2.4.1). Such observations are consistent with observations from other localities in Lofoten and Vesterålen (cf. Bergh et al., 2007; Hansen et al., 2009) and within the West Troms Basement Complex (cf. Koehl, 2013; Indrevær et al., 2014), indicating that ductile basement fabrics may have controlled the development of brittle faults and fractures, at least locally.

The NNE-SSW to NE-SW striking fractures are most abundant in the studied areas near the Andfjorden basin, although they might be under-represented elsewhere. These fractures commonly dip steeply either to the NW or SE, with a slight predominance of dip to the NW. In fracture mechanics, the displacement field of fractures is commonly classified into three different modes: Mode I, II and III (Kulander et al., 1979). Mode I fractures are characterized by extension perpendicular to the fracture walls, Mode II represents slip perpendicular to the edge while Mode III involves slip parallel to the edge of the fracture (Kulander et al., 1979). At outcrop scale the NNE-SSW to NE-SW striking fractures can be interpreted as steeply dipping, continuous extensional fractures (Mode I), but closer inspections revealed they may be both shear fractures (Mode II) and hybrid fractures (combinations of Mode I and Mode II and/or Mode III) with left- and right-lateral displacement and right-stepping patterns (Figs. 31, 38, 39 & 42).

Although shear indicators (e.g. slickensides) are generally absent on fault-fractures on Andøya, the presence of cataclastic fault rocks along steep, NE-SW striking fractures at Skarstein (Figs. 17 & 18), with apparent down-to-the-east movement, support they are true normal faults. Numerous slickensides have been observed on high-frequency fracture domains on ENE-WSW and NNE-SSW trending fractures in quarries on Andøya, Bjarkøya and on NE-SW trending fractures in the small quarry in Skrolsvik (Figs. 23 b, 28, 35 & 40), suggesting the fractures may be part of two major rhombic shaped fault systems. The sense of shear on these faults is largely similar, i.e. normal dip-slip and both dextral oblique and sinistral oblique-slip components (Figs. 28 & 40). Moreover the offset of a pegmatite vein along a NE-SW striking fracture at Senjehesten (Fig. 43), also revealed down-to-the-east movement, as was inferred for the Skarsteinsdalen fault (Fig. 23).

The genetic relationships between the NE-SW striking and the c. E-W striking faults/fractures is uncertain, but of great importance. Sometimes the two sets are observed to bisect each other systematically (Figs. 31 & 38), while clockwise bending (rotation) of the NE-SW striking fractures towards the E-W striking fractures are observed at Skarstein, Fiskenes and Sundsvoll (Figs. 15, 20, 22 & 32). The bisecting nature and geometry of the fractures suggest they represent a *fundamental joint system* (Mandl, 2005) consisting of an older systematic set of joints and a younger, less systematic set orthogonal to each other. Consequently, they are not temporally linked (see chapter 4.4). Given the small acute bisecting angle ($60-70^{\circ}$) between them, and the numerous evidence for shear, it can be argued that they are conjugate shear fractures related to pure shear deformation (Mode II) and/or as oblique Riedel shear fractures (R and R') with dextral (NE-SW) and sinistral (E-W) strike-slip movements in a simple shear regime (Smith & Durney, 1992; Crider, 2001; Katz et al., 2004), and thus, they may be genetically linked (see chapter 4.4).

The ENE-WSW to E-W striking fractures make out the second most abundant set, and generally dip steeply to the north or south. They are both continuous and discontinuous, but appear to be slightly less systematic than the NE-SW (Figs. 31 & 38). Slickensides from shear fractures (Mode II) in the quarries on Bjarkøya and Senja reveal several senses of shear: dominantly dextral oblique-slip, but also components of sinistral oblique-slip and normal dip-slip sense of shear. These data indicate they formed as both extensional fractures/joints as part of a *fundamental joint system* and/or as a conjugate shear fracture set. The former is supported by cross-cutting relationships (at the Sundsvoll and Skrolsvik localities) and by the presumed rotation of the NE-SW striking fractures into parallelism with the E-W striking fractures (Figs. 22 & 32)

The ENE-WSW to E-W striking fractures in addition have a more complex relationship to the NW-SE striking fractures than what is observed for the NE-SW striking set. Whereas the NW-SE striking fractures usually cross-cut or abut against the other sets, they are observed to have been rotated clockwise towards E-W strike at Skrolsvik, similarly to what is observed for the NE-SW striking fractures at Skarstein and Fiskeenes.

The NW-SE striking fractures are present over the entire study area, but are far less common than the other sets. These fractures are sometimes parallel to the host rock gneiss foliation (Figs. 15 & 21), dipping gentle or steeply to the NE or SW. Moreover, they generally cross-cut or abut against the other two sets, but rotate clockwise towards E-W striking fractures in Skrolsvik (Fig. 39). No offset is observed, but kinematic indicators on Bjarkøya show pure dextral strike-slip, but also sinistral oblique-slip. Investigations in the Skrolsvik quarry also revealed pure dip-slip normal motions along gently dipping NNW-SSE striking fractures. These data and the fact that they cross-cut all other fracture sets suggest they are younger and unrelated to the Andfjorden basin-boundary fault systems (see chapter 2.3 and further discussion in chapter 4.4).

4.2 Discussion of seismic data and interpretation

Based on the interpreted seismic data (chapter 3.3), the overall crustal structure of the studied Andfjorden area is that of a Precambrian crystalline basement overlain by at least two sedimentary sequences in a basin-ridge architecture (Figs. 46, 47 & 48). The sedimentary sequences have been defined as: (i) A Mid Mesozoic (Jurassic?) sequence that displays a fairly constant thickness throughout the study area, and (ii) an Upper Mesozoic (Cretaceous?) sequence that experiences a gradual thickness increase from the inner to the outer parts of the Andfjorden basin, and a pronounced thickening of the strata towards the basin-bounding faults striking on average NNE-SSW and E-W. These offshore faults largely

correspond in attitude with the two main fault populations detected onshore. The NNE-SSW set dominantly dips to the west, while the E-W striking set dips both north and south.

This seismic data and interpretations (see chapter 3.3.6) have shown that the major fault activity and Andfjorden basin formation likely occurred during the Early Cretaceous rifting event. In the Andfjorden basin, the syn-rift sequence clearly thickens from south to north and towards the west dipping Senja Fault in the east, which is believed to be the basin's eastern boundary fault (Hansen et al., 2012). As a constituent of the Troms-Finnmark Fault Complex, the Senja fault continues into the Harstad Basin and northwards toward the Finnmark Platform (Indrevær et al., 2014). A western boundary fault has also been predicted (cf. Dalland, 1981; Løseth & Tveten, 1996), but this fault cannot be obtained with confidence in the present data set. Along with onlapping strata towards the horst in the west, the internal structuring of the Andfjorden basin shows internal fault blocks dipping mostly to the east, indicating that the Andfjorden basin is a half-graben rather than a full graben. If this is true, there is no need for a western boundary fault in the Andfjorden basin (cf. Gawthorpe & Hurst, 1993).

The Andfjorden area was probably part of a rift system in which the outcrop area of Andøya was situated on the western flank of this rift (Dalland, 1981). This tentative Jurassic rift system resembles that of the Vestfjorden Basin 100 km south (Fig. 1), which is bounded by the Hamarøya fault and the East Lofoten Border fault against the Lofoten Ridge to the west (Hansen & Bergh, 2012). One hypothesis is therefore that the Andøya and Andfjorden basins encompasses several sub-basins which are the southward extension of the Harstad Basin and that these continue towards the southwest joining the Sortlandsundet fault in Sortlandsundet (delimiting the Mesozoic basin here) and/or faults in Gullsfjorden and Raftsundet (Osmundsen et al., 2010). Alternatively, the Andfjorden basin and basin related faults terminate to the southwest (Løseth & Tveten, 1996), where they make a step to the northeast and continue as the Vestfjorden-Vanna Fault Complex in Troms (Olesen et al., 1997). Offshore, this rift system continues northwards as the Troms-Finnmark Fault Complex, genetically linking the Andfjorden basin to not only the Harstad Basin, but possibly also the Hammerfest Basin, where a similar thickness increase of Early Cretaceous strata is observed towards the Troms-Finnmark Fault Complex. Potential transform movements along the Senja Fracture Zone offshore may have caused the more complex subsidiary fault trends (NW-SE, WNW-ESE) in the Andfjorden area. Yet another interpretation suggest that the Harstad and Andfjorden basins are situated at the end of a *failed arm* linked to a triple junction offshore to the north (Fønstelien & Horvei, 1979).

4.3 Onshore-offshore fault correlation using bathymetry and magnetic anomaly data.

Andfjorden is characterized by both glacial landforms and structural escarpments. The central and inner parts of Andfjorden are by NE-SW to ENE-WSW striking depressions and ridges of varying extent and depth. The most conspicuous structure is the large NE-SW striking scarps defining the inner border of the Mesozoic basin. The prominent structural trend on the seabed links up with a similar trend on land and further offshore this trend is associated with Paleozoic to Mesozoic faulting and passive margin evolution. Although some of these lineaments might be an expression of ductile fabric, most of them can probably be linked genetically to Paleozoic and/or Mesozoic faults onshore and further offshore, as for example the Senja fault of the Troms Finnmark Fault Complex (e.g. Brekke & Riis, 1987; Gabrielsen et al., 1990; Hansen et al., 2012; Indrevær et al., 2014) that defines the eastern border of the Mesozoic basin in Andfjorden.

The interpreted offshore fault-lineament patterns based on seismic (Figs 46, 47 & 48), bathymetric (Fig. 9) and magnetic (Fig. 44) data from the Andfjorden area is remarkably similar to the pattern obtained from onshore topography/relief (DEM) and structural field data (Figs. 9, 12, 15, 20, 30 & 41). Of particular interest is that the c. NNE-SSW and c. E-W striking basin-boundary faults created a rhombic to lense-shaped pattern both onshore and offshore, a pattern that is also well documented from larger portions of the Norwegian continental margin (e.g. Roberts & Lippard, 2005; Bergh et al., 2007; Hansen et al., 2012; Indrevær et al., 2014). Several NNE-SSW striking horst-internal fault zones, e.g. the Rekvika, Bremneset, Hillesøya, belonging to the major Rekvika fault complex in the West Troms Basement Complex, also follow this pattern (Koehl, 2013; Indrevær et al., 2014; Fig. 6 this work). Magnetic anomaly data (see chapter 3.2) suggests that the basement rocks of Andøya may be related to the West Troms Basement Complex (Fig. 44), and, consequently, horst-internal faults zones equivalent to the Rekvika fault complex may also be present in the Andøya horst. However, major fault zones are hard to detect on Andøya due to a significant peat cover, and only one major fault zone was observed during the fieldwork (see chapter 2.3.4). More detailed studies in the mountains, focusing on this particular subject, may provide data that can confirm/negate this theory.

It is assumed that a direct (spatial?) onshore-offshore correlation of NNE-SSW and E-W striking faults and fractures can be made, and that they together bound rhombic-shaped Jurassic-Cretaceous basins. The most important observations supporting this correlation are: (i) The close correspondence of fault-fracture populations, their strikes, dip and genetically related geometries, e.g. systematic rotation of NNE-SSW and NE-SW striking fractures into parallelism with the ENE-WSW and E-W striking fractures. (ii) The trace of the

Stonglandseidet Fault Zone can easily be traced on bathymetric data both eastward and westward of Stonglandet, and minor NNE-SSW striking fractures on North Eastern Andøya clearly continue northwards on the offshore part of the Andøya horst (Fig. 9). (iii) The coincidence of magnetic lineaments and known faults such as the Andøya and Senja faults and direct linkage of onshore offshore lithological units from magnetic anomaly data (Fig. 44). (iv) The rhombic fault pattern that characterizes the sedimentary basins in Andfjorden, Sortlandsundet, Gavlfjorden and larger basins on the outer continental margin (e.g. the Ribban Basin), can as well be inferred for many smaller (sub)basins on Andøya and probably also the geometry (shape) of islands in eastern parts of Andfjorden, e.g. on Bjarkøya (Figs. 9 & 24). The rhombic geometry of Bjarkøya (Figs. 9 & 24) is especially intriguing. Not only does the bathymetry/topography appear to be controlled by NNE-SSW and ENE-WSW striking faults; the nature of the seafloor and erosion in the glacial trough between Bjarkøya and Senja is also similar to that observed in the Andfjorden trough (cf. Rydningen et al., 2013; Fig. 9 this work), where the extent of the trough defines the boundaries between Precambrian rocks and Mesozoic sedimentary rocks. Similar erosional characters can also be seen in Sortlandsundet and Gavlfjorden (see www.mareano.no), where small Mesozoic basins are located (Davidsen et al., 2001; Bøe et al., 2010). These similarities to known sedimentary basins, substantiates that the trough between Bjarkøya and Senja actually may be a previously unrecognized sedimentary basin itself, and that the glacial erosion here is not only a result of the confluence of ice streams. However, no erratic blocks were discovered during the fieldwork on Bjarkøya and Skrolsvik, and conclusive evidence may only be gained from seismic investigations and/or drilling; data that is not available from this location, with the exception of a few seismic 2D lines collected by NGU in 2000 that were completely uninterpretable (Børre Davidsen, pers.com to Tormod Henningsen, 2013).

Regarding the NW-SE striking lineaments of the inner Andfjorden area, they are not as well-displayed neither on the bathymetry, seismic and onshore DEM and structural data sets as the other lineament sets. They are largely absent on seismic data of the outer shelf, but admittedly abundant locally on the onshore part of the margin in Lofoten-Vesterålen (Bergh et al., 2007; Eig & Bergh, 2011; Hansen et al., 2012). This absence may either be caused by the high angle these lineaments have relative to the shelf margin and limited structural data from NE-SW trending seismic lines, or confirm that the faults are simply not there (Bergh et al., 2007; Olesen et al., 2007) (see further discussion in chapter 4.4).

4.4 Timing constraints on the fault-fracture sets related to the Andfjorden basin

Based on the offshore and onshore data obtained in discussed in chapter 4.1 through 4.3, the relative timing constraints on the formation of the Andfjorden basin and associated NE-SW and ENE-WSW trending fracture sets can be made and compared with other portions of the North Norwegian passive margin. Onshore faults and fractures with similar attitudes and geometries have previously been described from Lofoten and Vesterålen (e.g. Bergh et al., 2007; Hansen & Bergh, 2012) and Senja in the West Troms Basement Complex (e.g. Gagama, 2005; Koehl, 2013; Indrevær et al., 2014). The spatial and temporal relationship between the two dominant fault-fracture sets have been debated and variously explained as follows (Fig. 49): (i) simple shear rotation and/or drag of an older set of fractures towards a younger fracture set (Dyer, 1988; Koehl, 2013) and/or (ii) stress perturbations near open fractures (Dyer, 1988; Mandl, 2005) or faults (Rawnsley et al., 1992; Nüchter & Ellis, 2011), causing the younger fractures to grow and propagate in the direction of the perturbed stress field.

The first model implies that the NNE-SSW to NE-SW striking faults/fractures are older and were displaced into a new attitude parallel to younger ENE-WSW to E-W striking faults/fractures (Hansen & Bergh, 2012; Koehl, 2013; Fig. 49 this work) and thus cannot have produced rhombic-shaped boundary basins during the same tectonic event. Such a temporal fault separation would require dextral strike-slip displacement along the E-W trending fault-fracture set, and likely also pronounced offsets of ductile fabrics in the crystalline basement gneisses (Hansen & Bergh, 2012). Due to the lack of such offset and striations supporting sinistral shear along the ENE-WSW striking fractures, Hansen and Bergh (2012) favored the second model, in which the NNE-SSW to NE-SW striking fractures are younger and/or developed synchronously with the ENE-WSW to E-W striking fractures. In this case, the curving geometry would rather be the result of stress perturbations around the potentially sinistral ENE-WSW to E-W striking fractures. This model was also supported by Koehl (2013) for faults and fractures in the Rekvika and Vestfjorden-Vanna fault complexes. Previous and recent radiometric dating (cf. Olesen et al., 1997; Davids et al., 2013) yielding consistent Permian ages, also favors a single stage of major faulting along the Vestfjorden-Vanna fault complex (see further discussion below).

The present data based on fault-striations on Bjarkøya (Figs. 28 & 35) and Senja (Fig. 40) along with interpretations of the internal fault/fracture geometries (Figs. 22, 31, 32, 38 & 39), suggest dominantly dextral-oblique displacement on ENE-WSW striking faults/fractures. These data seem to fit the *first* model best, i.e. that the NNE-SSW to NE-SW striking faults/fractures are oldest and were dragged into parallelism with or offset by dextral shear

along younger ENE-WSW to E-W striking faults/fractures. We cannot, however, exclude synchronous formation basically since the faults-/fracture zones on both Bjarkøya and Senja may have formed as either oblique tension joints or conjugate Riedel shears (R and R') in a succession of events. Several mechanics of fault-fracture formation should be expected on a continental margin that has undergone several stages of rifting along with significant uplift during the last c. 300 Ma. Their development is further complicated by possible influence of pre-existing zones of weakness in the basement rocks. Such inhomogeneities have been observed to affect the orientation of fractures, especially on Senjehesten, where E-W striking fractures bend into parallelism with a NE-SW striking lithological boundary (Fig. 41).

Moreover, the seismic data and interpretations show that the NNE-SSW and E-W striking basin-boundary faults cut through and affected the sedimentary units of the Andfjorden basin in a similar manner (Figs. 46, 47 & 48). This advocates synchronous development, possibly in the Mid/Late Jurassic, but with the greatest displacement in the Early to Mid-Cretaceous (cf. Hansen et al., 2012), resulting in the development of major basin-bounding faults and associated ridges (Fig. 46). Correspondingly, and probably as a response to continued subsidence and instabilities due to large input of sediments (Gibbs, 1984), synthetic faults and detachments may have formed in the growing hanging-wall strata during the main Early Cretaceous rift forming event.

The Early Cretaceous rift event is well-documented both onshore and offshore northern Norway, and is recognized as the most prominent Mesozoic rift event on the Lofoten-Vesterålen margin (cf. Blystad et al., 1995; Tsikalas et al., 2001; Bergh et al., 2007; Hansen et al., 2012). This event was also important for the evolution of major basins like the Harstad, Tromsø and Hammerfest basins on the SW Barents Sea Margin (e.g. Gabrielsen et al., 1990; Faleide et al., 1993; Indrevær et al., 2014). Rifting probably continued at least until the Albian, as indicated by the general upward deepening nature of the Skarstein Formation on Andøya (Fig. 7) (Dalland, 1981).

The duration and margin-extent of the Mid/Late Jurassic and Early Cretaceous rifting is also somewhat debated. Some workers argue for a continuous rift episode (e.g. Brekke, 2000; Tsikalas et al., 2001), while others infer that the Mid/Late Jurassic and Early Cretaceous rift event were separated by a short period of tectonic quiescence (e.g. Doré, 1991; Doré et al., 1999; Hansen et al., 2012) and even uplift and erosion (Dalland, 1981; Shannon et al., 2005).

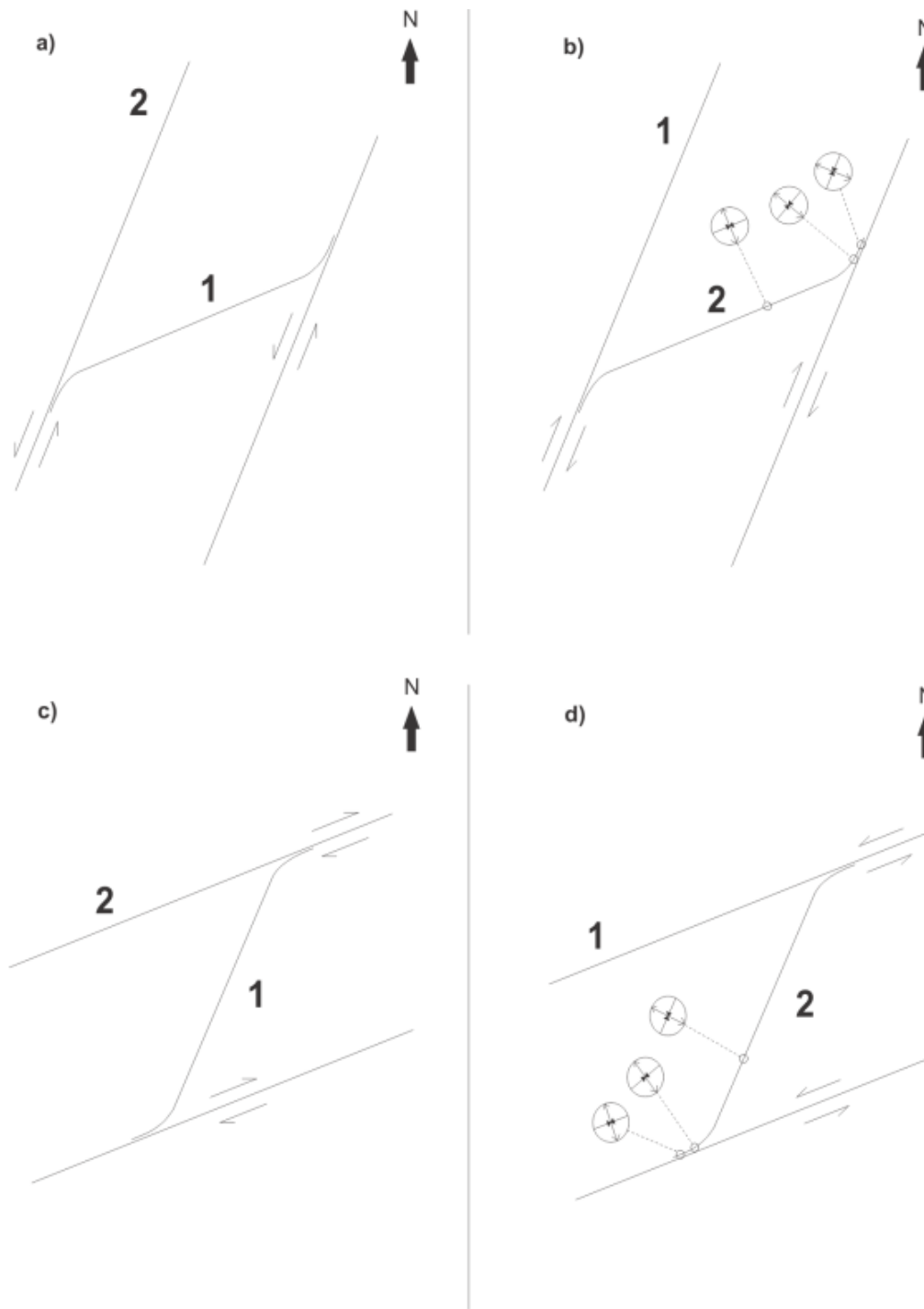


Figure 49 Models showing two potential kinematic interpretations and relative timing (indicated by numbers) for NNE-SSW and ENE-WSW striking fracture sets. a) Anticlockwise sigmoidal curving of ENE-WSW fractures that formed earlier (1), and that have been dragged toward younger NNE-SSW striking faults (2) during sinistral shearing and due to material rotation along the NNE-SSW striking faults. b) ENE-WSW trending fractures (2) are bent into parallelism with older or synchronous, NNE-SSW striking fractures (1). The anticlockwise curving is, here, due to local stress perturbation along the potentially dextral NNE-SSW striking faults. Note that shearing along the NNE-SSW striking fractures is not necessary to produce the curving geometry. c) Clockwise sigmoidal bending of NNE-SSW trending fractures that formed earlier (1), and that have been dragged toward younger ENE-WSW striking faults (2) during dextral shearing and due to material rotation along the ENE-WSW striking faults. d) NNE-SSW trending fractures (2) merge into parallelism with older/synchronous ENE-WSW striking fractures (1). The clockwise curving is due to local stress perturbation along the potentially sinistral ENE-WSW striking faults. Shearing along ENE-WSW striking fractures is not required to bend the NNE-SSW striking fractures. From Koehl (2013), redrawn and modified after Dyer (1988) and Hansen & Bergh (2012).

Onshore Andøya, the Jurassic-Cretaceous boundary is represented by an unconformity suggesting uplift and erosion before the Early Cretaceous rifting (Dalland, 1981). Seismic interpretation (see chapter 3.3) reveals a seemingly conformable boundary between the Jurassic and Early Cretaceous sequence, thus speaking against such an uplift. Instead, this indicates either a continuous rift episode from the Mid/Late Jurassic - Early Cretaceous times or two rift episodes separated by tectonic quiescence. In both of these latter scenarios, most of the displacement and syn-rift deposition occurred in the Early Cretaceous. Given the fact that the relative timing of faults/fractures onshore is somewhat inconclusive, it seems best to rely on the timing constraints from seismic data, suggesting the NNE-SSW and E-W striking faults and fractures developed synchronously sometime between Mid Jurassic to Early Cretaceous times.

Recently the brittle faulting onshore Senja and in the West Troms Basement Complex (Indrevær et al., 2014) have been radiometrically dated yielding dominantly Permian/Early Triassic movements (Davids et al., 2010; 2012a; 2012b; 2013), while faulting offshore and in Lofoten/Vesterålen show consistently younger, dominantly Mid/Jurassic to Early Cretaceous ages (e.g. Gabrielsen et al., 1990; Blystad et al., 1995; Tsikalas et al., 2001; Hendriks, 2003; Bergh et al., 2007; Faleide et al., 2008; Hendriks et al., 2010; Hansen et al., 2012; Davids et al., 2013). Rifting of the North-Norwegian margin is therefore postulated to have shifted westward from the Permian in Troms to the Early Triassic in Lofoten and Vesterålen (Davids et al., 2010; Davids et al., 2012b; Davids et al., 2013). Consequently, the faults and fractures onshore Senja, and possibly also on Bjarkøya, might have initiated e.g. earlier than those offshore and onshore Andøya. On the other hand, Paleozoic and Early Mesozoic rifting fault ages have been observed on Andøya (Davids et al., 2013; see chapter 2.3.4 this work) as well as in the northern Træna Basin, where an Early Triassic unit grows towards the western boundary fault of the basin (Hansen et al., 2012).

In this study, NW-SE striking fractures and faults are only observed onshore. They normally truncate all the other fractures, and are therefore believed to be the youngest fractures on the margin, and thus unlikely related to the Andfjorden basin formation. This is not conclusive however, since a fracture zone in Skrolsvik, Senja, apparently merges into parallelism with the E-W striking fractures (Fig. 39), suggesting a geometric relationship, at least locally. This merging could be caused by the same rotational processes as discussed for the relation between NNE-SSW to NE-SW and ENE-WSW to E-W striking fractures. If the NW-SE striking set is older, one would expect sinistral displacement along the ENE-WSW to E-W striking fractures. But as the slip is dominantly dextral oblique, the *second* model is favored, and the NW-SE striking fractures are therefore believed to have grown in a much younger perturbed stress field. Dip-slip normal movements along gently dipping NNW-SSE striking fractures in Skrolsvik (Fig. 40) also suggest that this fracture set may have formed

due to a late stage of NE-SW directed extension (Eig & Bergh, 2011; Koehl, 2013), e.g. in conjunction with NW-SE directed transform movements along the Barents Sea margin in the Early Cenozoic (cf. Faleide et al., 1993; Bergh & Grogan, 2003). This presumed transform-induced extension expressed in the Andfjorden area, is believed to have been the result of NW-SE crustal contraction due to e.g. ridge-push forces or Alpine closure phases (cf. Doré et al., 1999). Interestingly, NE-SW directed extension may have reactivated both sets of basin-bounding faults as reverse faults, thus advocating inversion tectonism (E-W striking faults may also be reactivated as normal faults) with a significant component of dextral shear (Fig. 50). Reverse reactivation of the two fault sets has not been observed in the study area (Reverse slip is only documented from a single NW-SE striking fault/fracture surface in Skrolsvik, see Fig. 40 c), but dextral movement was the dominant shear sense inferred from slickensides on faults in the quarries on Bjarkøya and Skrolsvik. These slickensides may thus have formed during late NE-SW directed extension, overprinting and/or extinguishing earlier striations formed during WNW-ESE oriented extension. If this is the case, the kinematic data collected on Bjarkøya and Senja may have no immediate relation to the formation and development of the Mesozoic sedimentary basins in Andfjorden and on Andøya. Also, it is necessary to point out that slickensides must be interpreted with care: Slip vectors with variable orientations may reflect a highly transient local stress state, e.g. due to fault interactions, in an otherwise constant regional stress field (Cashman & Ellis, 1994). Confident interpretation is thus dependent on a significant number of measurements, perhaps more than were collected during this study.

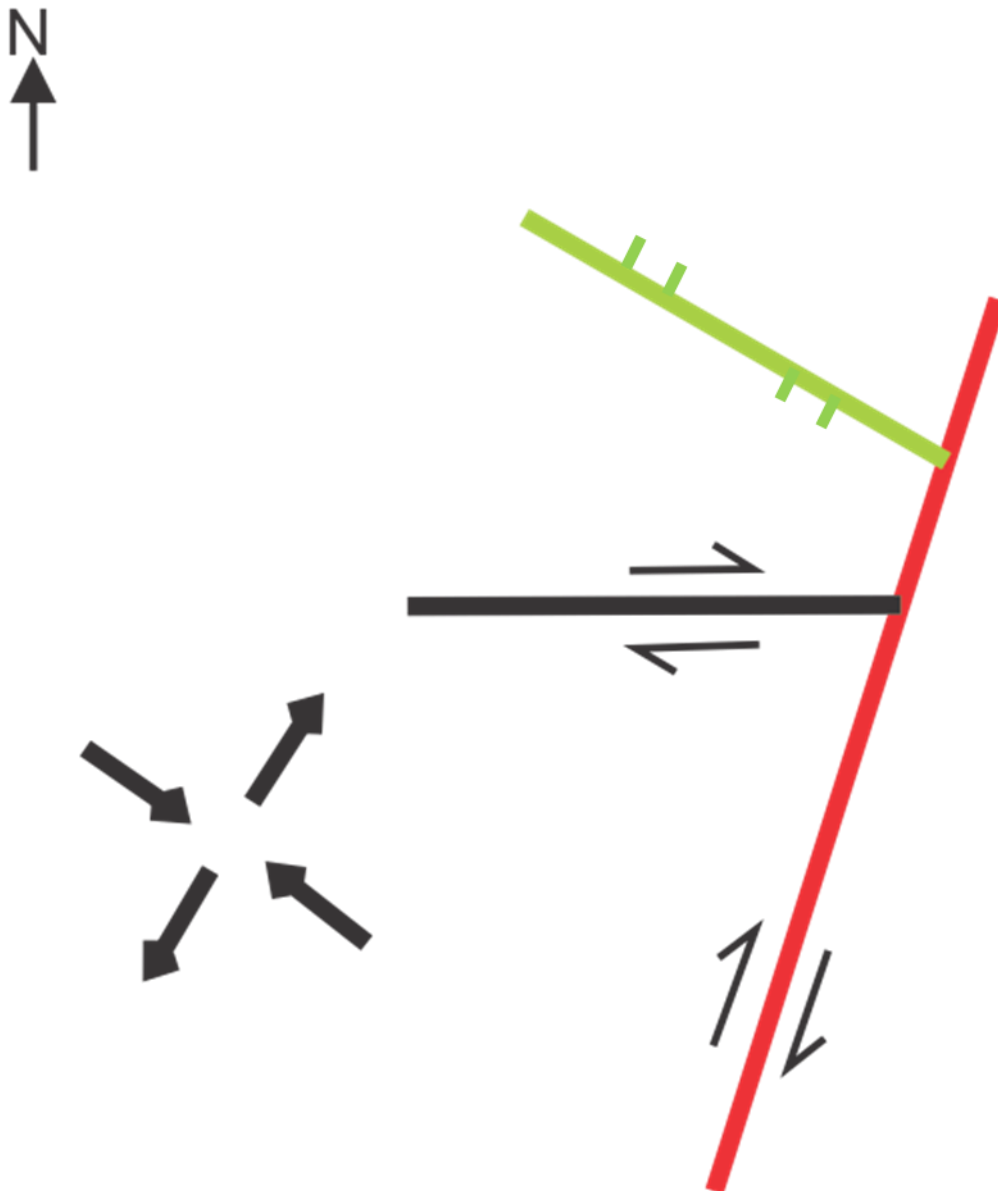


Figure 50 Sketch of how NE-SW directed extension causes NW-SE striking normal faults (green) and dextral slip along E-W (black) and NNE-SSW (red) striking faults. The large arrows marks directions for extension and compression.

4.5 Structural evolution of the Andøya/Andfjorden sedimentary basin

Having correlated onshore and offshore faults/fractures and established a temporal chronology of fault/fracture formation, a tentative model can be proposed and discussed for the structural evolution of the Andfjorden basin in the study area. All the inferred basins and sub-basins are believed to be a part of the same graben system, bounded by the Senja fault in the east and the East Andøya Fault Zone in the west (Figs. 2 & 3) (Dalland, 1981; Løseth & Tveten, 1996). Seismic interpretation (this study) has shown that the basin rather appears to have the architecture of a half-graben (Fig. 46), with only minor indications of possible east-dipping faults in the western margin of the basin. The east dipping fault observed in the

Skarsteinsdalen area (Fig. 23) is recently radiometrically dated to Devonian/Carboniferous age (Davids et al., 2013) and thus, does not seem to have any direct timing relationship to the sedimentary strata onshore further east. Maps from new gravity data cannot confirm the East Andøya Fault Zone, and support onlap relationship and further inland reaching sedimentary rocks (Brønner et al., 2008).

Half-grabens are the characteristic structural style of sedimentary basins developing along a rifted continental margin undergoing extension (Bally, 1981, 1982; Leeder, 1987), and such grabens may be bounded on one side by a main border fault zone (detachment?), which's throw is greater than the throw of other extensional faults within the basin (Gawthorpe & Hurst, 1993). The difference in throw creates an asymmetric subsidence profile, in which subsidence increases towards the border fault. In the Andfjorden basin, this border fault would be the Senja fault, which displays an asymmetric subsidence profile, created by increased subsidence towards the Senja fault in the east (Fig. 46). Asymmetric subsidence is also apparent towards the northeast (Fig. 47), but this can be explained by, e.g. a displacement maxima developed near the middle portion of the fault and diminishing throw towards the fault tip (Fossen, 2010). It is therefore likely that displacement along the Senja fault decreases to the southeast in Andfjorden, and that the southern boundary of the Andfjorden basin also marks the termination of the Senja fault.

In combination with the Andøya and Outer Andfjorden faults, the Senja fault is a part of a large system of NNE-SSW and c. E-W striking normal faults that created rhombic to lense-shaped fault-basin patterns both onshore and offshore (Figs 1, 2, 8, 9 & 44). Such patterns are also well-documented from the North Sea (Færseth et al., 1997) the Mid-Norwegian Shelf ((Blystad et al., 1995; Brekke, 2000), the Lofoten-Vesterålen margin (Bergh et al., 2007; Hansen et al., 2012) and the SW Barents Sea margin (Indrevær et al., 2014), as well as in other non-volcanic and volcanic rifted extensional margins, e.g. the Suez rift of Egypt (Gawthorpe et al., 2003), the East African rift system (Scott et al., 1992) and the Rio Grande Rift (Baldrige et al., 1994; Chapin & Cather, 1994). The rhombic fault-basin pattern can be attributed to either successive orthogonal extension, oblique extension (Bonini et al., 1997) or by a combination of the two (Bergh et al., 2007) due to switches in the spreading directions and/or rift axis migration (Mosar et al., 2002). Bergh et al. (2007) proposed a multi-phase and time-progressive-fault and basin evolution along the Lofoten margin, that indicated a switch in the regional rifting direction from c. E-W to NNW-SSE, resulting in the development of NNE-SSW striking and E-W striking faults, respectively, along with dextral reactivation of the NNE-SSW striking faults due to the rotation of the stress field. Hansen et al. (2012), however, argued for synchronous formation of the NNE-SSW striking, right-stepping *en echelon* faults and E-W striking *transfer zones* in a regional stress field oriented WNW-ESE. Both workers argue for a segmentation of the margin by linking of the *en*

echelon NNE-SSW striking faults by c. E-W striking *transfer faults*. Hansen et al. (2012) consequently applies the term *transfer zone*, to the areas between overlapping NNE-SSW striking fractures, which is an area where the sedimentary strata deformed between two normal faults formed at the same time (Morley, 1995; Faulds & Varga, 1998). Bergh et al. (2007) however, uses the term extensional *accommodation zone* or *twist zone*, where the stepping faults need not be active at the same time (Colletta et al., 1988).

The Senja and Andøya faults are spaced c. 30 kilometers apart, and have an overlap of c. 20 kilometers (Fig. 2). They appear to be linked together by the c. E-W striking Outer Andfjorden Fault, thus addressing the possibility that the Andfjorden area is a transfer or accommodation zone (Figs. 9 & 44). Seismic investigations in Andfjorden (chapter 3.3) reveal that the Senja and Andøya faults developed at the same time (Fig. 46). The Outer Andfjorden fault, separating the Andfjorden basin from the Harstad Basin, may have developed simultaneously either through linkage of the former in a perturbed stress field or as a new fault. The development of a new fault connecting two relaying branches has rarely been reported for natural cases (Ferrill et al., 1999; Peacock & Parfitt, 2002), and the most frequent way of breaching appears to be through propagation of the footwall fault towards the hanging-wall fault (Hus et al., 2005). Seismic section LO88R0752 shows a significantly larger displacement along the Andøya fault, than the Senja Fault in this area (Fig. 46), which probably can be related to the right-stepping nature of the NNE-SSW striking faults. The section is likely located in an area where displacement of the Andøya fault is close to maximum, whereas the displacement along the Senja fault gradually decreases towards the fault tip. Larger displacement along the Andøya fault and the Harstad Basin portion of the Senja fault, may also explain the relatively modest subsidence experienced in the Andfjorden basin compared to the Harstad Basin.

In such an interpretation, the Andfjorden basin is a hard-linked *synthetic interbasin transfer zone*, linking major faults with similar dip-polarity (Gawthorpe & Hurst, 1993). The internal structuring of the basin can then be explained by the development of smaller, intrabasin transfer zones that are characterized by *en echelon* steps, as seen in the NNE-SSW striking lineaments in the offshore continuation of Andøya (Fig. 9), and commonly display minor topographic changes within interbasin transfer zones (Machette et al., 1991). The separation of the onshore and offshore part of the Andfjorden Basin might be related to the main phase of exhumation of the Andøya horst, which is dated to c. 140 My (Hendriks 2003), i.e. simultaneously with the Early Cretaceous rifting. This uplift may thus have been initiated by *footwall uplift* along the Andøya fault, which again can have caused the initiation of east-dipping faults in the western Andfjorden basin, separating the onshore outcrops from the sedimentary strata in the fjord. This theory is supported by the asymmetric topography of northern Andøya, dipping towards the southeast (Fig. 10 b) and a provenance study of the

Mesozoic succession on Andøya (Morton et al. 2013), concluding that the Cretaceous sandstones in the Dragneset Formation were derived from Archean and Proterozoic rocks and Early Paleozoic granitoid rocks from the Lofoten-Andøya high, a conclusion also suggested by (Dalland, 1981).

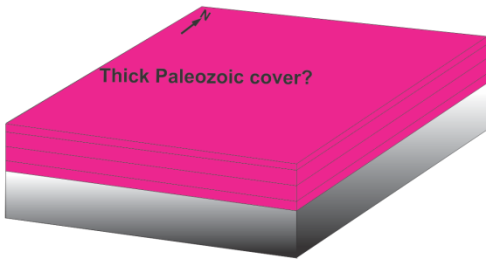
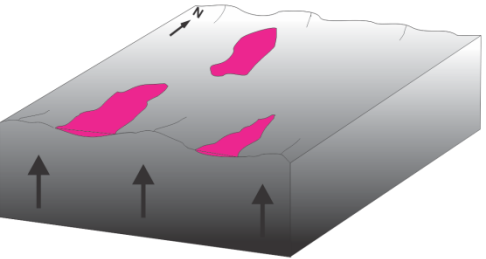
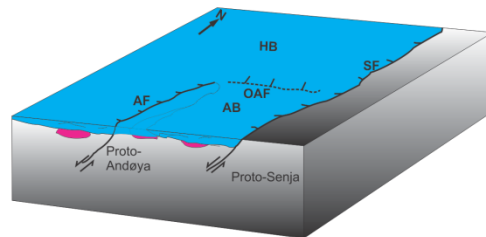
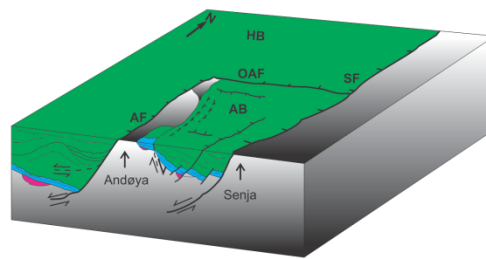
Based on the discussion above, the following evolutionary model advocated for the Mesozoic Andfjorden basin (Fig. 51):

1. The Andfjorden basin initiated as a part of the Harstad Basin in the Middle Jurassic along NNE-SSW striking and west/seaward-dipping and possibly also E-W striking rifted margin normal faults. Displacement was moderate, and was balanced by the sedimentation rate, resulting in a uniform thickness of Mid-Late Jurassic rocks that likely covered a large area, including Andøya.

2. The synthetic Senja and Andøya faults developed as major half-graben basin-boundary normal faults linked by a c. 30 km wide transfer zone. Propagation of these faults towards each other, or the development of a new fault (the Outer Andfjorden fault) breached the transfer zone, and separated the Andfjorden basin from the Harstad Basin. The separation leads to substantially more subsidence and, consequently, a shift of the depocenter toward the Harstad Basin relative to the Andfjorden basin.

3. Footwall uplift along the Andøya fault resulted in an asymmetric exhumation of the Andøya horst, and possibly also the antithetic NNE-SSW striking faults separating the Andfjorden basin from the Mesozoic rocks on Andøya.

4. Cenozoic uplift related to e.g., ridge-push, a critical taper, post-glacial rebounds, created the Late Cenozoic to recent topography.

Period	Tectonic event	Tectonic evolution	Conceptual model
Paleozoic	Tectonic subsidence	Subsidence and deposition of unknown sediments. The extent and shape of basin is poorly known.	
Early Mesozoic	Uplift and erosion	Uplift and erosion of Paleozoic sequence. Patches of Paleozoic rocks are preserved.	
Mid. Jurassic - Late Jurassic	WNW-ESE directed extension.	Rift initiation and sedimentation. Development of NNE-SSW striking faults (e.g. the AF and SF), and possibly E-W striking faults (e.g. the OAF). AB develops as a transfer zone between AF and SF in HB.	
Latest Jurassic - Early Cretaceous	WNW-ESE directed extension	Main rift stage on the LVM with evolution of major boundary faults (e.g. SF and AF) and basement ridges. AB develops as a half-graben and is separated from HB by the development of the E-W striking transfer fault OAF. Footwall-uplift of Andøya along AF, possibly causing development of east dipping faults in AB (EAF).	

Legend

-  Cretaceous
-  Jurassic
-  Paleozoic
-  Precambrian basement

Figure 51 Summary of the proposed structural model of the development of the Mesozoic Andfjorden basin. Abbreviations are given in Table 1. For structural legend, see Common legend in Figure 12.

5 Conclusions

The present study focuses on the onshore and offshore mapping of brittle faults and fractures in the Andfjorden basin and the surrounding basement islands Andøya, Senja and Bjarkøya. Structural field observations and interpretations of DEM-, magnetic anomaly- and seismic data provide the basis for the characterization of the geometry and kinematics of the faults and fractures that have been used to correlate onshore and offshore structures. Further, this correlation has been used to develop a model for the structural formation and evolution of the Andfjorden basin.

- 1) Three major structural lineament populations exist in the Andfjorden area. They trend c. NNE-SSW, c. ENE-WSW and NW-SE. The two first sets have the largest effect on the topography, and define a zigzag/rhombic to lense-shaped pattern. The NW-SE striking fractures truncate all other structures and do not seem to be related to the formation of the Andfjorden basin.
- 2) A satisfying spatial onshore-offshore correlation has been made between NNE-SSW and ENE-WSW striking faults and fractures. NW-SE striking faults and fractures are present in the inner Andfjorden, but cannot be identified in the offshore portion of the Andfjorden basin or further out on the shelf.
- 3) The NNE-SSW and ENE-WSW striking boundary faults of the Andfjorden basin are likely a part of the right-stepping Troms-Finnmark Fault Complex that displays a zigzag pattern along the North Norwegian margin. The NNE-SSW striking faults are thought to represent the main orthogonal fault system perpendicular to the WNW-ESE oriented extension, while the ENE-WSW striking faults possibly correspond to transfer zones that developed oblique to the extension direction, linking the right stepping, NNE-SSW striking fault array. These transfer faults may have initiated simultaneously or later than the main fault set. In the Andfjorden basin, NNE-SSW and E-W striking fractures likely developed synchronously.
- 4) The Andfjorden basin likely initiated as a part of the Harstad Basin in the Mid/Late Jurassic. Formation and linkage of the NNE-SSW striking Senja and Bjarkøya in the Early Cretaceous, separated the two basins, and the Andfjorden basin developed as a half-graben transfer zone between these major basin-boundary faults.
- 5) The syn-rift exhumation of Andøya in the Early Cretaceous may be related to footwall uplift along the Andøya fault. This may also have caused the asymmetric topography on northern Andøya, and the separation of the onshore and offshore parts of the Andfjorden basin along east-dipping NNE-SSW striking faults.
- 6) A late stage of NW-SE directed contraction and NE-SW directed extension is believed

to be responsible for the development of NW-SE trending fractures and dextral reactivation along NNE-SSW and E-W striking faults.

- 7) Basement inhomogeneities and pre-existing zones of weakness, such as ductile foliation and lithological boundaries, likely influenced the localization of brittle faults and/or fractures, at least on a local scale.

6 References

- Anderson, E. M. (1951). *The Dynamics of Faulting and Dyke Formation with Applications to Britain*: Oliver and Boyd, London.
- Andreassen, K. (2009). Marine Geophysics: Lecture notes for Geo-3123, University of Tromsø. 106 pp.
- Antonsdóttir, V. (2006). Structural and kinematic analysis of the Rekvika fault zone, kvaløya, Troms. *Unpublished master thesis, University of Tromsø*.
- Badley, M. E. (1985). *Practical seismic interpretation*: Prentice Hall
- Baldrige, W. S., Ferguson, J. F., braile, L. W., Wang, B., Eckhardt, K., Evans, D., . . . Biehler, S. (1994). The western margin of the Rio Grande Rift in northern New Mexico; an aborted boundary? *Geological Society of America Bulletin*, 106, 1538-1551.
- Bally, A. W. (1981). Atlantic-type margins. In *Geology of passive continental margins. American Association of Petroleum Geologists Education Course Note Series*, 19, 1-48.
- Bally, A. W. (1982). Musings over sedimentary basin evolution. *Royal Society of London Philosophical Transactions v. A305*, 325-328.
- Bartley, J. M. (1982). Mesozoic high-angle faults, east Hinnøy, North Norway. *Norsk Geologisk Tidsskrift*, 61, 291-296.
- Bergh, S. G., Corfu, F., & Corner, G. D. (2008). Proterozoic igneous and metamorphic rocks: a template for Mesozoic-Cenozoic brittle faulting and tectonically inherited landscapes in Lofoten-Vesterålen, North Norway. *33 IGC Excursion Guidebook No 38, IGC The Nordic Countries*, 71 p.
- Bergh, S. G., Eig, K., Kløvjan, O. S., Henningsen, T., Olesen, O., & Hansen, J. A. (2007). The Lofoten-Vesterålen continental margin: a multiphase Mesozoic-Paleogene rifted shelf as shown by offshore-onshore brittle fault-fracture analysis. *Norwegian Journal of Geology*, 87, 29-58.
- Bergh, S. G., & Grogan, P. (2003). Tertiary structure of the Sørkapp-Hornsund Region, South Spitsbergen, and implications for the offshore southern extension of the fold-thrust Belt. *Norwegian Journal of Geology*, 83, 43-60.
- Bergh, S. G., Kullerud, K., Armitage, P. E. B., Zwaan, K. B., Corfu, F., Ravna, E. J., & Myhre, P. I. (2010). Neoproterozoic to Svecofennian tectono-magmatic evolution of the West Troms Basement Complex, North Norway. *Norwegian Journal of Geology*, 90(21-48).
- Blystad, P., Brekke, H., Færseth, R. B., Larsen, B. T., Skogseid, J., & Tørudnakken, B. (1995). Structural elements of the Norwegian Continental Shelf, Part II: The Norwegian Sea region. *Norwegian Petroleum Directorate Bulletin*, 8, 45 pp.
- Bonini, M., Souriot, T., Boccaletti, M., & Brun, J. P. (1997). Successive orthogonal and oblique extension episodes in a rift zone: Laboratory experiments with application to the Ethiopian Rift. *Tectonics*, 16(2), 347-362.
- Braathen, A., Osmundsen, P. T., & Gabrielsen, R. H. (2004). Dynamic development of fault rocks in a crustal-scale detachment: An example from Western Norway. *Tectonics*, 23(4), 21pp.
- Brekke, H. (2000). The tectonic evolution of the Norwegian Sea continental margin with emphasis on the Vøring and Møre basins. *Geological Society, London, Special Publications* 167, 327-378. doi: 10.1144/GSL.SP.2000.167.01.13
- Brekke, H., & Riis, F. (1987). Tectonics and basin evolution of the Norwegian shelf between 62°N and 72°N. *Norwegian Journal of Geology*, 67, 295-321.
- Brønner, M., Koziel, J., & Gellein, J. (2008). Ramså Aeromagnetic Project 2007 (AP-07). Acquisition - processing report and interpretation. *NGU Report*, 2008.002, 27 pp.
- Bøe, R., Fossen, H., & Smelror, M. (2010). Mesozoic sediments and structures onshore Norway and in the coastal zone. *Norges geologiske undersøkelse Bulletin*, 450, 15-32.

- Caine, J. S., Evans, J. P., & Forster, C. B. (1996). Fault zone architecture and permeability structure. *Geology*, 24(11), 1025-1028.
- Cashman, P. H., & Ellis, M. A. (1994). Fault interaction may generate multiple slip vectors on a single fault surface. *Geology*, 22, 1123-1126.
- Chapin, C. E., & Cather, S. M. (1994). Tectonic setting of the axial basins of the northern and central Rio Grande Rift. *Geological Society of America Special Paper*, 291, 5-25.
- Clark, D. A., & Emmerson, D. W. (1991). Notes on rock magnetization characteristics in applied geophysical studies. *Exploration Geophysics*, 22, 547-555.
- Colletta, B., Quélélec, L., Letouzey, P., & Moretti, I. (1988). Longitudinal evolution of the Suez rift structure (Egypt). In LePichon, X. & Cochran, J.R. (eds): The Gulf of Suez and Red Sea Rifting. *Tectonophysics*, 153, 221-233.
- Corfu, F. (2004). U-Pb age, setting and tectonic significance of the anorthosite-mangerite-charnockite-granite-suite, Lofoten-Vesterålen, Norway. *Journal of Petrology* 45, 1799-1819.
- Corfu, F., Armitage, P. E. B., Kullerud, K., & Bergh, S. G. (2003). Preliminary U-Pb Geochronology in the West Troms Basement Complex, North Norway: Archean and Palaeoproterozoic events and younger overprints. *Norges geologiske undersøkelse Bulletin*, 441, 61-72.
- Crider, J. G. (2001). Oblique slip and the geometry of normal fault linkage: mechanics and a case study from the Basin and Range in Orgeon. *Journal of Structural Geology*, 23, 1997-2009.
- Crider, J. G., & Peacock, D. C. P. (2004). Initiation of brittle faults in the upper crust: a review of field observations. *Journal of Structural Geology*, 26, 691-707.
- Cunningham, D. (2007). Structural and topographic characteristics of restraining bend mountain ranges of the Altai, Gobi Altai and easternmost Tien Shan. In D. Cunningham & P. Mann (Eds.), *Tectonics of strike-slip restraining and releasing bends: Geological Society Special Publications* (Vol. 290, pp. pp. 219-237).
- Dalland, A. (1974). Geologisk undersøkelse av den mesozoiske lagrekka på Andøya, Nord-Noreg. *Unpublished thesis, University of Bergen*, 223 pp.
- Dalland, A. (1975). The Mesozoic Rocks of Andøy, Northern Norway. *Norges geologiske undersøkelse Bulletin*(316), 271-287.
- Dalland, A. (1979). The sedimentary sequence of Andøy, Northern Norway - Depositional and structural history. *Norwegian Sea Symposium, Norwegian Petroleum Society*, 26, 31 pp.
- Dalland, A. (1981). Mesozoic sedimentary succession at Andøy, Northern Norway, and relation to structural development of the North Atlantic area. *Canadian Society of Petroleum Geologists, Memoir*(7), 563-584.
- Davids, C., Benowitz, J. A., & Layer, P. (2012a). Constraining the Caledonian tectonic overprint in a Precambrian gneiss terrane in northern Norway. *Thermo 2012, 13th International Conference on Thermochronology, 2012-08-24 - 2012-08-28*.
- Davids, C., Bergh, S. G., Wemmer, K., & Layer, P. (2010). K-Ar and ⁴⁰Ar/³⁹Ar dating of post Caledonian brittle faults in northern Norway. *Thermo 2010, 12th International Conference on Thermochronology, Glasgow, UK, 16-20 August 2010*.
- Davids, C., Kohlmann, F., Hansen, J. A., Benowitz, J. A., Layer, P., & Jacobs, J. (2012b). Post-Caledonian onshore exhumation history of Troms, northern Norway, as constrained by K-feldspar ⁴⁰Ar/³⁹Ar and apatite fission track thermochronology. *Abstract and proceedings of the Geological Society of Norway. Onshore-Offshore relationship on the North Atlantic margin, Trondheim, October 17-18, 2012. NGF. Number 2, 2012*.
- Davids, C., Wemmer, K., Zwingmann, H., Kohlman, F., Jacobs, J., & Bergh, S. G. (2013). *K-Ar illite and apatite fission track constraints on brittle faulting and the evolution of the northern Norwegian passive margin*. University of Tromsø.
- Davidsen, B., Sommaruga, A., & Bøe, R. (2001). Final Report: Sedimentation, tectonics and uplift in Vesterålen. Phase 1 - Localizing near-shore faults and Mesozoic sediment basins. (pp. 16): Norges Geologiske Undersøkelse.

- Doré, A. G. (1991). The structural foundation and evolution of Mesozoic seaways between Europe and the Arctic. *Palaeogeography, Palaeoclimatology, Palaeoecology*, 87, 441-492.
- Doré, A. G., Cartwright, J. A., Stoker, M. S., Turner, J. P., & White, N. E. (2002). Exhumation of the North Atlantic Margin: Timing, Mechanisms and Implications for Petroleum Exploration. *Special Publications - Geological Society of London*, 196, 45-65.
- Doré, A. G., Lundin, E. R., Jensen, L. N., Birkeland, Ø., Eliassen, P. E., & Fichler, C. (1999). Principal tectonic events in the evolution of the northwest European Atlantic margin. In: Fleet, A.J. & Boldy, S. A. R. (eds) *Petroleum Geology of Northwest Europe: Proceedings of the 5th Conference*(41-61).
- Dunne, W. M., & Hancock, P. L. (1994). Palaeostress Analysis of Small-Scale Brittle Structures. In Hancock, P.L. (ed.): *Continental Deformation*, Pergamon Press, Oxford. 101-120.
- Dyer, R. (1988). Using joint interactions to estimate paleostress ratios. *Journal of Structural Geology*, 10, 685-699.
- Eig, K. (2008). *Onshore and offshore tectonic evolution of the Lofoten passive margin, north Norway*. (PhD), University of Tromsø, Unpublished.
- Eig, K., & Bergh, S. G. (2011). Late Cretaceous-Cenozoic fracturing in Lofoten, North Norway: Tectonic significance, fracture mechanisms and controlling factors. *Tectonophysics*, 499, 190-205. doi: 10.1016/j.tecto.2010.12.002
- Eig, K., Bergh, S. G., Henningsen, T., Kløvjan, O. S., & Olesen, O. (2008). *Kinematics and relative timing of brittle faults and fractures in Lofoten, North Norway: Constraints on the structural development of the Lofoten margin*. (PhD), University of Tromsø, Unpublished.
- Faleide, J. I., Tsikalas, F., Breivik, A. J., Mjelde, R., Ritzmann, O., Engen, Ø., . . . Eldholm, O. (2008). Structure and evolution of the continental margin off Norway and the Barents Sea. *Episodes*, 31(1).
- Faleide, J. I., Vågnes, E., & Gudlaugsson, S. T. (1993). Late Mesozoic-Cenozoic evolution of the southwestern Barents Sea in a regional rift-shear tectonic setting. *Marine and Petroleum Geology*, 10, 186-214.
- Faulds, J. E., & Varga, R. J. (1998). The role of accommodation zones and transfer zones in the regional segmentation of extended terranes. In Faulds, J.E. & Stewart, J.H. (eds): *Accommodation zones and Transfer Zones: the regional Segmentation of the Basin and Range Province*. *Geological Society of America, Special Publication*, 323, 1-45.
- Ferrill, D. A., Stamatakos, J. A., & Sims, D. (1999). Normal fault corrivation: implications for growth and seismicity of active normal faults. *Journal of Structural Geology*, 21, 1027-1038.
- Forslund, T. (1988). Post-Kaledonske forkastninger i Vest-Troms, med vekt på Kvaløyslettaforkastningen, Kvaløya. *Unpublished master thesis, University of Tromsø*.
- Fossen, H. (2010). *Structural Geology* (3 ed.): Cambridge University Press.
- Fürsich, F. T., & Thomsen, E. (2005). Jurassic bioata and biofacies in erratics from the Sortland area, Vesterålen, northern Norway. *Norges geologiske undersøkelse Bulletin*, 443, 37-53.
- Færseth, R. B., Knudsen, T., Liljedahl, T., Midbøe, P., & Søderstrøm, B. (1997). Oblique rifting and sequential faulting in the Jurassic development of the northern North Sea. *Journal of Structural Geology*, 19(10), 1285-1302.
- Fønstelién, S., & Horvei, A. (1979). Thoughts and considerations arising from the study of a "prospective" feature in the Troms I area. *Proceedings, Norwegian Sea Symposium, Tromsø: Norwegian Petroleum Society*, v. NSS/20. 1-10.
- Gabrielsen, R. H., Braathen, A., Dehls, J., & Roberts, D. (2002). Tectonic lineaments of Norway. *Norwegian Journal of Geology*, 82, 153-174.
- Gabrielsen, R. H., Færseth, R. B., Jensen, L. N., Kalheim, J. E., & Riis, F. (1990). Structural elements of the Norwegian continental shelf - Part I: The Barents Sea region. *Norwegian Petroleum Directorate Bulletin* 6, 33.

- Gabrielsen, R. H., & Ramberg, I. B. (1979). Fracture patterns in Norway from Landsat imagery: Results and potential use. Proceedings, Norwegian Sea Symposium, Tromsø, 1979. *Norwegian Petroleum Society NSP/1-28*.
- Gagama, M. F. V. (2005). Strukturell analyse av post-kaledonske lineamenter ved Sifjorden, Vest-Senja, Troms. *Unpublished master thesis, University of Tromsø*.
- Gawthorpe, R. L., & Hurst, J. M. (1993). Transfer zones in extensional basins: their structural style and influence on drainage development and stratigraphy. *Journal of the Geological Society London*, 150, 1137-1152.
- Gawthorpe, R. L., Jackson, C. A. L., Young, M. J., Sharp, I. R., Moustafa, A. R., & Leppard, C. W. (2003). Normal fault growth, displacement localisation and the evolution of normal fault populations: The Hamman Faraun fault block, Suez rift, Egypt. *Journal of Structural Geology*, 25, 883-895.
- Gernigon, L., & Brönnner, M. (2012). Late Palaeozoic architecture and evolution of the southwestern Barents Sea: Insights from a new generation of aeromagnetic data. *Journal of the Geological Society of London*, 169, 449-459.
- Gibbs, A. D. (1984). Structural evolution of extensional basin margins. *Journal of the Geological Society*, 141, 609-620.
- Goldstein, A., & Marshak, S. (1988). Analysis of fracture array geometry. . In S. Marshak & G. Mitra (Eds.), *Basic Methods of Structural Geology* (pp. 249-268). Englewood Cliffs, NJ: Prentice-Hall.
- Griffin, W. L., Heier, K. S., Taylor, P. N., & Weigland, P. W. (1974). General geology, age and chemistry of the Raftsund mangerite intrusion, Lofoten-Vesterålen. . *Norges geologiske undersøkelse* 312, 1-30.
- Grønlie, A., Nilsen, B., & Roberts, D. (1991). Brittle deformation history of fault rocks on the Fosen Peninsula, Trøndelag, Central Norway. *Norges geologiske undersøkelse Bulletin*, 421(39-57).
- Gustavson, M. (Cartographer). (1974). Geologisk kart over Norge 1:250000, Narvik.
- Hansen, J. A., & Bergh, S. G. (2012). Origin and reactivation of fracture systems adjacent to the Mid-Norwegian continental margin on Hamarøya, North Norway: use of digital geological mapping and morphotectonic lineament analysis. *Norwegian Journal of Geology*, 92, 391-303.
- Hansen, J. A., Bergh, S. G., & Henningsen, T. (2012). Mesozoic rifting and basin evolution on the Lofoten and Vesterålen Margin, North-Norway; time constraints and regional implications. *Norwegian Journal of Geology*, 91(203-228).
- Hansen, J. A., Bergh, S. G., Olesen, O., & Henningsen, T. (2009). Onshore offshore fault correlation on the Lofoten and Vesterålen margin: Architecture, evolution and basement control. In Hansen, J.A., *Onshore and offshore tectonic relations on the Lofoten and Vesterålen margin: Mesozoic and Early Cenozoic structural evolution and morphological implications*. Unpublished PhD-article, University of Tromsø.
- Hendriks, B. W. H. (2003). Cooling and denudation of the Norwegian and Barents Sea Margins, Northern Scandinavia. Constrained by apatite fission track and (U-Th)/He thermochronology. *PhD thesis, Vrije Universiteit Amsterdam*, 192pp.
- Hendriks, B. W. H., Osmundsen, P. T., & Redfield, T. F. (2010). Normal faulting and block tilting in Lofoten and Vesterålen constrained by Apatite Fission Track data. *Tectonophysics*, 485, 154-163.
- Henkel, H., & Guzman, M. (1977). Magnetic features of fracture zones. *Geoexploration*, 15, 173-181.
- Henningsen, T., & Tveten, E. (Cartographer). (1998). Geologisk kart over Norge. Bergrunnskart ANDØYA, M 1 : 250 000.
- Hobbs, B. E., Means, W. D., & Williams, P. F. (1976). *An outline of structural geology*. John Wiley & Sons.
- Hus, R., Acocella, V., Funicello, R., & De Batist, M. (2005). Sandbox models of relay ramp structure and evolution. *Journal of Structural Geology*, 27, 459-473.
- Indrevær, K., Bergh, S. G., Koehl, J. B., Hansen, J. A., Schermer, E. R., & Ingebrigtsen, A. (2014). Post-Caledonian brittle fault zones on the hyper-extended SW Barents Sea

- Margin: New insights into onshore and offshore margin architecture. *Norwegian Journal of Geology*.
- Katz, Y., Weinberger, R., & Aydin, A. (2004). Geometry and kinematic evolution of Riedel shear structures, Capitol Reef National Park, Utah. *Journal of Structural Geology*, 26(3), 491-501. doi: <http://dx.doi.org/10.1016/j.jsq.2003.08.003>
- Kløvjan, O. S. (1988). Tektonikk i den sørlige delen av Troms 2. *Hovedfagsoppgave (Cand. Scient.)*, Endogen geologi, geologisk avdeling, IBG, Universitetet i Tromsø, 277 pp.
- Koehl, J. B. (2013). Late Paleozoic-Cenozoic fault correlation and characterization of fault rocks in western Troms, North Norway. *Unpublished master thesis, University of Tromsø*, 100.
- Kulander, B. R., Barton, C. C., & Dean, S. L. (1979). The application of fractography to core and outcrop fracture investigations. *Tech Rep. U.S. Dept. Energy METC/SP-79/3 Morgantown Energy Center*, pp 1-174.
- Kullerud, K., Skjerlie, K. P., Corfu, F., & de la Rosa, J. D. (2006). The 2.40 Ga Ringvassøy mafic dykes, West Troms Basement Complex, Norway: The concluding act of early Palaeoproterozoic continental breakup. *Precambrian Research*, 150, 183-200.
- Larsen, G. B., Elvebakk, G., Henriksen, L. B., Kristensen, S. E., Nilsson, I., Samuelsberg, T. J., . . . Worsley, D. (2002). Upper Palaeozoic lithostratigraphy of the Southern Norwegian Barents Sea. *Norges geologiske undersøkelse Bulletin*, 444, 76pp.
- Leeder, M. R. G. R. L. (1987). Sedimentary models for tilt-block/half-graben basins. *Geological Society, London, Special Publications*, 28, 139-152.
- Løseth, H., & Tveten, E. (1996). Post-Caledonian structural evolution of the Lofoten and Vesterålen offshore and onshore areas. *Norsk Geologisk Tidsskrift*, 76, 215-230.
- Machette, M. N., Persounius, S. F., & Nelson, A. R. (1991). The Wasatch fault zone, Utah - segmentation and history of Holocene earthquakes. *Journal of Structural Geology*, 13, 137-149.
- Mandl, G. (2005). *Rock Joints - The Mechanical Genesis*. Springer, 221 pp.
- Manum, S. B., Bose, M. N., & Vigran, J. O. (1991). The Jurassic flora of Andøya, northern Norway. *Review of Palaeobotany and Palynology*, 68, 233-256.
- McGrath, A. G., & Davison, I. (1995). Damage zone geometry around fault tips. *Journal of Structural Geology*, 17(7), 1011-1024.
- Mokhtari, M., & Pegrum, R. M. (1992). Structure and evolution of the Lofoten continental margin, offshore Norway. *Norsk Geologisk Tidsskrift*, 72, 339-355.
- Morley, C. K. (1995). Developments in the structural geology of rifts over the last decade and their impact on hydrocarbon exploration. In Labiase, J.J. (ed): *Hydrocarbon Habitat in Rift Basins. Geological Society of London Special Publication*, 80, 1-32.
- Morley, C. K. (2004). Nested strike-slip duplexes, and other evidence for Late Cretaceous-Palaeogene transpressional tectonics before and during India-Eurasia collision in Thailand, Myanmar and Malaysia. *Journal of the Geological Society London*, 161, 799-812.
- Morley, C. K. (2007). Development of crestal normal faults associated with deepwater old growth. *Journal of Structural Geology*, 29, 1148-1163.
- Mosar, J., Eide, E. A., Osmundsen, P. T., Sommaruga, A., & Torsvik, T. H. (2002). Greenland-Norway separation: A geodynamic model for the North Atlantic. *Norwegian Journal of Geology*, 82, 281-298.
- Nielsen, S. B., Paulsen, G. E., Hansen, D. L., Gemmer, L., Clausen, O. R., Jacobsen, B. H., . . . Gallagher, K. (2002). Paleocene initiation of Cenozoic uplift in Norway. In A.G. Doré, J.A. Cartwright, M.S. Stoker, J.P. Turner, N. White (Eds), *Exhumation of the North Atlantic Margin: Timing, Mechanisms and Implications for Petroleum Exploration. Special Publications - Geological Society of London*, 196, 45-65.
- Nüchter, J. A., & Ellis, S. (2011). Mid-crustal controls on episodic stress-field rotation around major reverse, normal and strike-slip faults. In Fagereng, Å., Toy, V.G. & Rowland, J.V. (eds): *Geology of the Earthquake Source: A volume in honour of Rich Sibson. Geological Society of London Special Publication*, 359, 187-201.

- Olesen, O., Ebbing, J., Lundin, E., Muring, E., Skilbrei, J. R., Torsvik, T. H., . . . Sand, M. (2007). An improved tectonic model for the Eocene opening of the Norwegian-Greenland Sea: Use of modern magnetic data. *Marine and Petroleum Geology*, 24(1), 53-66.
- Olesen, O., Torsvik, T. H., Tveten, E., & Zwaan, K. B. (1993). The Lofoten-Lopphavet project - an integrated approach to the study of a passive continental margin. *NGU Report*, 93(129), 54.
- Olesen, O., Torsvik, T. H., Tveten, E., Zwaan, K. B., Løseth, H., & Henningsen, T. (1997). Basement structure of the continental margin in the Lofoten-Lopphavet area, northern Norway: Constraints from potential field data, on-land structural mapping and paleomagnetic data. *Norsk Geologisk Tidsskrift*, 77, 15-30.
- Opheim, J. A., & Andresen, A. (1989). Basement-cover relationships on northern Vanna, Troms, Norway. *Norsk Geologisk Tidsskrift*, 69, 67-81.
- Osmundsen, P. T., & Redfield, T. F. (2011). Crustal taper and topography at passive continental margins. *Terra Nova*, 00, 1-13. doi: 10.1111/j.1365-3121.2011.01014.x
- Osmundsen, P. T., Redfield, T. F., Hendriks, B. W. H., Bergh, S. G., Hansen, J. A., Henderson, I. H. C., . . . Davidsen, B. (2010). Fault-controlled apline topography in Norway. *Journal of the Geological Society*, 167, 83-98. doi: 10.114/0016-76492009-019
- Pascal, C., & Olesen, O. (2009). Are the Norwegian mountains compensated by a mantle thermal anomaly at depth? *Tectonophysics*, 475, 160-168.
- Passchier, C. W., & Trouw, R. A. J. (2005). *Microtectonics*. Berlin; New York: Springer.
- Peacock, D. C. P., Knipe, R. J., & Sanderson, D. J. (2000). Glossary of normal faults. *Journal of Structural Geology*, 22, 291-305.
- Peacock, D. C. P., & Parfitt, E. A. (2002). Active relay ramps and normal fault propagation on Kilauea Volcano, Hawaii. *Journal of Structural Geology*, 24, 729-742.
- Plassen, L. K., J. (2009). Fluid flow structures and processes; indications from the North Norwegian continental margin. *Norwegian Journal of Geology*, 89, 57-64.
- Prosser, S. (1993). Rift-related linked depositional systems and their seismic expression. In Williams, G.D. (ed): *Tectonics and Seismic sequence stratigraphy*. *Geological Society of London Special Publication*, 71, 35-66.
- Rasmussen, E. (1985). Summary of the Mesozoic rocks on Andøya, Northern Norway, with emphasis on reservoir geology, source rock potential and dating of unconformities. *Inhouse Norsk Hydro report*, 19 pp.
- Rawnsley, K. D., Rives, T., Petit, J. P., Hencher, S. R., & Lumsden, A. C. (1992). joint development in perturbed stress fields near faults. *Journal of Structural Geology*, 14, 939-951.
- Redfield, T. F., & Osmundsen, P. T. (2013). The long-term topographic response of a continent adjacent to a hyperextended margin: A case study from Scandinavia. *Geological Society of America Bulletin*, 125(1-2), 184-200.
- Reeves, C. (2005). *Aeromagnetic Surveys: Principles, Practice & Interpretation* (pp. 155).
- Reynolds, J. M. (1997). *An Introduction to Applied and Environmental Geophysics*: John Wiley and Sons, Ltd. New York.
- Roberts, D., Chand, S., & Rise, L. (2011). A half-graben of inferred Late Paleozoic age in outer Varangerfjorden Finnmark: evidence from seismic-reflection profiles and multibeam bathymetry. *Norwegian Journal of Geology*, 91(191-200).
- Roberts, D., & Lippard, S. J. (2005). Inferred Mesozoic faulting in Finnmark: Current status and offshore links. *Norges Geologiske Undersøkelse Bulletin*, 55-60.
- Rohrman, M., & van der Beek, P. (1996). Cenozoic postrift domal uplift of North Atlantic margins: an asthenospheric diapirism model. *Geology*, 24(10), 901-904.
- Root, K. G. (1990). Extensional duplex in the Purcell Mountains of Southeastern British Columbia. *Geology*, 18(5), 419-421.
- Rydningen, T. A., Vorren, T. O., Laberg, J. S., & Kolstad, V. (2013). The marine-based NW Fennoscandian ice sheet: glacial and deglacial dynamics as reconstructed from submarine landforms. *Quaternary Science Reviews*, 68, 126-141.

- Sandstad, J. S., & Nilsson, L. P. (1998). Gullundersøkelser på Ringvassøya; sammenstilling av tidligere prospektering og feltbefaring i 1997. *Norges geologiske undersøkelse Report*, 98, 61.
- Scott, D. L., Etheridge, M. A., & Rosendahl, B. R. (1992). Oblique-slip deformation in extensional terrains; a case study of the lakes Tanganyika and Malawi zones. *Tectonics*, 11, 998-1009.
- Shannon, P. M., Faleide, J. I., Smallwood, J. R., & Walker, I. M. (2005). The Atlantic Margin from Norway to Ireland: geological review of a frontier continental margin province. *In: Petroleum Geology: North-West Europe and Global Perspectives - Proceedings of the 6th Petroleum Geology Conference* (edited by Doré, A.G. & Vining, B.A.). Geological Society, London, 733-737.
- Smelror, M., Mørk, A., Mørk, M. B. E., Weiss, H. M., & Løseth, H. (2001). Middle Jurassic-Lower Cretaceous transgressive-regressive sequences and facies distribution off Nordland and Troms, Norway,. *In O. J. Martinsen & T. Dreyer (Eds.), Sedimentary environments offshore Norway - Palaeozoic to Recent* (Vol. 10, pp. 211-232): Norwegian Petroleum Society Special Publications.
- Smith, J. V. (1996). Geometry and kinematics of convergent conjugate vein array systems. *Journal of Structural Geology*, 18, 1291-1300.
- Smith, J. V., & Durney, D. W. (1992). Experimental formation of brittle structural assemblages in oblique divergence. *Tectonophysics*, 216, 235-253.
- Stelthenpohl, M. G., Moecher, D., Andresen, A., Ball, J., Mager, S., & Hames, W. E. (2011). The Eidsfjord Shear Zone, Lofoten-Vesterålen, North Norway: An early devonian, paleoseismigenic low-angle Normal Fault. *Journal of Structural Geology*, 33(5), 1023-1043.
- Stemmerik, L., Dalhoff, F., Larsen, B. D., Lyck, J., Mathiesen, A., & Nilsson, I. (1998). Wandel Sea Basin, eastern North Greenland. *Geology of Greenland Survey Bulletin*, 180, 55-62.
- Sturt, B. A., Dalland, A., & Mitchell, J. G. (1979). The age of the sub Mid-Jurassic tropical weathering profile of Andøya, northern Norway, and the implications for the Late Paleozoic palaeogeography in the North Atlantic region. *Geologische Rundschau*, 68(2), 523-542.
- Thorstensen, L. (2011). Land-sokkel korrelasjon av tektoniske elementer i ytre del av Senja og Kvaløya i Troms. *Unpublished master thesis, University of Tromsø*.
- Trudgill, B., & Cartwright, J. A. (1994). Relay-ramp forms and normal-fault linkages, Canyonlands National Park, Utah. *Geological Society of America Bulletin*, 106, 1143-1157.
- Tsikalas, F., Faleide, J. I., & Eldholm, O. (2001). Lateral variations in tectono-magmatic style along the Lofoten-Vesterålen volcanic margin off Norway. *Marine and Petroleum Geology*, 18, 807-832.
- Tveten, E. (Cartographer). (1978). Geologisk kart over Norge, berggunnskart SVOLVÆR 1:250000.
- Tveten, E., & Zwaan, K. B. (1993). Geology of the coast region from Lofoten to Loppa with special emphasis on faults, joints and related structures. *NGU Report* (Vol. 93, pp. 25).
- Vajda, V., & Wigforss-Lange, J. (2009). Onshore Jurassic of Scandinavia and related areas. *GFF*, 131, 5-23.
- Veeken, P. (2007). Seismic stratigraphy, basin analysis and reservoir characterisation. *Handbook of Geophysical Exploration* 37. 509.
- Voct, J. H. L. (1905). Om Andøens jurafelt (On the Jurassic field of Andøy). *Norges Geologiske Undersøkelse Aarbok*, 5, 67 pp.
- Wilson, R. W., McCaffrey, K. J. W., Holdsworth, R. E., Imber, J., Jones, R. R., Welbon, A. I. F., & Roberts, D. (2006). Complex fault patterns, transtension and structural segmentation of the Lofoten Ridge, Norwegian margin: Using digital mapping to link onshore and offshore geology. *Tectonics*, 25(TC4018). doi: 10.1029/2005TC0011895

- Woodcock, N. H., & Fischer, M. (1986). Strike-slip duplexes. *Journal of Structural Geology*, 8, 725-735.
- Woodcock, N. H., & Schubert, C. (1994). Continental strike-slip tectonics. In P. Hancock (Ed.), *Continental deformation* (pp. pp 251-263). New York: Pergamon Press.
- Ziegler, P. A. (1989). Evolution of the North Atlantic; an overview. *American Association of Petroleum Geologist Memoir*, 46, 111-129.
- Zwaan, K. B. (1995). Geology of the West Troms Basement Complex, Northern Norway, with emphasis on the Senja Shear Belt: A preliminary account. *Norges geologiske undersøkelse Bulletin*, 427, 33-36.
- Zwaan, K. B., & Grogan, P. W. (Cartographer). (1998). Geologiske Kart over Norge, Berggrunnskart TROMSØ, M: 1:250000.
- Ørvig, T. (1960). The Jurassic and Cretaceous on Andøya in northern Norway. In O. Holtedahl (Ed.), *Geology of Norway* (Vol. 208, pp. 344-350): Norges geologiske undersøkelse.

